The Dielectric Properties of Simple Polar Liquids at Millimetre Wavelengths

a thesis submitted for
the degree of
Doctor of Philosophy
in the
University of London

by

Elisabeth Ann Carter
Bedford College

August 1968

Abstract

Previous methods of determining the complex permittivity, $\epsilon^* = \epsilon' - j\epsilon''$, at millimetre wavelengths are reviewed, and at a wavelength of 0.848cms six different ways of determining this quantity from the experimental observations are compared. It is found that the method first described by Fatuzzo and Mason is the most suitable for determining the temperature variation of the complex permittivity at wavelengths of 3.332cms, 0.848cms and 0.435cms, and the three sets of apparatus are adapted to cut down experimental errors to a minimum. The complex permittivity, for several simple liquids, is determined at each of the three wavelengths over a temperature range from 50°C down to the freezing point of the liquid. The static permittivity ϵ_s and the refractive index at the Sodium-D line n_D are also measured over this same temperature range.

Assuming that the dispersion of ϵ^* is given by Debye's equations, then, knowing the static permittivity and the experimental value of ϵ^* at one other wavelength, the permittivity at the high frequency end of the

dispersion curve ϵ_∞ and the critical wavelength λ_c can be calculated. Using the value of ϵ^* at each of the three experimental wavelengths in turn, three different values for ϵ_∞ and λ_c at each temperature are calculated. The value of ϵ_∞ and λ_c at 3.332cms are taken as the correct values, and the deviation of the values at the other two wavelengths from this value noted. This deviation is to smaller values of ϵ_∞ and λ_c as the wavelength shortens and the deviation increases with decreasing temperature. This type of deviation is explained by the presence of a second absorption band centered at sub-millimetre wavelengths. By considering the amount of the deviation and the difference $\epsilon_\infty - n_D^2$ as compared with $\epsilon_s - n_D^2$ it is concluded that the second absorption band is due to a resonance absorption, rather than a Debye type absorption, and having a resonant frequency which decreases slightly with increasing temperature.

Index

Survey of the Theories of Polar Dielectrics.

Introduction.

The original meaning of the word 'dielectric' was a non-conductor of electricity, but most dielectrics exhibit a small amount of conduction, making it difficult to distinguish sharply between dielectrics and conductors.

These dielectrics, when placed between the plates of a charged condenser, have the property of lowering the potential between the plates. This property is characterized by the permittivity of the material and is due to a redistribution of the charges in the material, polarization, due to the applied external field. The total polarization is due to three main processes;-

1) a displacement of the electrons with respect to the nucleus, electronic polarization,

2) a relative displacement of the positive and negative ions within the molecule, atomic polarization,

3) an orientation of the permanent molecular moments, which in the absence of an external field have a random distribution and hence produce no resultant moment, orientational polarization.

Provided that the frequency of the external field is not too high the first two effects are always present. The third effect is only exhibited by those materials whose molecules have permanent electrical moments, polar molecules, again only if the frequency is not too high. These polar materials are characterized by high static permittivities, e.g. water80.1, and chlorobenzene 5.69, compared with non-polar benzene 2.28.

In a slowly alternating external field, e.g. at audio frequencies, the permittivity of a polar material shows no deviation from the static value. As the frequency is increased a point is reached when the rotation of the polar molecules starts to lag behind the applied field due to the resistance to their motion produced by the surrounding molecules. This causes a decrease in the permittivity and an absorption of energy. This observed lag of the polarization behind the applied field is referred to as 'relaxation', and the relaxation time τ of the material is defined as the time taken for the orientation polarization to fall to $\frac{1}{e}$ of its equilibrium value when the applied field is removed. The decrease in permittivity continues with increasing frequency until

the orientation polarization ceases to be effective. This point is usually reached by the far infra-red frequencies. The other two types of polarization give resonant absorption peaks, the atomic polarization at infra-red frequencies, and the electronic polarization at ultra-violet frequencies.

Static Dielectric Permittivity

The polarizability, α, of a molecule is defined by the equation $\mathbf{m} = \alpha \mathbf{F}$ where $\mathbf{m}$ is the average over a sufficient length of time of the electric moment aquired under the influence of an electric field intensity $\mathbf{F}$. All molecules have a polarizability α_o due to the atomic and electronic vibrations, but in the case of polar molecules there is an additional effect due to the permanent moments of the molecules. Debye found an expression for this orientational effect for a system of dipoles between which there are no forces other than the electrical forces.

Consider the molecule as a rigid system of charges, each molecule having an electric moment $\vec{m}$. With no forces

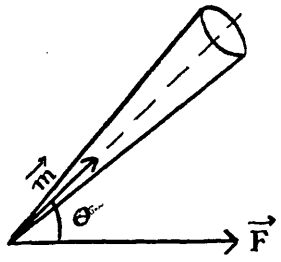

fig.1.

acting, the average of the electric moments of the molecules in any particular direction will be zero, and the number of molecules pointing in a direction confined within a solid angle $d\Omega$ as shown in fig.1, will be

$$A\, d\Omega$$

where A is a constant depending on the number of molecules under consideration. In a field of intensity $\vec{F}$, acting at an angle θ with respect to the molecules within the solid angle $d\Omega$, the number confined to this solid angle, according to Boltzmann's law, will be

$$A\, e^{-u/kT}\, d\Omega$$

where k is Boltzmann's constant, T the absolute temperature, and u is the potential energy of the molecule, given by

$$u = -\vec{m}\cdot\vec{F}$$

For a molecule within the solid angle $d\Omega$

$$u = -\mu F \cos\theta$$

where μ is the absolute value of the electric moment. Thus the average moment $\overline{m}_o$ in the direction of the field is given by

$$\overline{m}_o = \frac{\int A\, e^{\left(\frac{\mu F}{kT}\cos\theta\right)}\, \mu\cos\theta\, d\Omega}{A\, e^{\left(\frac{\mu F}{kT}\cos\theta\right)}\, d\Omega}$$

where the integration is taken over all possible directions. Remembering that

$$d\Omega = 2\pi \sin\theta \, d\theta$$

this gives $$\frac{\overline{m_o}}{\mu} = \coth \frac{\mu F}{kT} - \frac{1}{\mu F/kT}$$

For most substances $\frac{\mu F}{kT} \ll 1$ as $k = 1.38 \times 10^{-16}$ erg deg^{-1}, μ is of the order 10^{-18} e.s.u. (e.g. water 1.84×10^{-18} e.s.u., nitrobenzene 3.95×10^{-18} e.s.u.) and taking values for T of 300° A, and F of 1e.s.u., giving a value of

$$\frac{\mu F}{kT} = 2{\cdot}42 \times 10^{-5}$$

Because of this all orders of $\frac{\mu F}{kT}$ above the first in the expansion of $\frac{\overline{m_o}}{\mu}$ can be ignored giving

$$\frac{\overline{m_o}}{\mu} = \frac{1}{3}\frac{\mu F}{kT} \quad \text{or} \quad \overline{m_o} = \frac{\mu^2}{3kT} F$$

Hence the total polarizability is

$$\alpha = \alpha_o + \frac{\mu^2}{3kT}$$

The field F is the field acting on the molecule, and is not the same as the applied external field due to the presence of the surrounding dielectric.

Debye calculated this internal field by imagining the molecule in question enclosed by a small sphere, whose radius was large compared with molecular dimensions, but small compared with macroscopic dimensions, so that the

dielectric inside the sphere could be treated microscopically while the rest was treated macroscopically. Let the small sphere be in a homogeneous field obtained by a surface density of charge σ distributed uniformly over two plates whose dimensions are large compared with their separation, as shown in fig.2. Debye assumed that

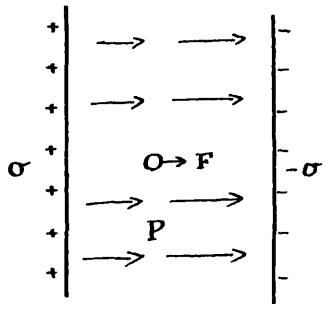

fig.2.

the force F, acting on the sphere carrying unit positive charge, to be made up of three compnents

$$F = F_1 + F_2 + F_3$$

F_1 is the force due to the external field, $= 4\pi\sigma$

The force F_2 is due to the dielectric outside the sphere, and is made up of two parts, one due to the layers of induced charge on the dielectric facing the conducting plates, and the second due to the layer of charge on the surface of the sphere. As the sphere is filled the polarization at its surface is parallel to the applied field, hence

$$F_2 = -4\pi P + \frac{4\pi}{3} P$$

where P is the polarization of the medium.

The force F_3 is due to the dielectric contained within the sphere. Generally F_3 is a complicated function,

though in a few cases it can be shown to be zero, e.g. cubic crystals, gases, and non-associating liquids. Debye assumed that F_3 was zero, and hence obtained

$$F = E + \frac{4\pi}{3} P$$

As the polarization is also the electric moment per unit volume $P = N \alpha F$

where N is the number of molecules per unit volume, and α is the polarizability. Combining these last two with

$$D = \epsilon E = E + 4\pi P$$

Debye obtained

$$\frac{\epsilon - 1}{\epsilon + 2} = N \frac{4\pi}{3} \alpha \qquad (1)$$

This is the same as the Clausius-Mosotti equation for non-polar materials, but Debye substituted

$$\alpha = \alpha_0 + \frac{\mu^2}{3kT}$$

giving

$$\frac{\epsilon - 1}{\epsilon + 2} = \frac{4\pi N}{3} \left(\alpha_0 + \frac{\mu^2}{3kT} \right) \qquad (2)$$

As this equation has been derived assuming F_3 to be zero, it can be expected to be valid for cases where F_3 does equal zero, i.e. gases, dilute solutions of polar liquids in a non-polar solvent, and non-polar liquids. By comparing values for μ calculated from measured values of ϵ for the pure polar liquid, a dilute solution of the

polar liquid in a non-polar liquid, and the vapour, it was found that , in general, dilute solutions gave approximately the same value for μ as the vapour, but there was a considerable discrepancy with the value for pure liquids, e.g. for water, measurements on the vapour gave $\mu = 1.84 \times 10^{-18}$ while those on the pure liquid gave $\mu = 0.95 \times 10^{-18}$ e.s.u. The main difficulty with Debye's formula can be shown if the formula is written in the form

$$\frac{\epsilon - 1}{\epsilon + 2} = x$$

or

$$\epsilon = \frac{1 + 2x}{1 - x}$$

According to this $\epsilon \to \infty$ as $x \to 1$, or

$$T \to T_c = \left(1 - \frac{4\pi N}{3}\alpha_0\right)\frac{4\pi N}{9k}\mu^2$$

i.e. T_c is a Curie point, and at temperatures below T_c the material should show spontaneous polarization. Inserting numerical values, T_c for water is 1,100° C, and for chlorobenzene 120° C. Similar values for other liquids mean that at ordinary temperatures spontaneous polarization should be a common occurance, but no liquid shows it.

This difficulty was put down to 'association', i.e. the forces between the polar molecules were so strong that no simple description would suffice. This was found

not to be the case when Wyman[2] showed that a large number of polar liquids, water included, obeyed the simple relation $(\epsilon+1)T \sim$ constant.

For polar liquids the assumption that $F_3 = 0$ cannot be made. Onsager[3], in deriving his formula, took into account the effect of an individual dipole molecule on the surrounding medium.

Onsager considered a typical molecule of the medium as a point dipole, having a permanent moment μ_o, and polarizability α_o, at the centre of a real spherical cavity of radius a, in a continuous medium of dielectric permittivity ϵ. With an electric field $\vec{F}$ acting on the sphere its total moment is the sum of the permanent and induced moments

$$\vec{m} = \mu_o \vec{u} + \alpha_o \vec{F} \qquad (3)$$

where $\vec{u}$ is a unit vector in the direction of the dipole axis. This moment at the centre of the cavity will cause a reaction field in the cavity

$$\vec{R} = \frac{2(\epsilon-1)}{(2\epsilon+1)} \frac{\vec{m}}{a^3}$$

When an external field $\vec{E}$ is applied to the dielectric it

it will produce a field in an empty cavity of

$$\vec{G} = \frac{3\epsilon}{(2\epsilon+1)}\vec{E}$$

Thus the total field in the cavity is

$$\vec{F} = \vec{G} + \vec{R} = \frac{3\epsilon}{(2\epsilon+1)}\vec{E} + \frac{2(\epsilon-1)}{(2\epsilon+1)}\frac{\vec{m}}{a^3} \qquad (4)$$

Using (3) and defining the internal refractive index n by

$$\alpha_o = \frac{n^2-1}{n^2+2}\,a^3$$

one obtains

$$\vec{m} = \frac{(n^2+2)(2\epsilon+1)}{3(2\epsilon+n^2)}\mu_o\vec{u} + \frac{\epsilon(n^2-1)}{(2\epsilon+n^2)}a^3\vec{E}$$

or

$$\vec{m} = \mu\vec{u} + \frac{\epsilon(n^2+2)}{(2\epsilon+n^2)}\alpha_o\vec{E} \qquad (5)$$

where

$$\mu = \frac{(n^2+2)(2\epsilon+1)}{3(2\epsilon+n^2)}\mu_o$$

Thus $\vec{F}$ can be written as

$$\vec{F} = \left[1 + \frac{n^2(\epsilon-1)}{(2\epsilon+n^2)}\right]\vec{E} + \frac{2(\epsilon-1)}{(2\epsilon+1)}\frac{\mu}{a^3}\vec{u} \qquad (6)$$

To find the average orientation of a molecule it is not permissible to assume that the orientating couple is proportional to the time average of $\vec{F}$, since $\vec{F}$ depends on the orientation. Thus the orientating couple must be computed for each direction of $\vec{u}$.

The couple is $\vec{M} = \vec{F} \times \vec{m}$

As $\vec{R}$ is parallel to $\vec{m}$ this does not contribute, hence

$$\vec{M} = \vec{G} \times \vec{m}$$

$\vec{G}$ is parallel to $\vec{E}$, so, using (5)

$$\vec{M} = \mu \vec{G} \times \vec{u}$$

With an angle θ between the field and the dipole axis

$$M = \mu G \sin\theta$$

If ω is the work of orientation

$$\frac{\partial \omega}{\partial \theta} = M$$

or $$\omega = -\mu G \cos\theta$$

The mean orientation is given by Boltzmann's formula

$$\overline{\cos\theta} = \frac{\int \cos\theta \; e^{-\omega/kT} \sin\theta \, d\theta \, d\phi}{\int e^{-\omega/kT} \sin\theta \, d\theta \, d\phi}$$

$$\overline{\cos\theta} = \coth \frac{\mu G}{kT} - \frac{1}{\mu G/kT}$$

For small field intensities, i.e. when $\frac{\mu G}{kT} \ll 1$

$$\overline{\cos\theta} = \frac{\mu G}{3kT} = \frac{\mu}{3kT} \frac{3\epsilon}{(2\epsilon+1)} E$$

Hence, from (5)

$$\vec{m} = \left[\frac{\mu^2}{3kT} \frac{3\epsilon}{(2\epsilon+1)} + \frac{\epsilon(n^2+2)}{(2\epsilon+n^2)} \alpha_0 \right] \vec{E}$$

The polarization per unit volume

$$\vec{P} = N \vec{m} = \frac{(\epsilon - 1)}{4\pi} \vec{E}$$

where N is the number of molecules per unit volume. If it is assumed that the volume of the liquid equals the sum of the volume of the individual molecules,

$$N \frac{4\pi a^3}{3} = 1$$

Hence

$$(\epsilon - 1) = \frac{4\pi N \mu^2}{3kT} \frac{3\epsilon}{(2\epsilon+1)} + \frac{3\epsilon(n^2-1)}{(2\epsilon+n^2)}$$

or

$$\frac{(\epsilon-1)}{(\epsilon+2)} - \frac{(n^2-1)}{(n^2+2)} = \frac{3\epsilon(n^2+2)}{(2\epsilon+n^2)(\epsilon+2)} \frac{4\pi N \mu_o^2}{9kT} \qquad (7)$$

When ϵ is large compared with n^2 the equation can be approximated to

$$\frac{\epsilon}{(n^2+2)^2} \simeq \frac{2\pi N \mu_o^2}{9kT}$$

which explains the empirical formula $(\epsilon+1)T \sim$ constant which Wyman found.

The difference between Onsager's and Debye's equations is the quantity

$$\frac{3\epsilon(n^2+2)}{(2\epsilon+n^2)(\epsilon+2)}$$

which tends to unity when $\epsilon \simeq n^2$, i.e. for small dipole moments, or for low densities e.g. gases.

If Onsager's equation (7) is written in the form

$$\frac{(\epsilon - n^2)(2\epsilon + n^2)}{(n^2+2)^2 \epsilon} = \frac{4\pi N \mu_o^2}{9kT}$$

it will be seen that $\epsilon \to \infty$ only when $T \to 0$. So, according to this, dielectrics cannot show spontaneous polarization.

Kirkwood[4] points out that a defect of the Onsager theory is the assumption of a uniform local permittivity, identical with the macroscopic permittivity of the medium. He approximates the local permittivity to the macroscopic permittivity outside the molecule and its first shell of neighbours, rather than to the entire region outside the molecule. Also taking into account hindered rotation of the neighbours of a molecule relative to itself, he obtains the formula

$$\frac{(\epsilon - 1)}{3} = \frac{3\epsilon}{(2\epsilon+1)} \frac{4\pi N}{3} \left(\alpha_o + \frac{\mu \bar{\mu}}{3kT} \right) \qquad (8)$$

where μ is the electric moment of the dipole in the liquid, and $\bar{\mu}$ is the sum of the dipole moment of a molecule and the moment induced due to the hindered rotation of the surrounding molecules in the absence of an external field. $\mu\bar{\mu}$ can be written in the form $g\mu^2$, where g is the correlation parameter. In principle

g can be calculated by statistical mechanics, but in practice this is usually prevented by insufficient knowledge of the liquid structure. Kirkwood's theory contains an incorrect approximation for the local field which is put right in Frohlich's theory.

Frohlich[5] considered a spherical region, large compared with microscopic dimensions, but small compared with macroscopic dimensions. He then applied statistical mechanics to the charges within this sphere, and treated the material outside the sphere as a continuous medium. By this means he obtained the formula

$$\frac{(\epsilon-1)}{(\epsilon+2)}-\frac{(n^2-1)}{(n^2+1)}=\frac{4\pi N}{9kT}\frac{3\epsilon(n^2+2)}{(2\epsilon+n^2)(\epsilon+2)}g\mu_o^2 \qquad (9)$$

which is the same as Onsager's equation apart from the correlation factor.

A group of measurements[6] upon a considerable number of pure polar liquids has been made to compare the equations of Debye (2), Onsager (7), and Kirkwood (8), the dipole moment being calculated in each case. Since there is no way of calculating g with accuracy for these liquids it is included in the value for the moment, hence

Onsager's and Frohlich's equations are indistinguishable.

The following table shows a comparison of the values of the vacuum dipole moments as calculated by the three equations from observed values at 25°C

Substance	Debye	Onsager	Kirkwood	Observed
Ethyl Bromide	1.28	1.80	1.90	2.20 (gas)
n-Butyl Bromide	1.41	1.80	1.92	2.15 (gas)
n-Octyl Bromide	1.56	1.81	1.88	1.96 (solution)
n-Dodecyl Bromide	1.61	1.79	1.89	
n-Hexadecyl Bromide	1.66	1.80	1.87	
Chlorobenzene	1.22	1.45	1.54	1.72 (gas)
Bromobenzene	1.17	1.37	1.52	1.77 (gas)
Ethylene Chloride	1.31	1.89	2.94	1.47 (gas)
Ethylene Bromide	0.93	1.04	1.14	1.04 (gas)

The calculated values depend on the value chosen for n.

Comparing the Bromide chains, the Debye values for μ increase with chain length while the Onsager, Kirkwood and Observed show no significant increase. This is to be expected because the Debye equation takes no account

of intermolecular forces, thus, as the molecules become larger so that the dipoles are further apart and the forces become less, the equation will become more exact. The Kirkwood values are higher than the Onsager, and the nearness of both to the observed values show that g is close to unity for these liquids.

Dielectric Relaxation

The preceeding theories have all been concerned with the behaviour of the dielectric under the influence of a time independent field, or one alternating with a low enough frequency that the polar molecules can follow the field with no detectable lag. At frequencies which are too high for the polar molecules to follow the applied field exactly, the permittivity drops below the static value and there is a dissipation of energy in the dielectric, known as dielectric loss.

Assume that the polarization P at these frequencies is made up of two parts, P_e resulting from the atomic and electronic polarizations, and P_a from the dipolar contribution. At the frequencies under consideration

the part $P_1 = \chi_1 E$

follows the field intensity E with negligible lag, χ_1 being the dielectric susceptibility. The part P_2 lags behind the field such that, if $\chi_2 E$ is the final value approached when E is held constant, P_2 at any instant approaches this value at a rate proportional to the difference still remaining

$$\frac{dP_2}{dt} = \frac{1}{\tau_m}(\chi_2 E - P_2)$$

where τ_m is a constant. Integrating this for the case where P_2 is initially zero, and E is suddenly applied at $t = 0$ and held constant, gives

$$P_2 = \chi_2 (1 - e^{-t/\tau_m}) E$$

Thus P_2 increases exponentially with a time constant τ_m, the relaxation time.

Let an alternating field $E = E_0 e^{j\omega t}$ be applied.

Here $$\frac{dP_2}{dt} = j\omega P_2 = \frac{1}{\tau_m}(\chi_2 E - P_2)$$

hence $$P_2 = \frac{\chi_2}{1 + j\omega \tau_m} E$$

This gives a total polarization

$$P = P_1 + P_2 = \left(\chi_1 + \frac{\chi_2}{1 + j\omega \tau_m}\right) E$$

The polarization is thus complex and corresponds to a complex permittivity

$$\epsilon = \epsilon' - j\epsilon'' = 1 + 4\pi P/E$$

At $\omega = 0$ the permittivity is real and has the value

$$\epsilon_s = 1 + 4\pi(\chi_1 + \chi_2)$$

At $\omega = \infty$ the permittivity is again real, having the value

$$\epsilon_\infty = 1 + 4\pi\chi_1$$

Hence the complex permittivity can be written as

$$\epsilon - \epsilon_\infty = \frac{\epsilon_s - \epsilon_\infty}{1 + j\omega\tau_m} \qquad (10)$$

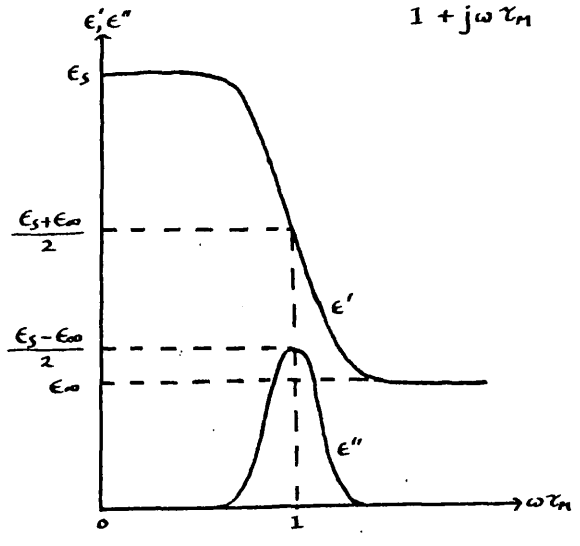

fig.3.

This gives

$$\epsilon' = \epsilon_\infty + \frac{\epsilon_s - \epsilon_\infty}{1 + \omega^2\tau_m^2}$$

$$\epsilon'' = \frac{\epsilon_s - \epsilon_\infty}{1 + \omega^2\tau_m^2}\,\omega\tau_m$$

The value of ϵ'' has a maximum at $\omega\tau_m = 1$

or $\omega = \omega_c = \frac{1}{\tau_m}$

where ω_c is the critical frequency.

Cole and Cole showed that the above equations can be written in the combined form

$$\epsilon''^2 + \left[\epsilon' - \frac{\epsilon_s + \epsilon_\infty}{2}\right]^2 = \left[\frac{\epsilon_s - \epsilon_\infty}{2}\right]^2 \qquad (11)$$

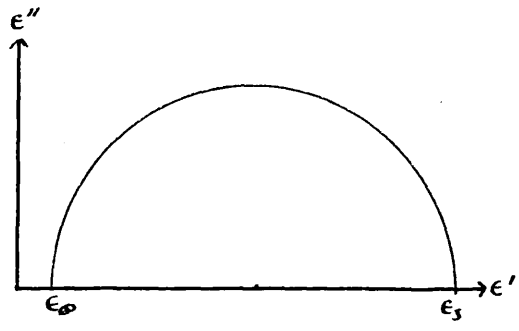

fig.4.

As only positive values of ϵ'' can occur, a plot of ϵ'' against ϵ' is a semicircle of radius $\frac{\epsilon_s - \epsilon_\infty}{2}$, and centre at $0, \frac{\epsilon_s + \epsilon_\infty}{2}$. The two points at which $\epsilon'' = 0$ are $\epsilon' = \epsilon_s$ and ϵ_∞. This means that, knowing the values of ϵ_s and ϵ_∞, the ϵ'', ϵ' curve can be completely defined, the frequency range in which the absorption takes place having no influence on its shape.

So far only the macroscopic properties of the liquid have been used, τ_M being termed the macroscopic relaxation time. Equations for the permittivity in the dispersion region have been developed using the microscopic properties of the liquid.

Debye[1] gave the first theoretical treatment, and W. F. Brown[8] gave a simplified version of his theory. It is assumed that there is negligible interaction between neighbouring molecules, and that there are no induced moments.

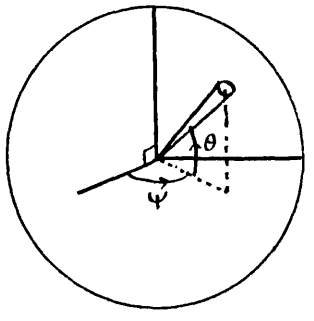

fig.5.

A molecule in a particular orientation (θ,ψ) as shown in fig.5. can be represented by a point on the unit sphere. The distribution of orientations at any instant can be represented by a distribution of points over the unit sphere.

Let $f(\theta,t)\,d\Omega$ be the number of points in a solid angle $d\Omega$ at time t. If J_θ is the net number of points that pass across unit length of the parallel θ = constant in unit time in the direction of positive θ, then it is assumed that

$$J_\theta = -C\frac{\partial f}{\partial \theta} + f\langle v_\theta\rangle_\omega$$

The first term is due to a diffusion process resulting from thermal agitation which tends to produce uniform distribution, and is assumed to obey the usual type of diffusion law where C is a constant. The second term is due to the effect of the field F which gives the molecules a mean angular velocity proportional to the orientating couple

$$\langle v_\theta\rangle_\omega = -\frac{1}{\zeta}\frac{\partial u}{\partial \theta}$$

where ζ is a constant measuring the inner friction, and the couple

$$\frac{\partial u}{\partial \theta} = \mu F \sin\theta$$

u being the potential energy. Hence

$$T_\theta = -C\frac{\partial f}{\partial \theta} - \frac{f}{\zeta}\frac{\partial u}{\partial \theta}$$

When the molecules are in thermal equilibrium $T_\theta = 0$.

This gives $f = A e^{-u/C\zeta}$

According to Boltzmann's law, this means that

$$C\zeta = kT$$

In unit time the net number of points entering the strip between the parallels θ and $\theta + d\theta$ is

$$-d\theta \frac{\partial}{\partial \theta}(2\pi \sin\theta\, T_\theta)$$

This must equal the rate of increase of $f\, d\Omega$ where

$$d\Omega = 2\pi \sin\theta\, d\theta$$

hence

$$\frac{\partial f}{\partial t} = \frac{1}{\zeta \sin\theta}\frac{\partial}{\partial \theta}\left[kT\sin\theta\frac{\partial f}{\partial \theta} + \mu F \sin^2\theta\, f\right] \qquad (12)$$

Debye now considered this equation after the removal of the field at $t = 0$. With no field the torque is zero, hence

$$\zeta\frac{\partial f}{\partial t} = \frac{kT}{\sin\theta}\frac{\partial}{\partial \theta}\left(\sin\theta\frac{\partial f}{\partial \theta}\right)$$

An exact solution of this is

$$f = A\left[1 + \frac{\mu F}{kT} e^{-\frac{2kT}{\zeta}t}\cos\theta\right]$$

The variable part of the distribution function falls

to $\frac{1}{e}$ of its initial value after a time of $\zeta/2kT$ seconds. This means that the relaxation time is

$$\tau = \frac{\zeta}{2kT}$$

Equation (12) can thus be written as

$$2\tau \frac{\partial f}{\partial t} = \frac{1}{\sin\theta} \frac{\partial}{\partial \theta} \left[\sin\theta \frac{\partial f}{\partial \theta} + \frac{\mu F}{kT} \sin^2\theta f \right] \qquad (13)$$

If the field is of the form

$$F = F_0 e^{j\omega t}$$

a solution to equation (13) is

$$f = A \left[1 + \frac{1}{1+j\omega\tau} \frac{\mu F}{kT} \cos\theta \right]$$

provided $\mu F \ll kT$, so that orders of $\mu F/kT$ higher than the first can be ignored. This gives the mean moment of the molecules

$$\overline{m_0} = \mu \frac{\int f \cos\theta \, d\Omega}{\int f \, d\Omega} = \frac{1}{1+j\omega\tau} \frac{\mu^2}{3kT} F$$

The polarizability at these frequencies is now given by

$$\alpha = \alpha_0 + \frac{1}{1+j\omega\tau} \frac{\mu^2}{3kT}$$

Using the same form of internal field as he used at zero frequency, except that ϵ is now the complex permittivity corresponding to the frequency ω, Debye obtains the equation

$$\frac{\epsilon - \epsilon_\infty}{\epsilon_s - \epsilon_\infty} = \frac{1}{1 + j\omega \left(\frac{\epsilon_s + 2}{\epsilon_\infty + 2} \right) \tau} \qquad (14)$$

The relaxation time in this case refers to the individual molecules and is the microscopic relaxation time. Comparing (14) with (10) it will be seen that

$$\tau_m = \frac{\epsilon_s + 2}{\epsilon_\infty + 2} \tau$$

According to this the ratio of τ_m to τ can be very large, e.g. for water $\tau_m/\tau = 20$.

Cole[9] used Onsager's equation (7) for the alternating field case, substituting $\mu^2/(1+j\omega\tau)$ instead of μ^2. This gives

$$\frac{(\epsilon - \epsilon_\infty)(2\epsilon + \epsilon_\infty)}{\epsilon} = \frac{(\epsilon_s - \epsilon_\infty)(2\epsilon_s + \epsilon_\infty)}{\epsilon_s} \frac{1}{(1+j\omega\tau)} \qquad (15)$$

Powles[10] pointed out that this equation could not be written in the form of (10) and hence could not correspond to a single relaxation time. Also the points on a plot of ϵ'' against ϵ' always lay outside the curve obtained from (10), whereas experimental points tend to lie inside this curve.

In the Onsager theory, the field inside a spherical cavity is given by

$$\vec{G} = \frac{3\epsilon}{2\epsilon + 1} \vec{E}$$

Substituting (10) in this equation one obtains

$$\frac{\vec{G}}{\vec{E}} = \frac{3\epsilon_\infty}{2\epsilon_\infty+1} + \left[\frac{3\epsilon_s}{2\epsilon_s+1} - \frac{3\epsilon_\infty}{2\epsilon_\infty+1}\right]\left[\frac{1}{1+j\omega\tau_m\left(\frac{2\epsilon_s+1}{2\epsilon_\infty+1}\right)}\right]$$

This imposes a single relaxation time on the permittivity. As Onsager's internal field had been so successful in determining the static permittivity, Powles decided to keep a similar field, and assumed

$$\frac{\vec{H}}{\vec{E}} = \frac{3\epsilon_\infty}{2\epsilon_\infty+1} + \left[\frac{3\epsilon_s}{2\epsilon_s+1} - \frac{3\epsilon_\infty}{2\epsilon_\infty+1}\right]\left[\frac{1}{1+j\omega\tau^*}\right]$$

where $\vec{H}$ is the field in the spherical cavity, and τ^* is unknown. This leads to the equation

$$\frac{\epsilon-\epsilon_\infty}{\epsilon_s-\epsilon_\infty} = \frac{2\epsilon_s+\epsilon_\infty}{2\epsilon_s}\,\frac{1+\left(\frac{\epsilon_s-\epsilon_\infty}{2\epsilon_s+\epsilon_\infty}\right)\frac{1}{1+j\omega\tau^*}}{1+j\omega\tau} \qquad (16)$$

This reduces to (10) only if

$$\tau^* = \tau_m = \frac{3\epsilon_s}{2\epsilon_s+\epsilon_\infty}\,\tau$$

The maximum ratio of τ_m/τ is $3/2$, which is likely to be of little significance in relating τ to molecular processes.

Collie, Hasted and Ritson[11] treated Onsager's theory with respect to an alternating field in a different way. The reaction field $\vec{R}$, in the absence of an applied field, is given by

$$\vec{R} = \vec{\mu}\,\frac{2(\epsilon_s-1)}{(2\epsilon_s+1)a^3}$$

where $\vec{\mu} = \mu_o \vec{u} + \alpha_o \vec{R}$

Hence $$\vec{R} = \frac{2(n^2+2)(\epsilon_s-1)}{3(2\epsilon_s+n^2)a^3}\mu_o \vec{u}$$

In an alternating field of frequency ω, with a corresponding permittivity ϵ, the additional field at the cavity is $\vec{E'}$, where, by Onsager's theory

$$\vec{E'} = \vec{E}\frac{3\epsilon}{2\epsilon+1} + \vec{E'}\alpha_o \frac{2(\epsilon-1)}{(2\epsilon+1)a^3}$$

the first term being the cavity field, the second the additional reaction field due to the distortion polarization. The total field

$$\vec{F} = \vec{E'} + \vec{R} = \vec{E}\frac{(n^2+2)\epsilon}{(2\epsilon+n^2)} + \frac{2(n^2+2)(\epsilon_s-1)}{3(2\epsilon_s+n^2)a^3}\mu_o \vec{u}$$

The orientating couple

$$\vec{M} = \vec{F} \times \vec{m} = \vec{F} \times (\mu_o \vec{u} + \alpha_o \vec{F})$$

becomes

$$M = \mu_o E \frac{(n^2+2)\epsilon}{(2\epsilon+n^2)} \sin\theta$$

If Debye's theory as discussed above is now adopted, this couple must be used instead of $\mu F \sin\theta$, giving

$$f = 1 + \frac{\epsilon(n^2+2)\mu_o E}{(2\epsilon+n^2)kT(1+j\omega\tau)}\cos\theta$$

The mean orientation of the permanent moments is thus

$$\overline{\cos\theta} = \frac{\int f \cos\theta \, d\Omega}{\int f \, d\Omega}$$

$$\overline{\cos\theta} = \frac{\epsilon(n^2+2)}{(2\epsilon+n^2)}\frac{\mu_o}{3kT}\frac{E}{(1+j\omega\tau)}$$

The component of the total moment along the field is

$$\overline{m_o} = \left[\frac{(n^2-1)\epsilon}{(2\epsilon+n^2)}a^3 + \frac{(2\epsilon_s+1)(n^2+2)^2}{3(2\epsilon_s+n^2)}\frac{\epsilon}{(2\epsilon+n^2)}\frac{1}{(1+j\omega\tau)}\frac{\mu_o^2}{3kT}\right]E$$

Using $\frac{\epsilon-1}{4\pi} = \frac{\vec{P}}{\vec{E}} = \frac{N\vec{m}}{\vec{E}}$, and the fact that $\frac{4\pi N}{3}a^3 = 1$

$$(\epsilon - n^2) = \frac{(n^2+2)^2(2\epsilon_s+1)}{(2\epsilon_s+n^2)}\frac{\epsilon}{(2\epsilon+1)}\frac{\mu_o^2}{3kT}\frac{4\pi N}{3}\frac{1}{(1+j\omega\tau)} \qquad (17)$$

This cannot be written in the form of (10) as it stands, but, for values of $\epsilon >> 1$, Collie, Hasted and Ritson showed that the equation reduces to

$$\frac{\epsilon-\epsilon_o}{\epsilon_s-\epsilon_o} = \frac{1}{1+j\omega\tau}$$

where ϵ_o has the value $n^2-\frac{1}{2}$.

High Frequency Discrepancies

In deriving these equations it is assumed that $\epsilon_\infty = n^2$ where n is the internal refractive index. ϵ_∞ is the value of the permittivity at the high frequency end of the Debye dispersion region. Its value can be found either by drawing the Debye semi-circle through plotted experimental points of ϵ'' against ϵ', or by plotting $\frac{\epsilon''}{\omega\tau}$ against ϵ',

which, according to the Debye equation, gives a linear graph with $\epsilon' = \epsilon_\infty$ when $\frac{\epsilon''}{\omega\tau} = 0$.

For many substances the ϵ''-ϵ' curve can be fitted to a semi-circle, but Cole and Cole found that for some liquids, e.g. methyl alcohol, glycerine, the ϵ'', ϵ' values were better fitted to the arc of a circle with its centre lying below the real axis. This curve can be expressed by the formula

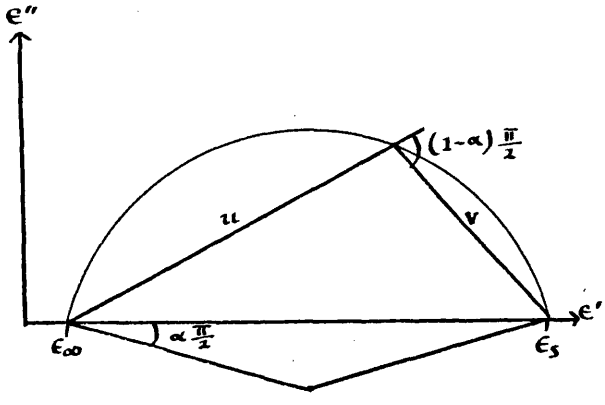

fig.6.

$$\epsilon = \epsilon_\infty + \frac{\epsilon_s - \epsilon_\infty}{1 + (j\omega\tau_0)^{1-\alpha}}$$

This type of behaviour could arise from a spread of relaxation times, the magnitude of α $(0 < \alpha < 1)$ being a measure of this spread. The most probable relaxation time, τ_0, corresponds to a point where ϵ'' has its maximum value, and can be calculated from the relation

$$\frac{V}{u} = (\omega\tau_0)^{1-\alpha}$$

The real and imaginary part of the complex permittivity can be written as

$$\epsilon' - \epsilon_\infty = \frac{1}{2}(\epsilon_s - \epsilon_\infty)\left[1 - \frac{\sinh(1-\alpha)x}{\cosh(1-\alpha)x + \sin\frac{\alpha\pi}{2}}\right]$$

$$\epsilon'' = \frac{\frac{1}{2}(\epsilon_s - \epsilon_\infty)\cos\frac{\alpha\pi}{2}}{\cosh(1-\alpha)x + \sin\frac{\alpha\pi}{2}}$$

where $x = \ln(\omega\tau_0)$.

Whether a semi-circle, or a circular arc is drawn through the experimental points, ϵ_∞ is still the value of ϵ' where the high frequency end of the curve cuts the ϵ'-axis. The higher the frequency at which the complex permittivity can be measured the more accurately can ϵ_∞, in principle, be found, as the extrapolation needed is less.

Poley[12], taking n as the value of the refractive index for the sodium D-line, compared n_D^2 with ϵ_∞ and found, for some liquids, a difference greater than that which could be attributed to experimental error

e.g.	Chlorobenzene	$\epsilon_\infty = 2.56$	$n_D^2 = 2.33$
	Nitrobenzene	4.07	2.43

n_D is not the correct value of n, but Poley showed that where infra-red values of n were available they did not differ appreciably from n_D. Recent infra-red measurements[45] support this assumption.

This difference between ϵ_∞ and n^2 could be due to the

Debye equation not being correct, or could be explained by the presence of at least one other absorption band having a relaxation frequency between that of the dipolar relaxation and the infra-red frequencies. Whichever explains the difference there must come a frequency at which the measured values of ϵ'' and ϵ' diverge from the Debye semi-circle, leading to a curve like that shown in fig.7. In such a case, extrapolation to ϵ_∞ using the high frequency values will lead to a lower value than the true one, due to this divergence.

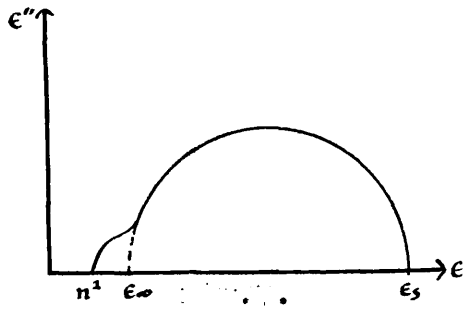

fig.7.

In polar liquids with chain molecules and polar polymers experimental values can show several distinct dispersion regions. In liquids with simpler molecules the evidence is less clear. Water and nitrobenzene show good semi-circles, with no divergence at the wavelengths so far reached, but a large discrepancy between ϵ_∞ and n^2. With the monohalogenated benzenes there is evidence for and against any divergence.

Poley[12] found, from measurements at 0.802cms and longer

wavelengths, a discrepency for chlorobenzene between ϵ_∞ and n^2 greater than that attributed to experimental error. The measurements of Heineken and Bruin[13] supported this, their values of the complex permittivity between 7.5mm and 3.0mm lying off the Debye curve. In contrast to this, Smyth[14-17] working with various people at 4.35mm and 2.19mm finds that the values he obtains fit a Cole-Cole plot with a small value of α, giving a value of $\epsilon_\infty = n^2$ within their experimental error. He has not included Poley's measurements when finding the Cole-Cole plot. Concurrent with the last measurements of Smyth, Chantry and Gebbie[18] have measured the absorption of chlorobenzene from 400cm^{-1} to 10cm^{-1} wavelength and found a broad but strong absorption band centred at 45cm^{-1}. These measurements also comfirm a single measurement[19] taken at a wavelength of 0.337mm, which lies off the Debye curve. Later measurements[20,21] also confirm this absorption band. More measurements are needed in the millimeter wavelength region and at shorter wavelengths to be able to discriminate between the two opinions.

The separate dispersion regions in the liquids with chain molecules or polymers can be explained by intra-

molecular rotation, i.e. apart from the molecules rotating as a complete entity, sections of the molecule can rotate independently giving rise to their own dispersion regions which can be described either by a Debye semi-circle or a Cole-Cole arc. Simple molecules with no intra-molecular rotation can, theoretically, have more than one dispersion region if the molecule is ellipsoidal. Then rotations about different axes will give rise to different relaxation times.

In Debye's equation these dispersion regions can be represented by replacing

$$\frac{\mu_o^2}{1+j\omega\tau} \qquad \text{by} \qquad \sum_{n=1} \frac{\mu_n^2}{1+j\omega\tau_n}$$

where n is the number of degrees of rotational freedom. If Debye's microscopic theory is adopted, this gives

$$\epsilon - \epsilon_\infty = \sum_n \frac{\epsilon_{sn} - \epsilon_{\infty n}}{1+\left(\frac{\epsilon_{sn}+2}{\epsilon_{\infty n}+2}\right) j\omega\tau_n} \qquad (18) \text{ cf.}(14)$$

where ϵ_{sn} and $\epsilon_{\infty n}$ are the static and infinite frequency values of the permittivity corresponding to the relaxation time τ_n only. For any value of n

$$\epsilon_{sn} = \epsilon_{\infty n-1}$$

The factor $\frac{\epsilon_{sn}+2}{\epsilon_{\infty n}+2}$, which can have very large values, is

peculiar to the Debye theory and is almost certainly incorrect.

Powles[10] extended his theory to cover the case of multiple relaxation times, and obtained a similar formula.

$$\epsilon - \epsilon_\infty = \sum_n \frac{\epsilon_{sn} - \epsilon_{\infty n}}{1 + \left(\frac{3\epsilon_{sn}}{2\epsilon_{sn} + \epsilon_{\infty n}}\right) j\omega\tau_n}$$

For polar liquids that have rigid molecules allowing no intra-molecular rotation, and have the same relaxation time about different axes of rotation, but still show a discrepancy between ϵ_∞ and n^2, there must be another explanation.

It could be that, although the Debye equation holds for values of $\epsilon' \gg 1$, it is no longer correct as $\epsilon' \to \epsilon_\infty$. Investigating the Collie, Hasted and Ritson[11] equation (17) by plotting $\epsilon''/\omega\tau$ against ϵ' (shown in graph 1a), it was found that, although it approximated to a straight line at high values of ϵ', as $\epsilon' \to \epsilon_\infty$ the values of ϵ'' became lower than those predicted from equation (10) for the same value of ϵ', hence ϵ_∞ was higher than the intercept of the straight line.

At these high frequencies another effect that the Debye theory does not take into consideration is that of the moment of inertia of the molecule. Debye derived his equation on the assumption that the terminal velocity of the molecule due to the couple

$$\frac{\partial\theta}{\partial t} = \frac{M}{\zeta}$$

is aquired instantaneously. If the frequency is such that the time taken to reach this velocity due to inertial effects, is an appreciable portion of the period, the apparent value of $\frac{\partial\theta}{\partial t}$ will be less and the loss in the liquid will decrease more quickly than the Debye equation predicts.

Powles[22] modified the Debye theory to take inertia into account. According to the Debye theory the equation of motion for the molecule is $\zeta \frac{\partial\theta}{\partial t}$

If inertial effects are included the equation becomes

$$M = \zeta \frac{\partial\theta}{\partial t} + I \frac{\partial^2\theta}{\partial t^2}$$

where M is the couple due to the field. As in Debye's theory $M = \mu F \sin\theta$ with $\mu F \ll kT$

giving an approximate solution as

$$\frac{\partial\theta}{\partial t} = \frac{M}{\zeta} \frac{1}{1 + j\omega\frac{I}{\zeta}}$$

Following the treatment as on page 21,

$C\zeta = kT$ is replaced by $C\zeta = \dfrac{kT}{1 + j\omega \frac{I}{\zeta}}$

Powles introduces an uncertainty factor $0 \leq \alpha \leq 1$ into the value of C, and uses

$$C = \frac{kT}{\zeta} \frac{1}{1 + j\omega\alpha \frac{I}{\zeta}}$$

This implies that the Brownian distribution of the molecules depends on their moments of inertia. If $\alpha = 0$, C becomes independent of I, and the moment of inertia only affects the motion due to the field. With $\alpha = 0$ Powles' equations become the same as that of Constant, Leroy and Raczy.[23] They used a correlation function $G(t)$ where

$$\frac{\epsilon - \epsilon_\infty}{\epsilon_s - \epsilon_\infty} = \int_0^\infty e^{-j\omega t} \dot{G}(t)\, dt$$

For the Debye equation $G(t) = e^{-t/\tau}$

With inertia included $G(t) = e^{-t/\tau_1} e^{-\tau_2/\tau_1} e^{\left(-\frac{\tau_2}{\tau_1} e^{-t/\tau_2}\right)}$

where τ_1 is the dipole relaxation time, and

$$\tau_2 = \frac{I}{\zeta} = \frac{I}{2kT\tau_1}$$

When $\tau_2 \ll \tau_1$ this gives

$$\frac{\epsilon - \epsilon_\infty}{\epsilon_s - \epsilon_\infty} = \frac{1}{(1 + j\omega\tau_1)} \frac{1}{(1 + j\omega\tau_2)} \qquad (19)$$

With typical values of $I \sim 900 \times 10^{-40}$ g-cm^2 and $\tau_1 \sim 10^{-11}$ sec, $\tau_2 \sim 10^{-13}$ sec, so the assumption that $\tau_2 \ll \tau_1$ is valid. Plotting values of $\epsilon''/\omega\tau_1$ against ϵ' for $\tau_1/\tau_2 = 10$ and 100 (graph 1b) shows that the apparent value of ϵ_∞ obtained by extrapolation from lower frequencies is lower than that obtained when $\tau_2 = 0$. Both these tend to show that the discrepancy between ϵ_∞ and n^2 is larger than that obtained from the extrapolated value, and not less.

In these liquids with rigid molecules there must be another mechanism causing a second absorption region. There is evidence to support the idea that it can be caused by the rotational oscillations of a molecule in a quasi-crystalline structure.

Investigating the monohalogenated benzenes, Poley[12] found that $\epsilon_\infty - n^2$ was proportional to μ^2, suggesting another polar dispersion region. He suggested that it might be caused by the vibration of the molecule about a temporary equilibrium position.

Chantry and Gebbie[18] compared the absorption of liquid chlorobenzene with that of the solid, and found that the

solid showed two sharp absorption features, characteristic of a lattice spectrum, in the same frequency range as the broad band in the liquid. Chanal, Decamps, Hadni and Wendling[21] compared liquid and solid states of several polar molecules, and found that they all possessed absorption maxima in the solid state.

Although molecules of non-polar liquids have no permanent dipole moment, it has been found[24-27] that they also show small dielectric losses in the millimetre and sub-millimetre region. For example, Garg, Kilp and Smyth[26] working at 2.11mm found

	ϵ'	ϵ''
benzene	2.2840	0.0073
carbon tetrachloride	2.2363	0.0056
toluene	2.2766	0.0307

Chantry et al[27] showed that these absorptions were at the low frequency end of a dispersion region centred in the far infra-red. Measuring the absorption of the liquid and solid states of carbon tetrachloride, carbon disulphide and benzene, over the range 20cm^{-1} to 120cm^{-1}, they found that the liquid absorption peak, in all cases, corresponded with the solid absorption peak. The absorption peaks of the non-polar molecules occur in the same frequency range

as those of the polar molecules, but the total absorption is smaller by a factor of the order 10.

e.g. chlorobenzene $\alpha_{max} \simeq 17$ nepers/cm at $40cm^{-1}$

benzene 5 nepers/cm at $70cm^{-1}$

These results point to a dispersion region present in both polar and non-polar liquids due to a similar type of mechanism.

Hill[28] considered the combination of oscillations of a molecule about an instantaneous equilibrium position with the Debye relaxation process, and obtained a value for the high frequency limit of the Debye dispersion region given by

$$\frac{\epsilon_\infty - n^2}{\epsilon_s - n^2} = \frac{2kT}{I\omega_o^2}$$

where I is the moment of inertia of the molecule, and ω_o is the frequency of the oscillations. Using the values of ϵ_∞, ϵ_s and n^2 obtained by Poley, this gives a value of $\omega_o = 23cm^{-1}$ for chlorobenzene, which is of the same order as the frequency of the absorption band actually found at $45cm^{-1}$.

Lassier and Brot[29] have presented a model for the

angular motion of molecules, taking into account their finite moment of inertia, submitted to thermal collisions in a multi-well potential. The finite moment of inertia means that the time taken for the molecules to jump from one well to another is finite, and also that the molecules oscillate when reaching the new well. They obtain an equation for the absorption of the liquid which not only contains the Debye relaxation, but also an absorption due to the oscillations of the molecules in the potential well, the absorption going to zero at high frequencies. The theoretical curves from this equation agree very well with the experimental shape.

Water shows a large discrepancy between ϵ_∞ and n^2, and possesses an absorption band centred at 140cm^{-1}. This absorption band is absent in weak solutions of water in dioxane, hence it must be due to inter-, and not intra-molecular forces. Stanevich and Yaroslavskii[30] found that this band actually consisted of many weak absorption bands, and they interpreted these as due to a quasi-crystalline structure, using a degenerate cubic lattice. They assumed that each molecule had four hydrogen bonds in one plane and a weaker oxygen-oxygen bond at right angles

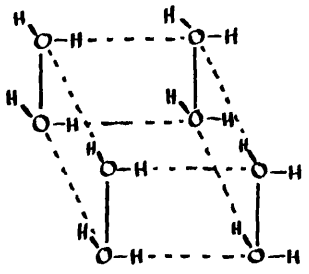

fig.8.

to this plane, as in fig.8. Calculating the modes of vibrations of this sort of lattice they found that the theoretical results were grouped about the experimental values. There is no evidence as to whether methyl and ethyl alcohols also display this type of absorption band, though they show the discrepancy between ϵ_∞ and n^2.

There definitely seems to be a dispersion region present in both polar and non-polar liquids which can be explained as due to rotational oscillations in a quasi-crystalline structure. More measurements, at a range of temperatures, at frequencies into the infra-red region are needed before full investigations can be carried out.

Survey of the Methods used to Measure the Complex Permittivity at Millimetre Wavelengths

To measure the complex permittivity of a liquid it is necessary to investigate the reflection and absorption (or transmission) of an electro-magnetic wave by a thickness of the liquid. At wavelengths greater than 10cms. coaxial transmission lines are used to carry the waves, while waveguides are used for shorter wavelengths. Below wavelengths of 3cms. the wavelength is becoming short enough that the wave can be launched into space before reaching the liquid without incurring too much error by diffraction. Hence measurements at millimetre wavelengths can be divided into two catagories, free space methods and those using guided waves.

Free Space Methods

If the electro-magnetic wave has its electric vector perpendicular to the plane of incidence, the complex reflection coefficient **R** off the surface of the liquid when terminated by a short circuit at a depth d is given by[31]

$$\frac{1+R}{1-R} = \frac{j\beta_o}{\alpha+j\beta}\,\frac{\cos i}{\cos r}\,\tanh\{(\alpha+j\beta)d\cos r\} \qquad (20)$$

where i is the angle of incidence, r the angle of refraction, $j\beta_o = j\frac{2\pi}{\lambda_o}$ is the propagation constant in free space, λ_o being the wavelength in free space, and $\alpha + j\beta$ is the propagation constant in the liquid, α being the attenuation constant and $\lambda_l = \frac{2\pi}{\beta}$ being the wavelength in the liquid. The complex permittivity is given by

$$\epsilon' - j\epsilon'' = \left(\frac{\alpha + j\beta}{j\beta_o}\right)^2 = \frac{\beta^2 - \alpha^2}{\beta_o^2} - j\frac{2\alpha\beta}{\beta_o^2} \qquad (21)$$

Experimentally the complex permittivity can either be found by measuring α and β directly, or by measuring the reflection coefficient at known depths of liquid.

Mungall and Hart[32], working at 9mm, found α by measuring the transmission of different thicknesses of the liquid, Then, using a gonimeter, they measured the reflectance at normal incidence of an infinite depth of liquid by measuring the reflectance over angles close to the normal and then extrapolating to zero. The two equations for α and the reflected power $|r_o|^2$ in terms of ϵ' and ϵ'' enable these latter to be calculated.

Saxton et al[33], at 9.0, 4.3, and 3.1mm, measured

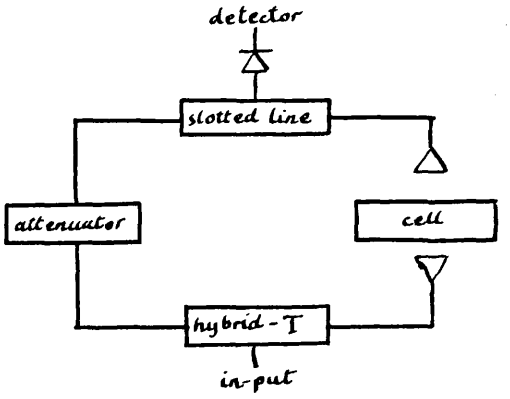

fig.9.

both α and β directly. A diagrammatic representation of their apparatus is shown in fig.9. With the polystyrene container empty a reference position was found in the slotted line, then the phase shift was measured for different thicknesses of the liquid, giving λ_ℓ. To find α, the reference arm was removed, and the attenuation of different depths of the liquid found by using a power ratio meter.

Then $$\epsilon' - j\epsilon'' = \frac{\beta^2 - \alpha^2}{\beta_0^2} - j\,\frac{2\alpha\beta}{\beta_0^2}$$

Rampolla, Miller and Smyth[14] measured the reflection off the surface of the liquid using an arrangement as in fig.10

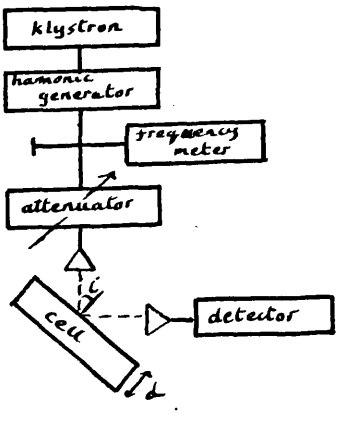

fig.10

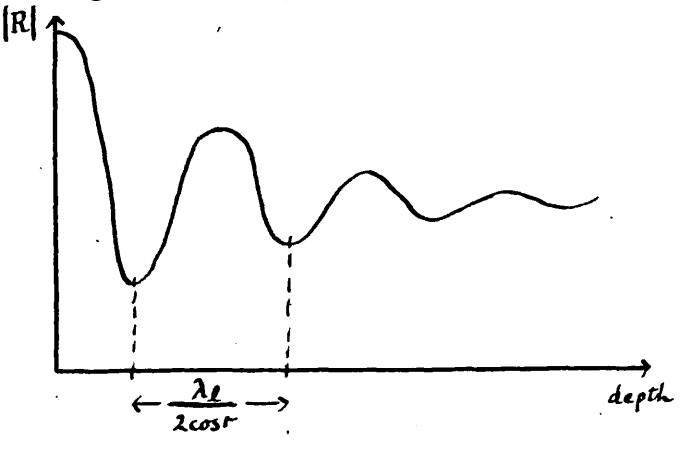

fig.11

If $|R|$ from equation (20) is plotted against depth, a curve as shown in fig.11 is obtained. The distance between successive minima is $\frac{\lambda_\ell}{2\cos r}$, and $\alpha \cos r$ can be found from the values of adjacent maxima.

If $\beta' = \frac{2\pi}{\lambda_\ell} \cos r$ and $\alpha' = \alpha \cos r$

then $$\epsilon = \frac{\beta'^2 - \alpha'^2}{\beta_o^2} - j\frac{2\alpha'\beta'}{\beta_o^2} + \sin^2 i$$

The value of the angle of incidence was found by using a lossless dielectric whose permittivity was known. To overcome inaccuracies due to evaporation, measurements were taken with the depth decreasing and then with the depth increasing, and the results were averaged. Horn-horn interaction was minimized by taking readings of the signal with the receiving horn at $0, \frac{\lambda_\ell}{4}, \frac{\lambda_\ell}{2}$, and $\frac{3\lambda_o}{4}$ from the surface of the liquid and averaging these results.

Smyth, Vaughan et al[15,16] have used this method working at 4.3, 3.1 and 2.2mm. Pine, Zoellner and Rohrbaugh[34] used the same principle, using a magnetron as oscillator, and a grating to separate the different wavelengths, obtaining 4.2, 3.2, 2.5 and 1.8mm.

Gerschel and Brot[35], at 2mm, used an interferometric

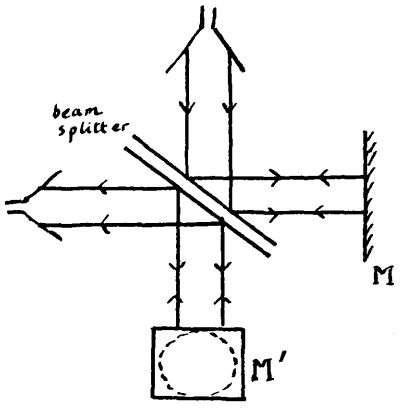

fig.12

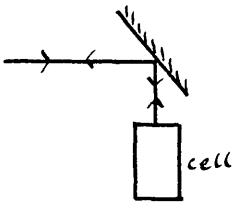

side view of M'

method, fig.12. The beam splitter was an air gap of adjustable thickness between two teflon prisms, so made that the wave was incident on their faces at the Brewster angle. The depth of dielectric in the cell was measured from the window to the terminating short circuit. With zero depth of dielectric, the apparatus was adjusted to give destructive interference. Then, with a depth d of dielectric in the cell, the voltage standing wave ratio (V.S.W.R.) ρ was measured, and also the distance that the mirror has to move to bring the minimum back to the initial zero position. This gives the reflection coefficient $|R|e^{j\varphi} = \frac{\rho-1}{\rho+1} e^{j\varphi}$ at the depth d. To calculate ϵ' and ϵ'' from this the method of Roberts and von Hippel[36] was used.

From the equation at normal incidence

$$\frac{1+|r|e^{j\varphi}}{1-|r|e^{j\varphi}} = \frac{j\beta_o}{\alpha+j\beta}\tanh(\alpha+j\beta)d$$

Roberts and von Hippel obtain the equation

$$\frac{\tanh(\alpha+j\beta)d}{(\alpha+j\beta)d} = \frac{-j\lambda_o}{2\pi d}\,\frac{\frac{1}{\rho}-j\tan\frac{\varphi}{2}}{1-j\frac{1}{\rho}\tan\frac{\varphi}{2}} = Ce^{j\xi} \qquad (22)$$

If $$(\alpha+j\beta)d = Te^{j\tau}$$

then $$\frac{\tanh Te^{j\tau}}{Te^{j\tau}} = Ce^{j\xi}$$

Knowing d, ρ, and φ, $Ce^{j\xi}$ can be calculated. The corresponding values of T and τ can be found from charts provided by Roberts and von Hippel. These charts are multivalued, but taking measurements at two different depths will eliminate any ambiguity.

Papoular[37] used a similar method at 2mm and 4mm.

Guided Waves

In a waveguide the propagation constant in air is $j\beta_g = j\frac{2\pi}{\lambda_g}$ where λ_g, the wavelength in the waveguide, is related to the free space wavelength λ_o by

$$\frac{1}{\lambda_g^2} = \frac{1}{\lambda_o^2} - \frac{1}{\lambda_c^2}$$

where λ_c is the cutoff wavelength of the guide. The propagation constant in the liquid contained within the waveguide is $\alpha + j\beta = j\frac{2\pi}{\lambda_o}\sqrt{\epsilon - \left(\frac{\lambda_o}{\lambda_c}\right)^2}$

Hence $$\frac{\alpha + j\beta}{j\beta_g} = \sqrt{\frac{\epsilon - \left(\frac{\lambda_o}{\lambda_c}\right)^2}{1 - \left(\frac{\lambda_o}{\lambda_c}\right)^2}}$$

Leading to $$\epsilon' = \frac{1 + \left(\frac{\lambda_c}{\lambda_g}\right)^2 (b^2 - a^2)}{1 + \left(\frac{\lambda_c}{\lambda_g}\right)^2} \qquad (23a)$$

$$\epsilon'' = \frac{2ab\left(\frac{\lambda_c}{\lambda_g}\right)^2}{1 + \left(\frac{\lambda_c}{\lambda_g}\right)^2} \qquad (23b)$$

where $b = \beta/\beta_g$ and $a = \alpha/\beta_g$.

The wave strikes the surface of the liquid normally, and hence the reflection coefficient r is given by

$$\frac{1 + r}{1 - r} = \frac{j\beta_g}{\alpha + j\beta} \tanh(\alpha + j\beta)d \qquad (24)$$

Lane and Saxton[38], working down to 6.2mm, found the absorption coefficient $k = \frac{\lambda_o \alpha}{2\pi}$ of the liquid measured at a free space wavelength λ_o in two waveguides having cutoff frequencies λ_{c_1} and λ_{c_2}.

Then

$$\epsilon' = \frac{\left(\frac{\lambda_0}{\lambda c_1}\right)^2 k_1^2 - \left(\frac{\lambda_0}{\lambda c_2}\right)^2 k_2^2}{k_1^2 - k_2^2} - \left(k_1^2 + k_2^2\right)$$

$$\epsilon'' = 2 k_1 \left[\epsilon' + k_1^2 - \left(\frac{\lambda_0}{\lambda c_1}\right)^2\right]^{1/2}$$

Poley,[12] working down to 0.802cms, measured the value of the V.S.W.R.

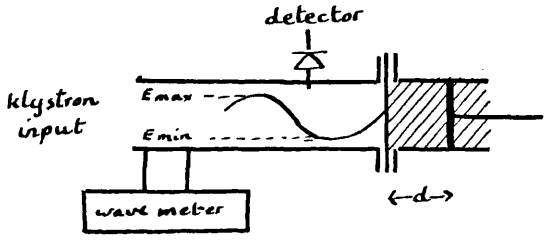

fig.13

$$\rho = \frac{|E|_{max}}{|E|_{min}} = \frac{1+|\tau|}{1-|\tau|}$$

as a function of the depth of liquid d, terminated by a short circuit (fig.13). A typical graph of ρ against depth is shown in fig.14. The distance between successive minima equals $\frac{\lambda_\ell}{2}$. Using the fact that ρ changes slowly at the maxima which occur at values

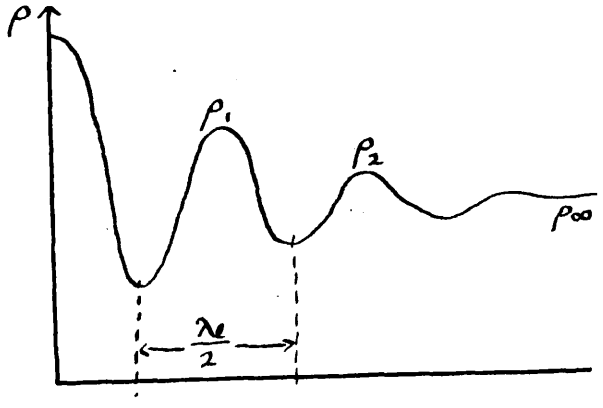

fig.14

of $d \simeq \frac{n\lambda_\ell}{2}$, Poley obtained

$$\frac{\rho_m}{\rho_n} = \frac{\tanh\left(n\pi\frac{\alpha}{\beta}\right)}{\tanh\left(m\pi\frac{\alpha}{\beta}\right)}\left(1-c\right)$$

where ρ_n is the value of the V.S.W.R. at the n^{th} maximum, and C is a correction term. Poley showed that, with the liquids that he was using $C \ll 1$, generally being less than 1%, and hence could be neglected. A correction was made for the loss at the junction of the measuring cell with the rest of the waveguide, using

$$\frac{1}{\rho} = \frac{1}{\rho_{measured}} - \frac{1}{\rho_{junction}}$$

Using this corrected value for ρ, a higher consistency in the values of α/β was obtained.

Heinenken and Bruin[13] used a similar method down to 3mm. By moving a short circuit (see fig.15) either backwards or forwards in the liquid filled guide, successive maxima and minima were displayed on the oscilloscope. β was found from the liquid depth between successive minima, and α from the ratio of the power in successive maxima.

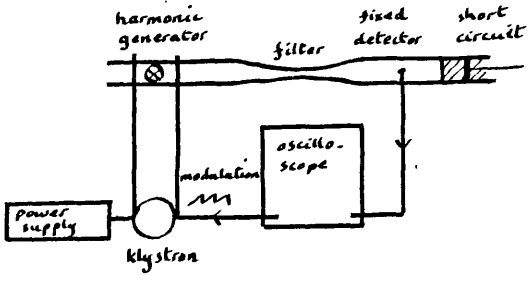

fig.15

Grant, at 8mm, found β as above, but measured α

directly by measuring the change in attenuation due to a change in liquid depth.

Mallikarjun and Hill[40], at 8.4mms, used a bridge arrangement as in fig.16. The two arms of the bridge were made as near equal in length as possible. When the total phase change and attenuation of the wave was the same in both arms there was zero signal at the detector. With a short circuit at the position of zero depth of liquid in the cell, the balance arm was adjusted to give zero signal, thus providing reference values. The cell was filled with liquid and terminated by a match, and the bridge balanced again. The change in short circuit position gave the phase change φ, and the change in attenuation the amplitude $|r|$ of the wave reflected from the surface of the liquid. Terminating the liquid by a match corresponds to using an infinite depth of liquid.

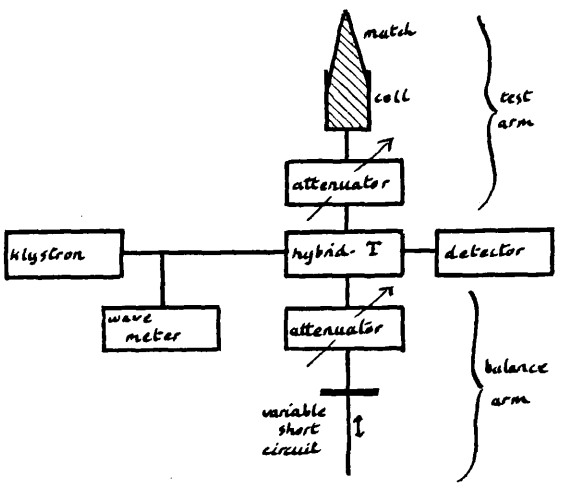

fig.16

At infinite depth

$$\frac{1 + |\Gamma| e^{j\varphi}}{1 - |\Gamma| e^{j\varphi}} = \frac{j\beta_g}{\alpha + j\beta}$$

Coupling this with $|\Gamma| = \frac{\rho - 1}{\rho + 1}$ one obtains

$$b = \frac{\rho\left(1 + \tan^2 \frac{\varphi}{2}\right)}{1 + \rho^2 \tan^2 \frac{\varphi}{2}}$$

$$a = \frac{(\rho^2 - 1) \tan \frac{\varphi}{2}}{1 + \rho^2 \tan^2 \frac{\varphi}{2}}$$

from which a and b can be found, and hence ϵ' and ϵ''. A correction was applied for the reflection from the mica window.

Roberts and von Hippel's method[36] can also be used with guided waves. With a depth of dielectric d, terminated by a short circuit; the V.S.W.R. ρ, and the distance x_o of the first minimum from the mica window is measured. In a waveguide

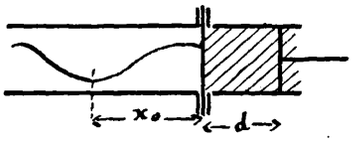

fig.17.

$$\frac{1 + |\Gamma| e^{j\varphi}}{1 - |\Gamma| e^{j\varphi}} = \frac{j\beta_g}{\alpha + j\beta} \tanh (\alpha + j\beta) d$$

where $\varphi = \frac{4\pi x_o}{\lambda_g}$. Giving

$$\frac{\tanh T e^{j\tau}}{T e^{j\tau}} = \frac{\tanh (\alpha + j\beta) d}{(\alpha + j\beta) d} = \frac{-j\lambda_g}{2\pi d} \frac{\frac{1}{\rho} - j \tan \frac{2\pi x_o}{\lambda_g}}{1 - j \frac{1}{\rho} \tan \frac{2\pi x_o}{\lambda_g}} = C e^{j\beta}$$

The corresponding values of ϵ' and ϵ'' can be found as before, by using Roberts' and von Hippel's charts.

Fatuzzo and Mason[4] used this method, but chose depths such that the reflection coefficient was real. With the short circuit up to the mica window the position of the first minimum of the standing wave was found. The depth of liquid in front of the short circuit was then increased until a minimum was again found at that position. The V.S.W.R. was measured at this depth. For this condition the equation simpifies to

$$\frac{\tanh\,(\alpha+j\beta)d}{(\alpha+j\beta)d} = \frac{-j\lambda_g}{2\pi d}\frac{1}{\rho}$$

This condition corresponds to $\xi = 90°$ and T and τ, and hence ϵ' and ϵ'' as before, can readily be found.

Experimental Procedure

8mm Apparatus

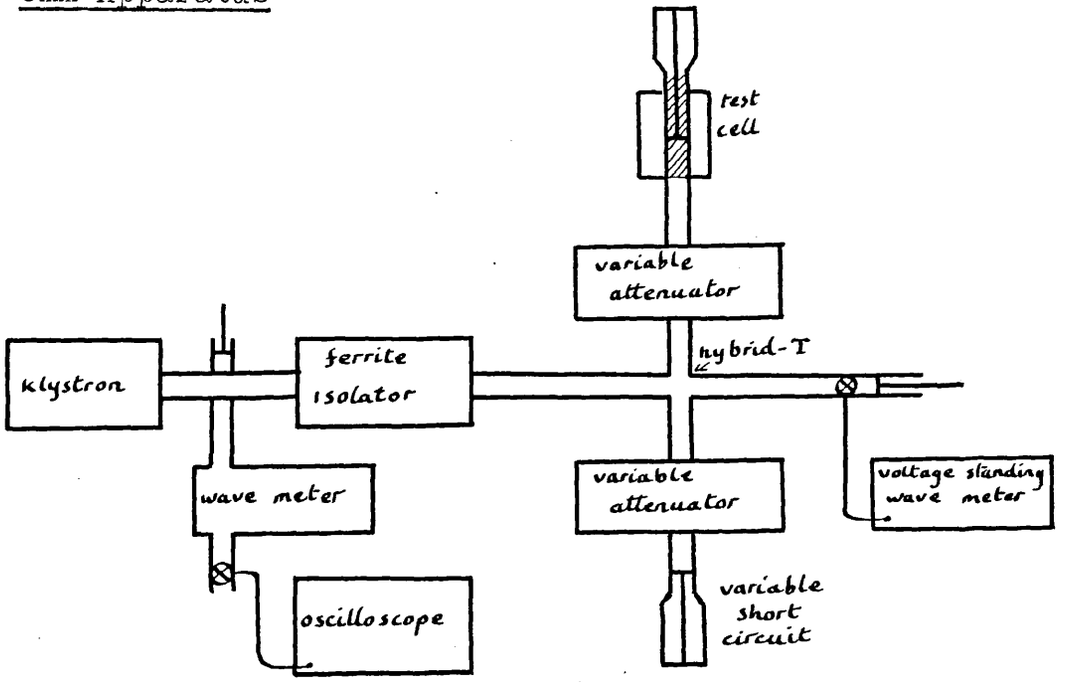

fig.18

In the present experiments a bridge arrangement was used for the 8mm waves. A schematic diagram of the apparatus is shown in fig.18. The complete apparatus was arranged so that the input and detection arms were horizontal with the two side arms in the vertical plane, the test cell being at the end of the top arm.

The output frequency from the fan-cooled klystron

could be changed by altering the klystron cavity itself, and by adjusting the reflector volts and grid volts supplied to the klystron. A small part of the wave from the klystron passed through a wavemeter and the resulting signal was displayed on an oscilloscope. When the wavemeter cavity was tuned to the klystron a pattern was displayed on the oscilloscope. By keeping the form of this pattern constant the frequency could be kept constant to within 3MHz. (0.01%). The ferrite isolator in the input arm prevented any waves reflected back along the arm reaching the klystron and upsetting the frequency.

A hybrid-T divided the beam along the two side arms. These arms were made as near equal in length as possible, and each consisted of a transition section from a rectangular to circular waveguide, a rotary-vane attenuator, and another transition section back to a rectangular guide. The wave was reflected at the end of one arm by the test cell, and at the end of the other arm by a variable short circuit. The two reflected waves recombined at the hybrid-T and the resultant wave was detected by a crystal in the fourth arm of the bridge, the output signal from the crystal being displayed on a voltage standing wave

meter. The property of the hybrid-T is that, if the impedance in both arms is the same, the two waves recombine in antiphase and the resulting signal is zero. Hence, with an unknown terminating impedance, i.e. the test cell, in one arm, zero signal can be obtained by adjusting either of the variable attenuators, and the variable short circuit, until the total impedance in each arm is the same. The advantage of making the two side arms equal in length is that the balance point is equivalent to the condition for white light fringes on a Michelson Interferometer, and hence the balance point becomes insensitive to small changes in frequency.

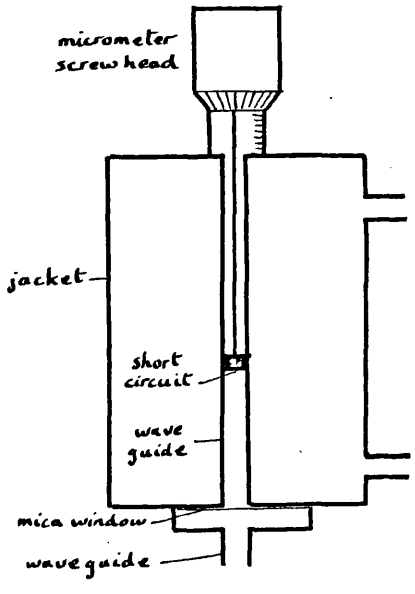

fig.19.

The cell, fig.19, consisted of a length of rectangular waveguide surrounded by a jacket for temperature control. The junction of the cell with the rest of the apparatus was closed by a thin mica window, held in place by the flanges of the guide itself. The liquid under test was

behind the mica and was terminated by a moveable short circuit, which just fitted the bore of the guide, and had two small grooves down one of the long sides to enable the liquid to flow past when the short circuit was moved. The depth of liquid from the mica to the front face of the short circuit was measured by a micrometer screw head attached to the short circuit.

The variable attenuators showed the angle through which the metallized glass vane inside had been rotated, zero angle corresponding to zero attenuation. When the vane is at an angle θ, the amplitude of the wave passing through it is reduced by $\cos^2\theta$, hence the complete attenuation of the reflected wave by the time it reaches the hybrid-T again is $\cos^4\theta$.

The klystron was first tuned to give maximum signal. This was done by removing the hybrid-T and placing the crystal detector on the end of the straight arm from the klystron. The reflector volts, the grid volts, the klystron cavity, and the tuning of the crystal, were all altered in turn until the signal from the crystal decreased which ever one was altered. As the klystron

cavity had been disturbed sometime was left for it to settle down again, and the tuning rechecked. When no change was noted the cavity of the wavemeter was adjusted until this was tuned to the klystron frequency. During all the experiments the wavemeter reading was kept at this setting, and the other variables adjusted to give resonance, so that the same frequency was used each time.

To find the wavelength in the guide the test cell was used empty as a short circuit, and the two attenuators and the variable short circuit adjusted to give zero reading on the voltage standing wave meter. The variable short circuit only was moved until another zero position was obtained. The distance that the short circuit had to move between these two positions was $\frac{\lambda_g}{2}$, λ_g being the guide wavelength. This wavelength could be checked against that obtained from the wavemeter, using the calibration tables to convert the linear reading of the micrometer head of the wavemeter cavity into the free-space wavelength λ_o, λ_o was found by using

$$\frac{1}{\lambda_o^2} = \frac{1}{\lambda_c^2} + \frac{1}{\lambda_g^2}$$

where λ_c is the cut-off wavelength of the guide.

It was found that varying the attenuation in the arms shifted the short circuit balance point. As the attenuator balance and the phase balance positions are independent of each other, though zero signal is obtained only when both are balanced, this meant that one, or both, of the attenuators had a phase change associated with its change in attenuation. Keeping one attenuator constant and checking the short circuit balance for different attenuations in the other, it was found that only one attenuator gave a phase change. This attenuator was kept constant during the experiments, and all the balancing was done with the other.

At the balance point above the two attenuators gave different readings. This could be due to the reflection coefficients of the two short circuits having different values, making at least one of them not a perfect short circuit, or else due to a difference in insertion loss of the two attenuators. When the two short circuits were interchanged the values of the attenuators for balance changed very little, so the difference was due to different insertion losses.

This difference had to be taken into account when measuring an unknown reflection coefficient. With the short circuit of the cell at zero depth the attenuators and the variable short circuit were balanced. Balancing again with the mica window in place these readings altered slightly. The values with the mica in were taken as the reference values, thus incorporating a correction for the reflection off the mica. At the balance point an attenuation corresponding to θ_o was needed in the test arm as against zero in the lower arm, showing that the insertion loss in the lower arm was higher than that in the test arm. This attenuator was kept at a setting of θ_o to prevent unwanted phase changes. Then an attenuation of θ in the lower arm was equivalent to a reflection coefficient of $\cos^4\theta$ in the test arm. Any phase change in the test arm was shown by a change in balance point of the variable short circuit. The phase change was given by $\frac{4\pi x_o}{\lambda_g}$, where x_o was the distance of the balance from the reference position.

4mm Apparatus

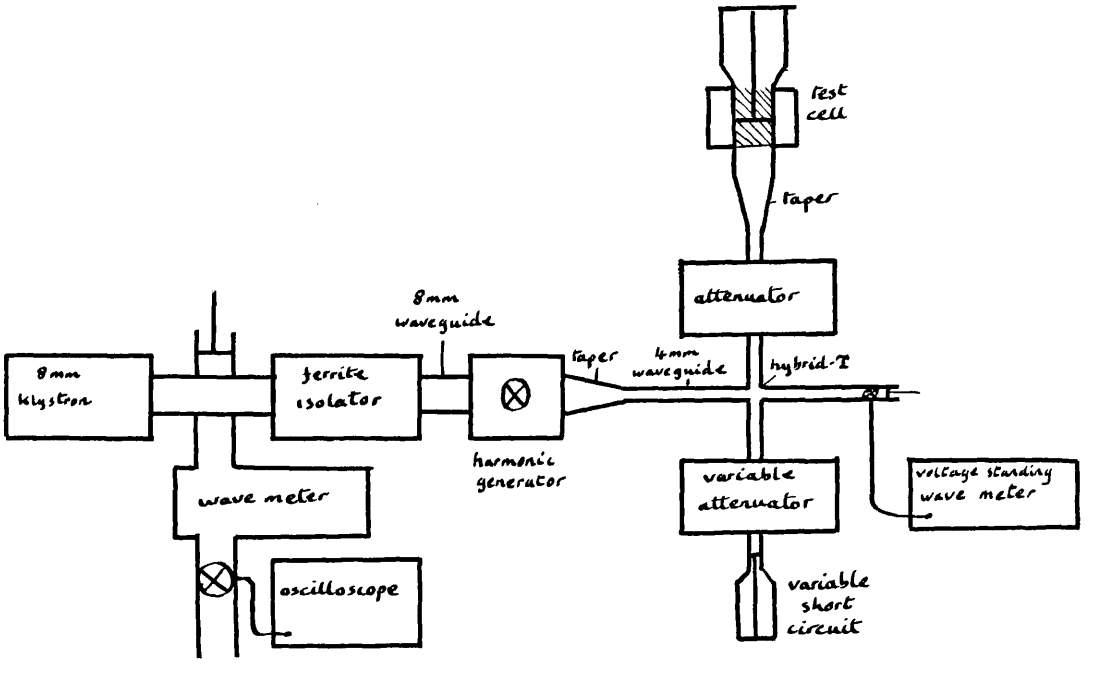

fig.20

The arrangement for the 4mm waves was slightly modified as a harmonic generator was used to obtain the first harmonic from an 8mm wave, and a tapering waveguide filtered off the fundamental. The power reduction for each successive harmonic is of the order of 30dbs, so any 2mm wave present with the resulting 4mm wave was too small an amplitude to be noticed.

The two attenuators were not identical. The one in

the lower arm was accurately calibrated directly in decibels. The other in the test arm was there to compensate for the insertion loss of the lower attenuator, and was not used to make any readings. A taper was used in the test arm back to an 8mm waveguide so that the same liquid cell could be used as in the measurements at 8mm. This was found to be more practicable than making a cell of the 4mm waveguide strong enough to withstand constant use.

The apparatus was tuned in the same way as the 8mm apparatus, and the wavelength in the 4mm guide found as before with the variable short circuit. The wavelength in the 8mm waveguide was found by using the fact that the free-space wavelength is the same, hence

$$\frac{1}{\lambda_o^2} = \frac{1}{\lambda_{c_4}^2} + \frac{1}{\lambda_{g_4}^2} = \frac{1}{\lambda_{c_8}^2} + \frac{1}{\lambda_{g_8}^2}$$

Change of attenuation was found to cause no phase change, but it was noticed that the signal was asymmetric about the short circuit balance point. Reflections off the crystal itself could cause this, but the crystal had been tuned to the frequency used, hence reflections off hybrid-T were likely to be the cause.

Investigations of Reflections from the Hybrid-T

With full attenuation (effectively a match) in the lower arm, and a match in the test arm, no signal above the noise level in the voltage standing wave meter was detectable. Thus the coupling between the input and detection arms was zero, or else very small.

With full attenuation in the lower arm, and a short circuit fixed directly to the hybrid-T in the test arm, the value of the detected signal was noted for various positions of the short circuit. For a perfect hybrid-T the signal should be independent of the short circuit position. The actual signal was found to vary systematically with the short circuit position as in fig.21. With the match and the short circuit interchanged the signal variation was just about identical in both phase and the maximum to minimum ratio to the first curve, comparisons being shown in the following table.

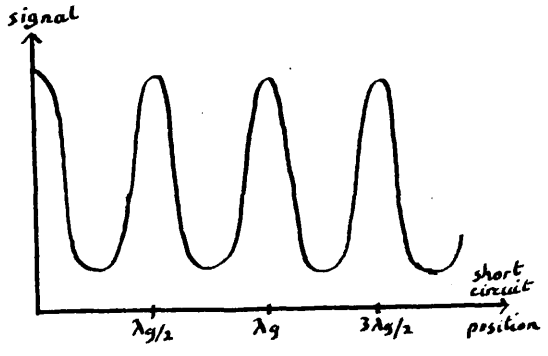

fig.21.

	1st curve	2nd curve
position of first maximum	0.212cm.	0.217cm.
maximum to minimum ratio	4.138	4.144

This shows that the hybrid-T can be considered symmetrical.

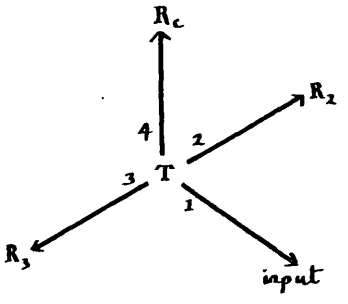

fig.22

Let 1, 2, 3, and 4 be the arms of the hybrid-T; R_2, R_3, and R_c the terminating reflection coefficients of the arms 2, 3 and crystal respectively, including any phase change incurred by the wave travelling from the hybrid-T to the actual termination. Due to the presence of the isolator $R_1 = 0$.

Let s_{22} be the reflection coefficient of the junction of arm 2 etc.

Let s_{12} be the coupling coefficient between arms 1 and 2 etc.

Then, with an input value of electric field E, the electric field E_i $(i = 2,3,4)$ entering the arm i of the hybrid-T is given by

$$E_2 = R_2 s_{22} E_2 + R_3 s_{32} E_3 + s_{12} E + R_c s_{42} E_4$$

$$E_3 = R_3 s_{33} E_3 + R_2 s_{23} E_2 + s_{13} E + R_c s_{43} E_4$$

$$E_4 = R_c s_{44} E_4 + R_2 s_{24} E_2 + R_3 s_{34} E_3 + s_{14} E$$

Assuming symmetry, which is justified by the above measurements

$$S_{12} = S_{21} \quad \text{or} \quad S_{ij} = S_{ji}$$

$$S_{13} = -S_{12}$$

$$S_{24} = S_{34}$$

$$S_{22} = S_{33}$$

Since there is no coupling between input and output arms, $S_{14} = 0$

Since the crystal is tuned independently of the hybrid-T, $R_c = 0$.

This gives

$$E_2 = R_2 S_{22} E_2 + R_3 S_{23} E_3 + S_{21} E$$

$$E_3 = R_3 S_{33} E_3 + R_2 S_{23} E_2 - S_{21} E$$

$$E_4 = R_2 S_{24} E_2 + R_3 S_{24} E_3$$

One of the side arms (say 2) is matched, so $R_2 = 0$. Then

$$E_4 = \frac{S_{24} S_{21} R_3 E}{R_3 S_{33} - 1}$$

S_{24}, S_{21}, S_{33} and R_3 are all complex, hence let

$$S_{24} = \mathcal{S}_{24} e^{j\theta_{24}} \qquad \text{etc.}$$

where $\mathcal{S}_{24}$ and θ_{24} are real.

R_3 is a short circuit at a distance x from the hybrid-T. As there may be attenuation due to the walls of the guide, R_3 can be given by

$$R_3 = -1\, e^{-(\alpha - j\beta)x}$$

The output signal

$$|E_4|^2 = |E|^2 \frac{s_{24}^2 s_{21}^2 e^{-2\alpha x}}{1 + s_{33}^2 e^{-2\alpha x} + 2\cos(\theta_{33} + \beta x) s_{33} e^{-\alpha x}}$$

This gives maximum and minimum values at $(\theta_{33} + \beta x) = 2n\pi$ and $(\theta_{33} + \beta x) = (2n+1)\pi$ respectively, where

$$\frac{|E_{4\,max}|^2}{|E_{4\,min}|^2} = \frac{\left[1 + s_{33} e^{-\alpha x}\right]^2}{\left[1 - s_{33} e^{-\alpha(x + \lambda/4)}\right]^2} \qquad (25)$$

Using this, α was found to be 0.081/cm, and $s_{33} = 0.347$. Using a value of $s_{33} = 0.4$, a theoretical curve was plotted of $|E_4'|^2$ against phase (the equivalent of short circuit position). The shape of this corresponded with that of the experimental curve, so it could be assumed that the reflection s_{33} was the main cause of the variation in signal.

In a measurement with the cell $R_2 \neq 0$.

Then

$$E_4 = E \frac{s_{24} s_{21} (R_3 - R_2)}{(1 - R_2 s_{22})(1 - R_3 s_{33})}$$

If

$$R_2 = r_2 e^{j\varphi_2}$$

$$R_3 = r_3 e^{j\varphi_3}$$

$$s_{22} = s_{33} = s e^{j\theta}$$

Then

$$E_4 = \frac{E\, s_{24} s_{21} \left(r_3 e^{j\varphi_3} - r_2 e^{j\varphi_2}\right)}{\left[1 - s r_2 e^{j(\varphi_2 + \theta)}\right]\left[1 - s r_3 e^{j(\varphi_3 + \theta)}\right]} \qquad (26)$$

The condition for balance is $E_4 = 0$. From equation (26) this condition is fulfilled if

$$r_2 e^{j\varphi_2} = r_3 e^{j\varphi_3}$$

or $r_2 = r_3$ and $\varphi_2 = \varphi_3$

This means that the correct balance point is obtained even though the hybrid-T is mismatched, provided that the hybrid-T is symmetrical.

Practically, this was not quite true, as a slight variation in both reflection coefficient and phase change was observed when a piece of resistive card was attached to the cell short circuit, and the bridge balanced for different positions of the cell short circuit. Both these values varied with a periodicity of $\frac{\lambda_g}{2}$. The effect of this is discussed on page 83.

Due to lack of power, the zero balance positions were not sharp, making it difficult to obtain the short circuit and attenuation readings at balance accurately. To increase this accuracy the short circuit was adjusted to as near balance as possible, then the value of the attenuation was taken for the same small signal value either side of the zero position. This was repeated

for the short circuit with the attenuation at the balance position. Just around the zero position the signal variation is symmetrical, although the signal variation as a whole was asymmetric. Thus the balance positions were given by the average of the two short circuit readings, and of the two actual attenuations, which equal antilog (-decibel/10).

The reference positions were found as before with the mica window in place and the cell short circuit at zero depth. The variable attenuator gave a small reading at balance, and hence, any subsequent values had to be divided by this value to give the correct attenuation. At any other depth of liquid, the phase change is given by $\frac{4\pi x_0}{\lambda_g}$, and the reflection coefficient is the average attenuation divided by the reference value.

3cm Apparatus

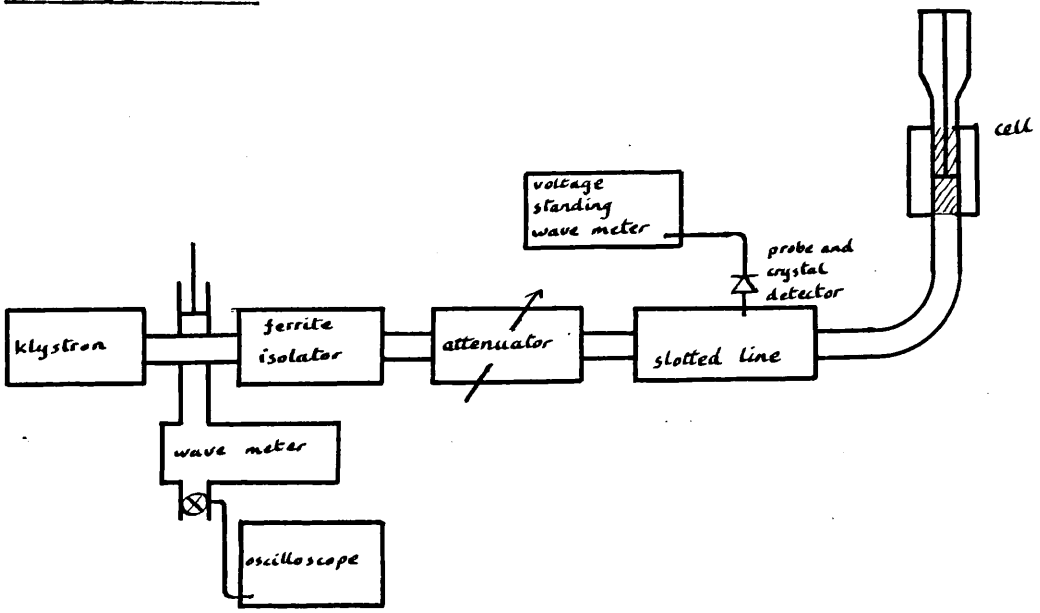

fig.23

With 3cm waves the bridge arrangement became impractical as both attenuators produced a phase shift with change in attenuation. To overcome this difficulty the arrangement shown in fig.23 was used. A standing wave was set up due to the reflection from the cell, and the variation of its voltage with position was found by means of the travelling probe. The signal from the crystal of the probe was displayed on a voltage standing wave meter. In taking measurements, the variable attenuator was adjusted so that this signal had a fixed value. This eliminated any error due to the crystal not

obeying a square law, and non-linearity in the response of the voltage standing wave meter. The cell was of the same design as the 8mm cell.

The apparatus was tuned. The wavelength in the guide was twice the distance that the probe had to move between two successive minima of the standing wave. The reflection coefficient was found from the ratio of the maximum to minimum voltages of the standing wave

$$\frac{1+r}{1-r} = \rho = \frac{|E_{max}|}{|E_{min}|} = \text{anti log}\left[\frac{A_{max} - A_{min}}{20}\right]$$

where A_{max} and A_{min} were the variable attenuator readings at the maximum and minimum to give the same signal on the voltage standing wave meter. With the mica window in place, and the cell short circuit at zero depth, the reference positions were found. ρ had a value such that r_o was slightly less than unity. This correction had to be applied at the other balance points by dividing the measured value of the reflection coefficient by the value r_o. The phase change at other balance points was $\frac{4\pi x_o}{\lambda_g}$, x_o being the distance of the minimum of the standing wave from the reference minimum.

To Compare Different Methods of Measuring the Permittivity

Using the 8mm apparatus, the reference values were found and the cell filled with a dielectric liquid. The liquid used was chloroform, unpurified, and the experiment performed at room temperature.

The short circuit in the test cell was withdrawn, thus increasing the depth of liquid in front of it, until there was no perceptible change in the balance point for a further increase in depth. This meant that this, and greater depths, were equivalent to an infinite depth of the liquid. Starting with this depth of liquid, the depth was decreased, and readings of the attenuation and variable short circuit position needed for balance taken at regular intervals of depth until zero depth was reached. A short time was allowed to elapse between the movement of the cell short circuit and the bridge being balanced to enable any excess liquid to move back past the short circuit, and so cut down the possibility of the mica window being distorted due to liquid pressure. From the readings of the attenuation and variable short circuit position, the reflection coefficient and phase change respectively were calculated, and these values

plotted against the corresponding depth of liquid. From these results, the values of ϵ' and ϵ'' were calculated in the following ways.

1/ Using the values at 'infinite depth', a and b are given by

$$a = \frac{(\rho_\infty^2 - 1)\tan\varphi/2}{1 + \rho_\infty^2 \tan^2 \varphi/2}$$

$$b = \frac{\rho_\infty (1 + \tan^2 \varphi/2)}{1 + \rho_\infty^2 \tan^2 \varphi/2}$$

where $r_\infty = \frac{\rho_\infty - 1}{\rho_\infty + 1}$ and φ are the values of the reflection coefficient and the phase change at 'infinite depth' respectively.

2/ Poley's Method[12].

The positions of the minima in the reflection coefficient were noted and from these λ_ℓ was found as twice the distance between adjacent minima. The value of $\rho_n = \frac{1 + r_n}{1 - r_n}$ at the n^{th} maximum was calculated.

From $$\frac{\rho_\infty}{\rho_n} = \tanh (n\pi \tan \tfrac{1}{2}\Delta)$$

$\tan \frac{1}{2}\Delta$ was calculated using the different maxima. It was found that as n increased $\tan \frac{1}{2}\Delta$ decreased. To

obtain a more consistant value of $\tan \frac{1}{2}\Delta$ the correction for junction loss, as discussed on page 48, was applied.

$$\frac{1}{\rho_{corrected}} = \frac{1}{\rho_{measured}} - \frac{1}{\rho_{junction}}$$

The value of $\rho_{junction}$ giving the smallest deviation in the mean value of $\tan \frac{1}{2}\Delta$ was found by trial and error. $\tan \frac{1}{2}\Delta = \frac{\alpha}{\beta}$ and $\beta = \frac{2\pi}{\lambda_g}$, giving a and b and hence ϵ' and ϵ''.

3/ Roberts and von Hippel's method[36]

At a depth d, the reflection coefficient r and phase φ were noted. Then

$$\frac{\tanh T e^{j\tau}}{T e^{j\tau}} = \frac{\tanh(\alpha+j\beta)d}{(\alpha+j\beta)d} = \frac{-j\lambda_g}{2\pi d} \frac{\left(\frac{1-r}{1+r}\right) - j\tan\frac{\varphi}{2}}{1-\left(\frac{1-r}{1+r}\right)j\tan\frac{\varphi}{2}}$$

Using Roberts and von Hippel's charts, the values of T and τ, and hence of a and b were found for several depths, and the average value found.

4/ Fatuzzo and Mason's method.[41]

The depth d for a real reflection coefficient, i.e. when $\varphi = 0$, was noted. Then

$$\frac{\tanh(\alpha+j\beta)d}{(\alpha+j\beta)d} = \frac{-j\lambda_g}{2\pi d} \frac{1-r}{1+r}$$

and a and b found as in method 3.

5/ Using the maxima of the reflection coefficient only. The maxima occur very nearly at $\frac{n\lambda_g}{2}$ giving $2\beta d = 2n\pi$.

Thus from

$$\frac{1+\tau e^{j\varphi}}{1-\tau e^{j\varphi}} = \frac{j\beta_g}{\alpha+j\beta}\tanh(\alpha+j\beta)d$$

$$\frac{1-\tau_{max}^2}{1+\tau_{max}^2} = \frac{2b\tanh\alpha d}{a^2+b^2+\tanh^2\alpha d}$$

As a first approximation it was assumed that $a^2 \ll b^2$, so that a^2 could be neglected with respect to b^2. At 'infinite' depth' $\tanh\alpha d = 1$, hence, using τ_∞, b can be found. The above equation is now a quadratic in $\tanh\alpha d$, enabling α to be found. If this approximate value of α is then substituted for $a = \frac{\alpha}{\beta_g}$, a closer value of $\tanh\alpha d$ can be calculated.

6/ The variable short circuit in the lower arm was replaced by a match. The signal detected was then the reflected wave from the cell only. The attenuator in the test arm was adjusted to give full scale deflection for zero depth of liquid. The depth of liquid was increased until the first minimum was reached and the position noted. At the next maximum the attenuator was adjusted to give full scale deflection again and the attenuation noted. This was continued until there was no difference

between maxima and minima. Using the attenuation at $d = 0$ as the reference for a reflection coefficient of -1, the reflection coefficients of the other maxima were calculated. λ_g was twice the distance between successive minima. Poley's equations were then used to calculate ϵ' and ϵ''.

The results obtained were

Method	a	b	ϵ'	ϵ''
1/	0.402	2.05	2.88 ± 0.04	1.02 ± 0.04
2/	0.447	2.24	3.35 ± 0.02	1.24 ± 0.02
3/	0.452	2.23	3.34 ± 0.1	1.25 ± 0.09
4/	0.443	2.24	3.36 ± 0.03	1.23 ± 0.03
5/	0.463	2.15	3.11 ± 0.02	1.23 ± 0.02
6/	0.479	2.24	3.29 ± 0.02	1.29 ± 0.02

Except for the values obtained by method 1/ the results were internally consistent.

In method 1/, the value of φ at infinite depth was small, being less than 10°. This meant that any error in the measured value of φ, e.g. due to the presence of the mica window, caused a large error in the value of

$\tan \frac{\varphi}{2}$. Because of this a correction for the mica window would have to be made. With low loss liquids there was also the difficulty in making sure that the measurements were taken at 'infinite depth'.

Method 6/ was unreliable for two reasons:-
a) the minima were flat, making it difficult to determine the actual position of the minima, and
b) the value of the maxima were critically dependent on the power output. Any slight frequency shift, small enough to produce no noticeable change in the oscilloscope picture, because of the change in power output, produced a large change in the attenuator reading.

Poley's method 2/ needed a complete run of depths from $d = 0$ to $d = \infty$. This was a distinct disadvantage when readings at temperatures other than room temperature were required. Though it did not need the value of a precise depth, it did need the distance between two minima. With low loss liquids the minima were sharply defined, and their positions determined easily, but with high loss liquids the minima were few, 2 or 3 at the most, and were very flattened, making an

accurate determination of λ_ℓ impossible. The higher the loss the worse this error became.

As method 5/ did not need the minimum positions this consideration did not enter in, but this method also needed a complete depth run. Also, with high loss liquids, the assumption that the maxima occured at $\frac{n\lambda_\ell}{2}$ was no longer true.

In Roberts and von Hippel's method 3/ the depth was the main source of error. Even with the fact that no mica correction had been applied, agreement with Poley's method, the only one that did incorporate any correction, was good.

Mason's method 4/ also gave good agreement with Poley's method. This individual value at $\varphi = 0$ gave better agreement than the individual values in method 3/ obtained at $\varphi \neq 0$.

A similar run on the 4mm apparatus also showed good agreement between Poley's, Roberts and von Hippel's, and Mason's methods. Again, Mason's value was in better

agreement with Poley's and the average Roberts and von Hippel's than the individual Roberts and von Hippel's values.

Taking all these results into consideration, it was decided to use Mason's method for finding the temperature variation of the complex permittivity at each of the three wavelengths.

Because the phases of the reflection coefficient at the reference position and the single depth position were the same, the variable short circuit remained fixed. On the 8mm apparatus, to eliminate any possibility of the attenuator with a phase change upsetting the readings, this attenuator was placed in the lower arm, and all balancing done with the attenuator in the test arm. This meant that, once the reference position had been found, the lower arm remained unchanged. The reflection coefficient at a depth d was given by $\frac{\cos^4 \theta_o}{\cos^4 \theta_d}$, where θ_o was the reference value, and θ_d the value at the depth.

To vary the temperature of the dielectric an arrangement as shown in fig.24 was used. Commercial

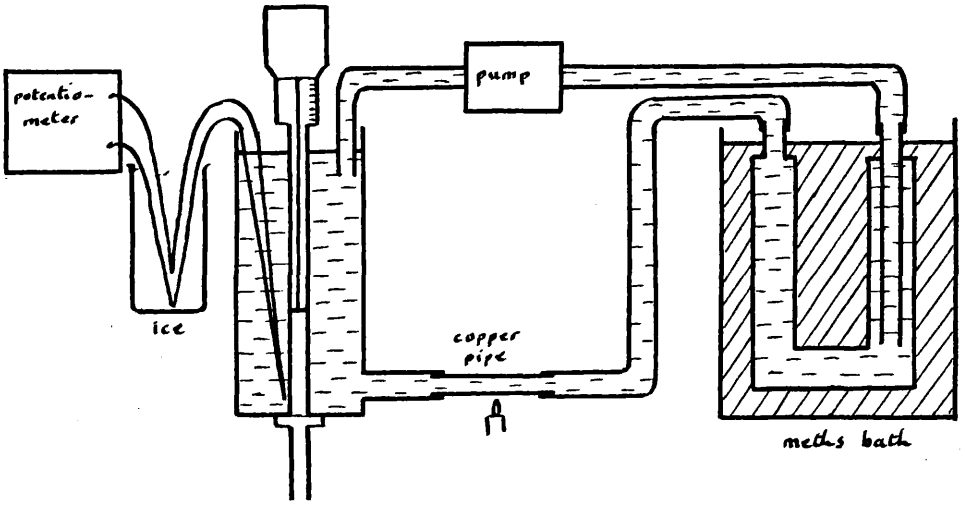

fig.24

meths was used, both as the circulating liquid and as the bath liquid. Below room temperature, the temperature of the bath was altered by adding dri-kold to the meths.

The temperature of the meths around the liquid cell was mainly determined by the temperature of the bath, but it could be controlled to a certain extent by the rate of pumping. Above room temperature it was further controlled by heating the meths as it flowed through a copper pipe. Below room temperature this copper pipe was removed to cut down heat intake, and the temperature controlled by keeping the bath temperature constant.

The jacket of the cell and the connecting tubing were all lagged to cut down heat loss. Below 0°C a layer of frost coated all these parts, cutting down the heat leakage even further. The temperature of the meths around the liquid cell was measured by means of a thermocouple, and could be controlled to within 0.1°C.

At each temperature a short time was allowed to elapse before any measurements were taken, to enable the dielectric to reach the temperature. On the 8mm and 4mm apparatuses the reference positions were found for zero depth of liquid. The depth of liquid was increased until the signal, which had increased from zero to a maximum, decreased to a minimum. Then the attenuation and depth were adjusted alternately until zero signal was obtained. On the 3cm apparatus the minimum of the standing wave was found at zero depth, then the depth increased until this probe position was again the minimum. The voltage standing wave ratio was taken in each case. The final depth setting in all three cases was made with the cell short circuit moving towards zero depth. This eliminated any back-lash in the micrometer head, and also made any deformation of

the mica window always occur in the same direction. After each measurement the reference positions were checked before altering the temperature.

For small ratios of a to b, $\frac{a}{b} < 0.20$, a second change depth with zero phase could be found the same way as the first one. For ratios between about 0.20 and 0.35 only one depth could be found to satisfy the phase condition, while for ratios > 0.35 there was no depth showing zero phase change. In the latter case a minimum signal was found with the cell short circuit and the attenuator, then the variable short circuit was moved to bring the signal to zero. This phase was noted, and Roberts and von Hippel's formular used to calculate the permittivity.

The measurements were taken over a range of temperatures, and graphs of ϵ' and ϵ'' against temperature plotted.

Discussion of Errors

The errors in these measurements arose from two sources, one from experimental uncertainty, and the other from systematic causes. On the three sets of apparatus

the depth and attenuations could be measured to the following accuracy:-

λ	depth	attenuation
3cm	0.01mm	0.005dbs.
8mm	0.002mm	0.01° of angle
4mm	0.005mm	0.01-0.02dbs

These gave errors of ±(0.5-1)% on ϵ'', and ±2% on ϵ'' on the 4mm apparatus, and ±0.5% on ϵ', and ±1% on ϵ'' for the 3cm and the 8mm apparatuses. These are average values, the actual errors depend on the ratio of ϵ'' to ϵ'. The higher this ratio the greater the error.

The reflection from the mica window was another source of error.

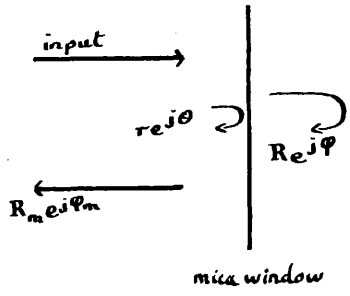

fig.25

Let $R_m e^{j\varphi_m}$ be the measured reflection coefficient,

$r e^{j\theta}$ be that of the mica window plus junction,

$R e^{j\varphi}$ be the actual reflection coefficient off the liquid surface,

t be the transmission coefficient at the junction.

This adds a constant phase on to the value of φ, and

hence can be treated as a real number, since the method involves measuring the liquid depth required to produce a certain change in φ.

The measured reflection coefficient

$$R_m e^{j\varphi_m} = \tau e^{j\theta} + t R e^{j\varphi}$$

The initial balance is obtained for a short circuit behind the mica window, i.e. $Re^{j\varphi} = -1$

$$R_m e^{j\varphi_m} = \tau e^{j\theta} - t$$

giving $$\tan \varphi_{m_o} = \frac{\tau \sin\theta}{\tau\cos\theta - t}$$

The next balance is obtained for the same value of φ_m, but a different value for $Re^{j\varphi}$.

$$\tan \varphi_m = \frac{\tau \sin\theta + tR\sin\varphi}{\tau\cos\theta + tR\cos\varphi} = \frac{\tau\sin\theta}{\tau\cos\theta - t}$$

Thus $$\tan\varphi = \frac{\tau\sin\theta(R-1)}{R(\tau\cos\theta - t)} \qquad (27)$$

The measured value for ,

$$R_m^2 = \tau^2 + t^2R^2 + 2t\tau R\cos(\varphi-\theta) \qquad (28)$$

The value $\tau e^{j\varphi}$ was the measured reflection coefficient when the test arm was terminated by a match with the mica window in place, and t was found from the

reflection coefficient with a short circuit termination. For the 3cm apparatus $re^{j\theta} = 0.004 - 0.012j$, and $t = 0.95$. For the first depth where $\varphi_m = \varphi_{m_o}$, $R \sim 0.7$, and at the second depth $R \sim 0.5$. With these values, the deviations from the ideal case were

R	φ	R_m whereas	tR
0.7	$180^\circ + 0.31^\circ$	0.669	0.665
0.5	$180^\circ + 0.75^\circ$	0.479	0.475

The effect of these deviations could be seen by the fact that the value of both a and b were always smaller for the second depth than for the first, e.g.-

	b	a	giving ϵ'	ϵ''
first	2.308	0.342	3.22	0.834
second	2.300	0.327	3.21	0.796

Recalculating these using the corrected phase instead of 180° gave

b	a	ϵ'	ϵ''
2.315	0.342	3.24	0.837
2.310	0.334	3.23	0.817

This correction had more effect on the second depth

values than on those of the first, and brought the two sets to agree within the experimental error. If the first depth, uncorrected, is taken, this also lay within the experimental error of the corrected values, and these were the values used. This approximation was more valid on the 8mm and 4mm apparatuses as a thinner piece of mica could be used for the window, and hence less correction had to be applied.

The systematic errors will also tend to increase the difference between the values at the two depths. These errors include those due to the mis-match of the hybrid-T, i.e. the slight variation in the value of the reflection coefficient and the phase change with the distance of the dielectric from the hybrid-T which was observed on the 4mm apparatus (see page 65). This error will be minimized due to the fact that the liquid surface was always at the same position, and that all measurements were taken with the same phase change. The effect of these errors could not be measured experimentally as any attempt at measuring them automatically incurred a change in the error to be measured. Their effect could not be very great as the

values at the two depths usually agreed within the experimental error when no correction for the mica window was applied, and always did when the correction was applied. Because of these systematic errors the difference between values at different temperatures will tend to be more accurate than the actual values themselves. This is shown in the case of methyl alcohol where the graph of ϵ' against temperature shows a knee in the curve (page 120), the values over the whole range of which are well within the experimental error. On repeating the run the knee again showed up while all the values of ϵ' were decreased within the experimental error.

Measurement of the Static Permittivity

The static permittivity of a substance can be found as the ratio of the capacitance of a condenser with the substance filling the space between its plates C_d to its capacitance with the space evacuated C_o

$$\epsilon_s = \frac{C_d}{C_o}$$

For polar liquids whose dispersion region lies in

the microwave range, the permittivity measured at frequencies as high as one megacycle is still equal to that measured at zero frequency. Because of this a resonance method of measuring the capacitances can be used.

If an inductance L, a capacitance C, and a resistance R, are arranged in series in a circuit, their total impedance is given by

$$\sqrt{R^2 + \left(L\omega - \frac{1}{C\omega}\right)^2}$$

where ω is the frequency of the e.m.f. induced in the circuit. This impedance is a minimum when

$$L\omega = \frac{1}{C\omega} \quad \text{or} \quad LC\omega^2 = 1$$

When this condition is satisfied the circuit is said to be in a state of resonance, and is shown by the current flowing in the circuit being at its maximum value.

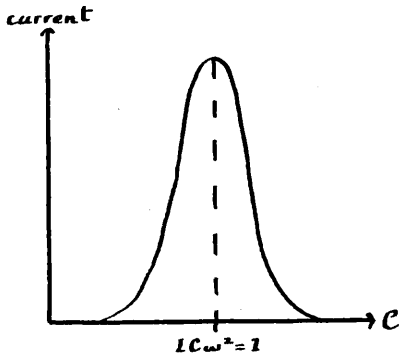

fig.26

Around the resonance state, the current varies with capacitance as shown in fig.26, the height of the resonance peak being governed by the value of R, the smaller the value of R the higher and

sharper the peak.

For constant values of both ω and L, resonance occurs at a definite value of C. Thus, if the dielectric cell is arranged in parallel with a variable condenser, resonance will occur when the sum of the two capacitances equals this required value, and changes in the capacitance of the dielectric cell can be measured by the changes in the variable condenser needed to maintain resonance.

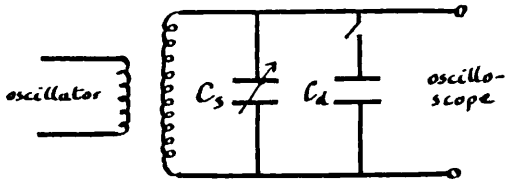

fig.27

Oscillations, at about 20KHz were loosely coupled to the circuit from a stable oscillator. The resonance of the circuit was found by using an oscilloscope to detect the maximum voltage across the condensers. The variable condenser was an accurate 0 - 1,100pf condenser. The dielectric cell was of the type introduced by Sayce and Briscoe[42] with modifications as described by Mallikarjun.[43]

For silvering the cell the process recommended by

Sugden[44] was used. He modified the previously used silvering solution in order to make the silver film long-lasting yet thin. It was found that the silver film was stable enough to allow the static permittivity of several liquids to be found before part of the coating disintegrated. To aid the stability of the silver coating the condenser was never left dry, but filled with benzene when not in use. The cell was never silvered right to the top, so it was always possible to check that the dielectric liquid covered the silvered portion completely. Between different liquids the cell was cleaned by washing with benzene and dried by drawing dry air through the cell.

The cell was placed in a temperature bath. Because of the thin walls of the silvered surfaces, the dielectric liquid quickly attained the temperature of the bath. With the cell disconnected, the variable condenser was adjusted to give the resonance position, and its value noted. The cell was then connected into the circuit, and the new value of the variable condenser needed for resonance found. The difference between these two values was the capacitance of the cell.

The capacitance of the cell in air C_o was found both directly, and by using a standard liquid such as benzene. It was found that there was a larger discrepancy between the two values of C_o than could be accounted for by experimental error. This discrepancy was due to the presence of stray capacitances.

Assuming that there is a stray capacitance c in parallel with the dielectric cell, then the apparent permittivity k will be

$$k = \frac{\epsilon_s C_o + c}{C_o + c}$$

where C_o is the capacitance of the air-filled cell, and ϵ_s the true permittivity. c was found using the values obtained from the air-filled and the benzene-filled cell, and then this value checked with another standard liquid. The stray capacitance was of the order of 7pf, and this value had to be subtracted from every reading taken.

The temperature variation of the capacitance of the air-filled condenser was found to be too small to be detected. Having thus found this capacitance, the static

permittivity of any liquid at any temperature can be found.

The variable condenser, at resonance, could be set, repeatedly, to within 0.1pf, thus capacitance changes at resonance could be found accurately. The main source of error was due to the determination of the stray capacitance. This value, when estimated from two liquids and a dry capacitance determination, had an error of about 0.8pf, giving an error of 0.4% on the final value.

Measurement of the Refractive Index

The refractive index of the dielectric liquid at the wavelength of the sodium-D line was found using an Abbe refractometer. It was not possible to use this instrument below the freezing point of water because of condensation. Readings over a range of temperatures above 0°C were taken, and the results plotted against temperature. It was found that, over this range of temperatures, the variation in refractive index was apparently linear with temperature, hence the

values of the refractive index at temperatures below 0°C were found by assuming this linearity to hold. This assumption is not true as the refractive index obeys a law of the kind

$$\frac{n^2-1}{n^2+2}\,\frac{1}{\rho} = \text{constant}$$

where ρ is the density. Using this formular, the values of the refractive index at 0°C and -40°C were calculated from the experimental value at 50°C, and compared with the values obtained by assuming linearity.

temperature	0°C	-40°C
calculated refractive index	1.5361	1.5612
experimental refractive index	1.5359	1.5604

The difference between the experimental and calculated values is thus less than 0.1%, and hence any non-linearity over this temperature range is negligible compared with the experimental errors in the other quantities.

Discussion of Results

Tables of the values of ϵ' and ϵ'' at various temperatures at each wavelength are shown on pages 124 to 130. At each wavelength and temperature values for ϵ_∞, the value of the permittivity at the high frequency end of the Cole-Cole arc, and λ_c, the wavelength at which ϵ'' is a maximum, were calculated using the equations

$$\epsilon_\infty = \epsilon' - \frac{\epsilon''^2}{\epsilon_s - \epsilon'} \qquad (29a)$$

$$\lambda_c = \lambda\left(\frac{\epsilon_s - \epsilon'}{\epsilon''}\right) \qquad (29b)$$

where λ is the wavelength at which ϵ' and ϵ'' were measured. Tables of these calculated values are shown on pages 131 to 135.

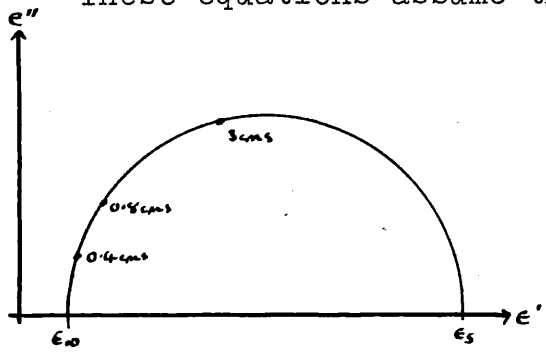

fig.28

These equations assume that a Debye semi-circle for a single relaxation time passes through the point $(\epsilon_s, 0)$ and (ϵ', ϵ'') at each temperature and wavelength. If, for one temperature, the values of ϵ_∞ and λ_c at each

wavelength lie on the same semi-circle, (fig.28) the three independent values of ϵ_∞ and λ_c will be the same.

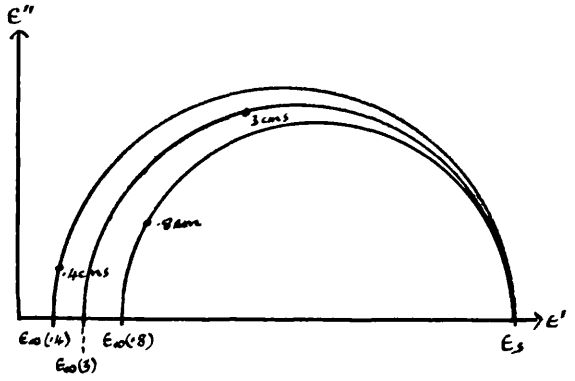

fig.29

Any deviation from a single semi-circle (fig29) will show up in differing values of ϵ_∞ and λ_c, the value of ϵ_∞ depending on the actual semi-circle, and the value of λ_c depending on the position of the point (ϵ', ϵ'') on the semi-circle.

Ethyl and methyl alcohol were not treated in this way due to lack of information. The values of ϵ_s and of the complex permittivity at 3.332cms were too high to be measured by the methods used. Because $\epsilon_s - \epsilon_\infty$ is large for these two liquids, and both the 8mm and the 4mm values lie near the high frequency end of the Cole-Cole plot, ϵ_∞ will be approximately equal to ϵ'. Hence, by comparing the values of ϵ' for 8mm and 4mm, it can be seen that the 4mm values lie off the semi-circle through the 8mm values.

The general trend for all the liquids studied was

that $\epsilon_\infty(3) > \epsilon_\infty(.8) > \epsilon_\infty(.4)$ and $\lambda_c(3) > \lambda_c(.8) > \lambda_c(.4)$, the differences between the values increasing with decreasing temperature. The fact that $\epsilon_\infty(3) > \epsilon_\infty(.8) > \epsilon_\infty(.4)$ means that the point (ϵ', ϵ'') at 8mm lies outside the semi-circle through the point (ϵ', ϵ'') at 3cms, and that (ϵ', ϵ'') at 4mm lies even further from this first semi-circle. The value of λ_c depends mainly on ϵ'', hence $\lambda_c(3) > \lambda_c(.8)$ means that (ϵ', ϵ'') at 8mm lies outside the 3cms semi-circle because ϵ'' at 8mm is greater than the value ϵ'' would have if it lay on the 3cm semi-circle. The 4mm values and the lower temperature values deviate even further. As a lower temperature is equivalent to a decrease in wavelength, this means that the shorter the wavelength the more the values of (ϵ', ϵ'') deviate from the semi-circle through the longest wavelength. This type of effect would occur if the values of (ϵ', ϵ'') at different wavelengths lay on an arc of a circle and not on a semi-circle as Cole and Cole[7] found to be the case for some liquids, but previous evidence[40] shows that this is not the case for the liquids under consideration. Another absorption region at shorter wavelengths than the Debye dispersion will also produce this deviation from the Debye semi-circle at wavelengths short compared to λ_c, hence the present

measurements support the evidence for a second absorption region.

Poley[11] found that, for the halogenated benzenes, $\epsilon_\infty - n^2 \propto \mu^2$. If the second absorption region depends on μ^2 in the same way that the Debye dispersion region does, $\frac{\epsilon_\infty - n^2}{\epsilon_s - n^2}$ will be approximately constant irrespective of the liquid. A table of this value is shown below, the value of ϵ_∞ used being the average of $\epsilon_\infty(3)$ and $\epsilon_\infty(\cdot 8)$.

Table A

temp	C_6H_5Cl	C_6H_5Br	C_6H_5I	$CHCl_3$	C_9H_7N	$(CH_3)_3CCl$	$C_6H_5NO_2$
°C	±.01	±.01	±.01	±.01	±.01	±.03	±.01
50		0.056	0.061	0.071	0.078		0.062
40	0.045	0.058	0.058	0.081	0.083	0.158	0.060
30	0.056	0.064	0.061	0.085	0.087	0.170	0.056
20	0.067	0.066	0.059	0.084	0.086	0.172	
10	0.071	0.071	0.062	0.086	0.083	0.184	
0	0.076	0.073	0.059	0.085	0.078	0.188	
-10	0.078	0.073	0.057	0.083	0.075	0.187	
-20	0.081	0.075	0.059	0.081		0.181	
-30	0.082	0.072	0.057	0.079			
-40	0.083			0.077			

These values are very much dependent on the value assumed

for n^2. The value used for the above results was n_D^2. Chamberlain[45] has measured the refractive index of chlorobenzene from 160cm^{-1} up to 2cm^{-1} at 20°C. Over this range n decreases to a minimum of 1.520 ± .002 at 70cm^{-1}, then increases up to the microwave region. This minimum value is less than n_D by 0.005. Assuming that there is a similar difference at all temperatures $\frac{\epsilon_\infty - n^2}{\epsilon_s - n^2}$ for chlorobenzene becomes

Table B

temp	40	20	0	-20	-40	°C
$\frac{\epsilon_\infty - n^2}{\epsilon_s - n^2}$	0.049	0.070	0.080	0.084	0.087	±.01

The change in the values, compared with those of table A, is well within the initial uncertainty of 15% on the larger values rising to 25% on the smallest.

Within the limits of this error the values show a consistency between the different liquids. The exception is 2chloro-2methyl-propane. This liquid is the only one of the group which Hill[46] terms a group II molecule, one that possesses dipole rotation in the solid phase. For this type of molecule Hill expected $\epsilon_\infty - n^2$ to be very small, hence one would expect $\frac{\epsilon_\infty - n^2}{\epsilon_s - n^2}$ to

be smaller for this liquid than for the others, whereas the present experimental results show it to be larger.

The consistency between liquids in the same group shows that the second absorption region could also be Debye like in origin. If this is so it is possible to calculate its relaxation wavelength λ_{c_2}. In a Debye dispersion region the dielectric loss is given by

$$\epsilon'' = \frac{\epsilon_s - \epsilon_\infty}{1 + \left(\frac{\lambda_c}{\lambda}\right)^2} \frac{\lambda_c}{\lambda}$$

Taking the relaxation wavelength for the main dispersion region as $\lambda_c(3)$, a value of ϵ'' was calculated at both 0.848cms and 0.435cms. The difference between this calculated value ϵ_c'' and the measured value ϵ'' was taken to be due to the second absorption region. Using this difference a value for λ_{c_2} was calculated from

$$\epsilon'' - \epsilon_c'' = \frac{\epsilon_\infty - n^2}{1 + \left(\frac{\lambda_{c_2}}{\lambda}\right)^2} \frac{\lambda_{c_2}}{\lambda}$$

This calculated value λ_{c_2} is shown in table C for both chlorobenzene and iodobenzene.

λ_{c_2} shows a tendency to be constant over the temperature range (the initial rise is mainly due to

Table C

	C_6H_5Cl		C_6H_5I	
temp °C	8mm ±.07	4mm ±.04	8mm ±.07	4mm ±.04
40		0.199	0.088	0.181
30	0.05	0.203	0.248	0.204
20	0.119	0.205	0.312	0.225
10	0.182	0.209	0.346	0.225
0	0.232	0.210	0.368	0.232
-10	0.292	0.211	0.386	0.244
-20	0.338	0.209	0.368	0.238
-30	0.347	0.210	0.350	0.226

the fact that $\epsilon'' - \epsilon_\infty''$ is very small here and subject to a large uncertainty), but at a value around 0.3cms ($\sim 3cm^{-1}$) whereas the experimental evidence shows the maximum of the second absorption region at about $45cm^{-1}$. This means that the observed deviation at 8mm and 4mm is larger than can be explained by a Debye type relaxation centered at $45cm^{-1}$.

This is also born out by some theoretical calculations on chlorobenzene.

The values of ϵ_s were calculated using Onsager's equation (7).

$$\epsilon_s - \epsilon_\infty = \frac{\epsilon_s(\epsilon_\infty + 2)^2}{(2\epsilon_s + \epsilon_\infty)} \frac{4\pi}{3kT} \frac{\rho}{M} N_A \mu^2$$

where N_A is Avogadro's number, M is the molecular weight, and ρ is the density of the liquid. This, to a rough approximation, can be expressed as

$$\epsilon_s - \epsilon_\infty \propto \frac{\rho}{T}$$

Similarly, treating the difference between ϵ_∞ and n^2 as another dispersion region of the same kind

$$\epsilon_\infty - n^2 \propto \frac{\rho}{T}$$

The refractive index obeys a law of the form

$$\frac{n^2 - 1}{n^2 + 1} \propto \rho$$

The relaxation times of the two dispersion regions τ and τ_2, were found using

$$\tau \propto \lambda_c \propto \frac{\eta}{T}$$

where η is the viscosity. This is a relationship which was found to be approximately true by Mallikarjun and Hill.[40] Hence $\lambda_c \propto \frac{e^{B/T}}{T}$

where B is a constant

Similarly $\lambda_{c_2} \propto \frac{e^{B'/T}}{T}$

Taking the experimental values for chlorobenzene at 20° C, the constants of proportionality were found, and hence ϵ_s, ϵ_∞, n^2, λ_c, and λ_{c_2} at different temperatures were calculated. From these values, ϵ' and ϵ'', with respect to both temperature and frequency were calculated using the equations

$$\epsilon' = n^2 + \frac{\epsilon_\infty - n^2}{1+\left(\frac{\lambda_{c_2}}{\lambda_c}\right)^2} + \frac{\epsilon_s - \epsilon_\infty}{1+\left(\frac{\lambda_c}{\lambda}\right)^2}$$

$$\epsilon'' = \frac{\epsilon_\infty - n^2}{1+\left(\frac{\lambda_{c_2}}{\lambda}\right)^2}\frac{\lambda_{c_2}}{\lambda} + \frac{\epsilon_s - \epsilon_\infty}{1+\left(\frac{\lambda_c}{\lambda}\right)^2}\frac{\lambda_c}{\lambda}$$

These theoretical relaxation curves are shown in graphs 2 and 3. The actual values for n^2, ϵ_∞, ϵ_s, λ_c and λ_{c_2} are shown below.

Table D

temp	n^2	ϵ_∞	ϵ_s	λ_c	λ_{c_2}
40	2.29	2,49	5.36	1.61	0.0159
30	2.30	2.51	5.50	1.89	0.0188
20	2.32	2.54	5.66	2.24	0.0222
10	2.33	2.56	5.83	2.68	0.0266
0	2.35	2.59	6.02	3.25	0.0322
-10	2.37	2.63	6.21	3.99	0.0400
-20	2.39	2.66	6.42	4.97	0.0491
-30	2.41	2.69	6.64	6.32	0.0626
-40	2.43	2.72	6.88	8.16	0.0809

The values of the first four variables correspond very closely with the experimental values for chlorobenzene (page 124), as do the shapes of the curves for 3cms, 0.8cms and 0.4cms wavelength.

Using equations (29), values for ϵ_∞ and λ_c were calculated for each theoretical value of (ϵ', ϵ'') obtained at 0.8cm, 0.4cm and 0.2cm. These values are shown below.

Table E

temp	ϵ_∞	$\epsilon_\infty(.8)$	$\epsilon_\infty(.4)$	$\epsilon_\infty(.2)$	λ_c	$\lambda_c(.8)$	$\lambda_c(.4)$	$\lambda_c(.2)$
40	2.49	2.49	2.49	2.49	1.61	1.60	1.58	1.55
30	2.51	2.51	2.51	2.51	1.89	1.88	1.86	1.79
20	2.54	2.53	2.54	2.54	2.24	2.23	2.19	2.07
10	2.56	2.56	2.56	2.55	2.68	2.66	2.60	2.41
0	2.60	2.60	2.59	2.59	3.25	3.20	3.13	2.80
-10	2.63	2.62	2.61	2.60	3.99	3.92	3.76	3.23
-20	2.66	2.65	2.65	2.64	4.97	4.87	4.57	3.66
-30	2.69	2.68	2.68	2.66	6.32	6.09	5.49	4.05
-40	2.72	2.71	2.70	2.67	8.16	7.69	6.56	4.37

These values show the same sort of deviations as the experimental ones do (page 131), but the deviation at a similar wavelength is much less. Hence a mechanism

giving rise to a higher absorption than a Debye type relaxation must be responsible.

Hill[28] proposes a resonance absorption, the resonant frequency ω_o of which is given by

$$\frac{\epsilon_\infty - n^2}{\epsilon_s - n^2} = \frac{2kT}{I\omega_o^2}$$

for a liquid whose molecules have a moment of inertia I. Using this formula the following values were obtained for λc_1, in cm^{-1}, the wavelength corresponding to ω_o.

Table F

temp \ I	C_6H_5Cl	C_6H_5Br	C_6H_5I	C_9H_7N	$(CH_3)_3CCl$	$C_6H_5NO_2$
	6.15	9.40	12.1	6.30	2.70	7.66
°C	±20%	±20%	±20%	±20%	±20%	±20%
50		22.5	18.7	23.5		31.1
40	30.4	21.7	18.7	22.4	25.6	31.1
30	26.7	20.5	18.2	21.6	24.5	31.4
20	24.3	19.7	18.3	21.4	23.8	
10	22.8	18.7	17.6	21.4	22.6	
0	22.1	18.2	17.5	21.5	22.0	
-10	21.5	17.9	17.5	21.6	21.9	
-20	20.6	17.4	17.4		21.9	
-30	20.1	17.3	17.3			

$\times 10^{-38}$ g cm^2

The value of the wavelength for chlorobenzene is still high compared with the experimental value of 45cm^{-1}, but all the values are of the correct order. For each liquid λ_{c_2} shows a tendency to increase with decreasing temperature, but only slightly. Due to the uncertainty in the actual value of ϵ_∞, and hence in $\epsilon_\infty - n^2$, this increase could be more or less than that shown, but would not make enough difference for the values to decrease with decreasing temperature.

This present work supports the evidence for a second absorption region at wavelengths shorter than the main dispersion region. The effect of a Debye type of dispersion region centered around 45cm^{-1} is smaller, at the wavelengths used, than that found experimentally, the experimental measurements fitting in more with an absorption region due to a resonance type of mechanism, whose resonant frequency varies little with temperature. A full investigation at wavelengths shorter than 0.2cms, and over a temperature range, is needed before this second absorption region can be fully understood.

Graph 1a Collie, Hasted and Ritson's equation

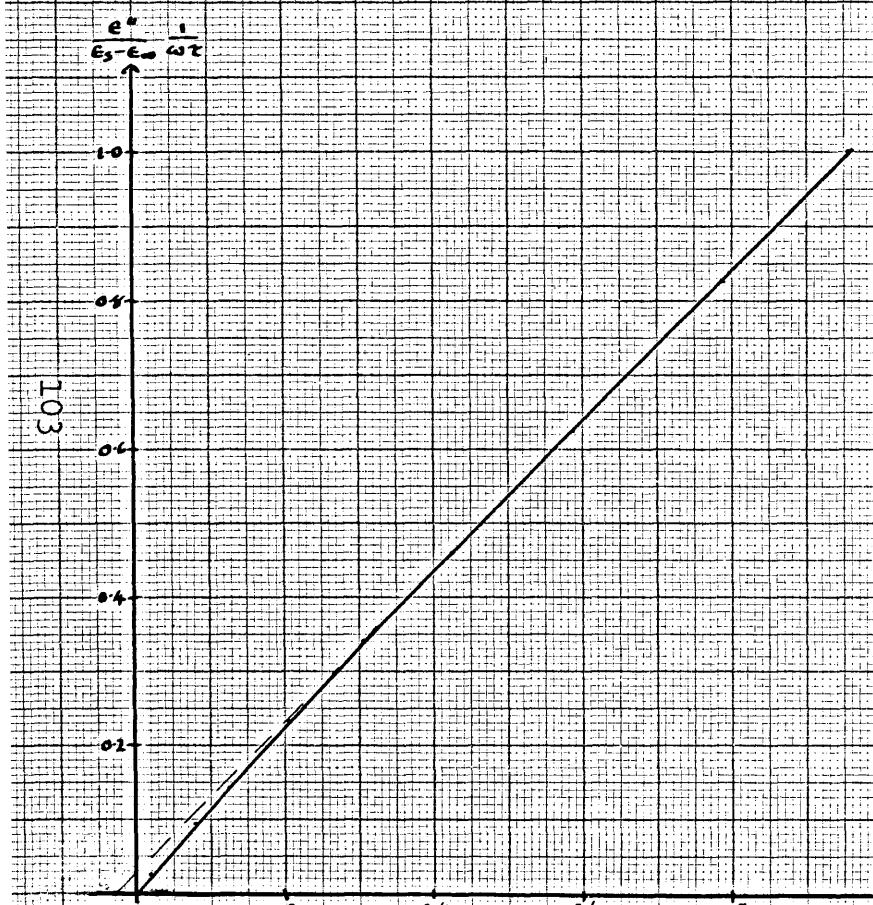

Graph 1b Effect of inertia

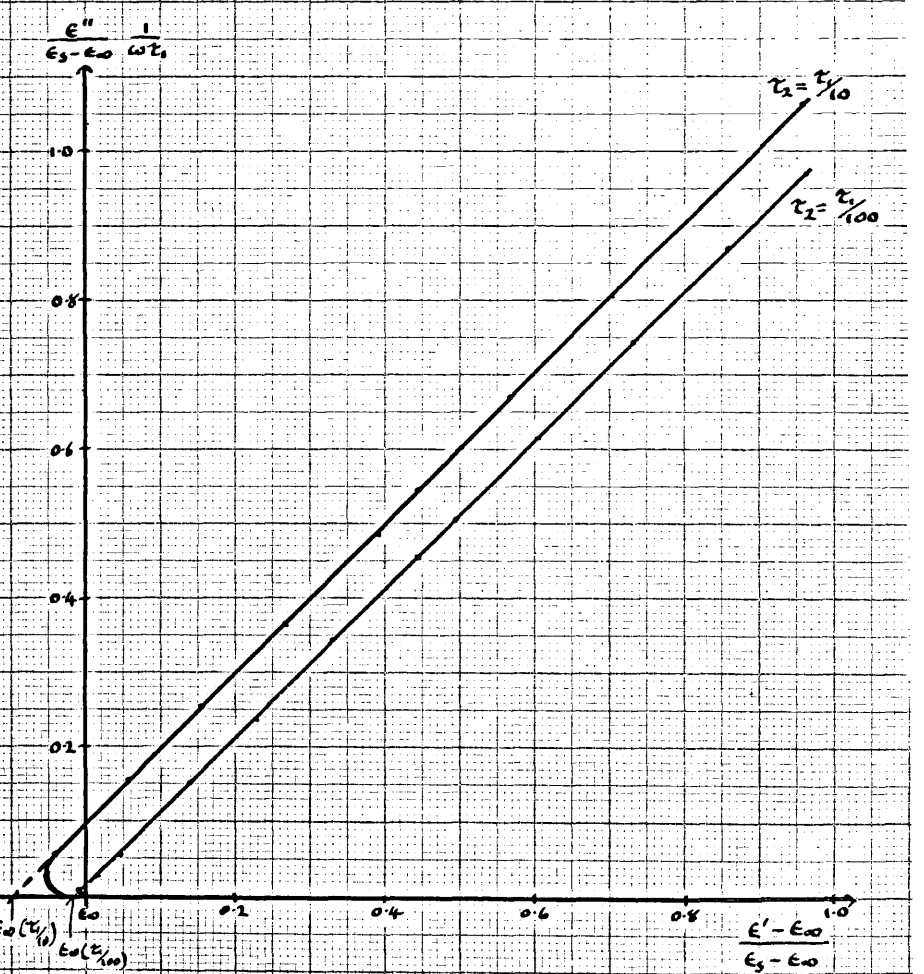

Graph 2

Theoretical curves of ϵ' for chlorobenzene

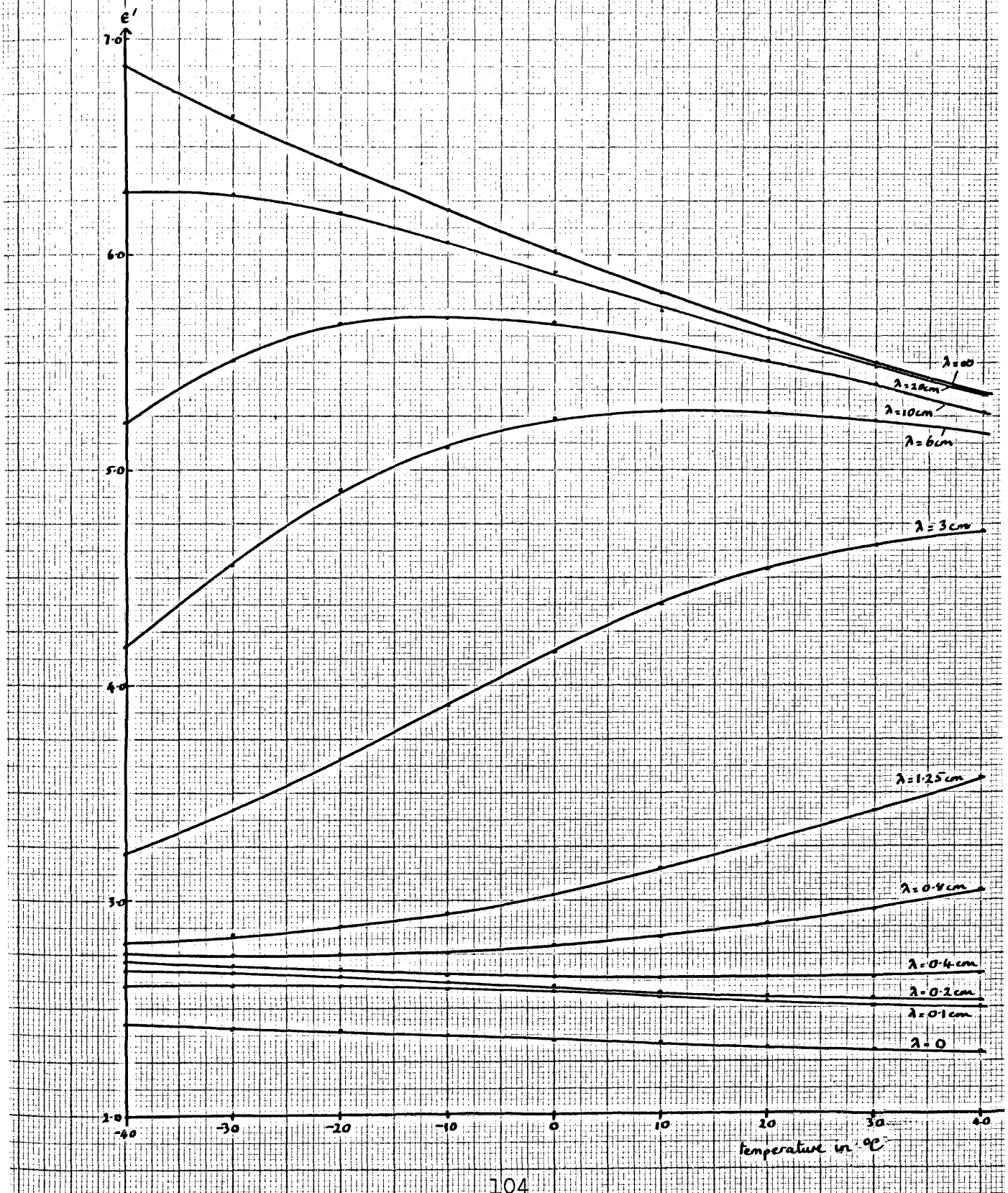

Graph 3

Theoretical curves of ϵ'' for chlorobenzene

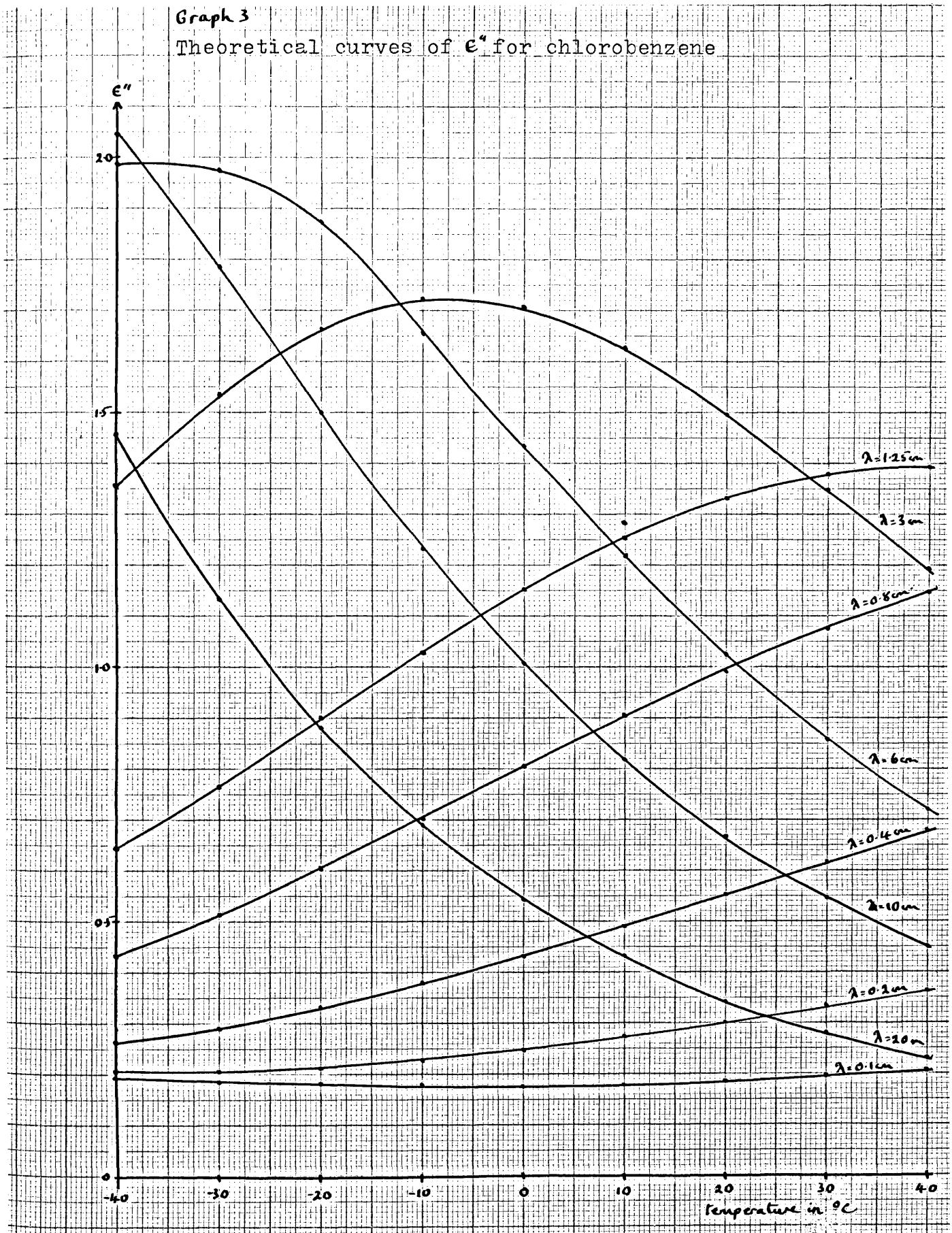

ϵ' against temperature for chlorobenzene

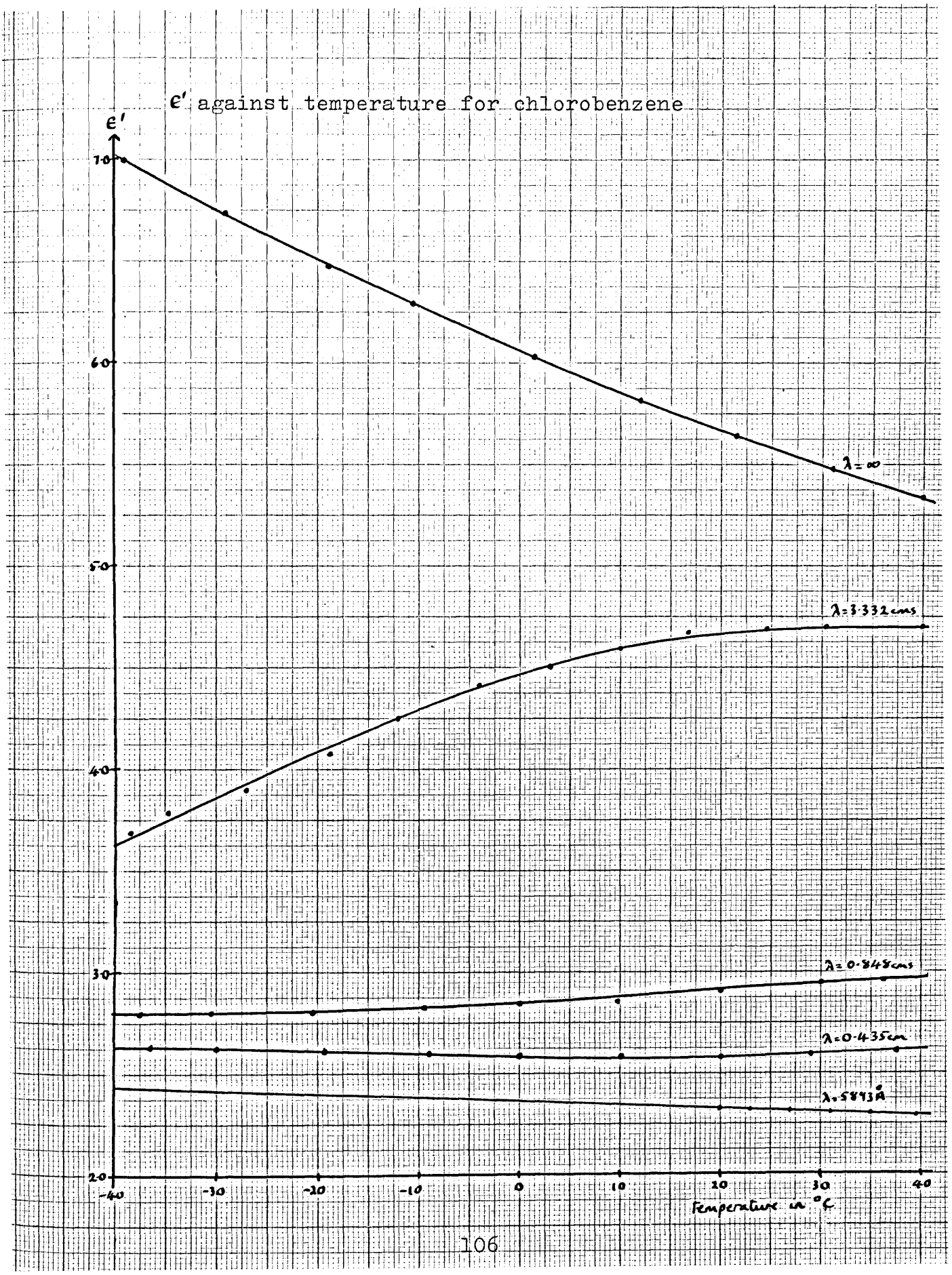

ϵ'' against temperature for chlorobenzene

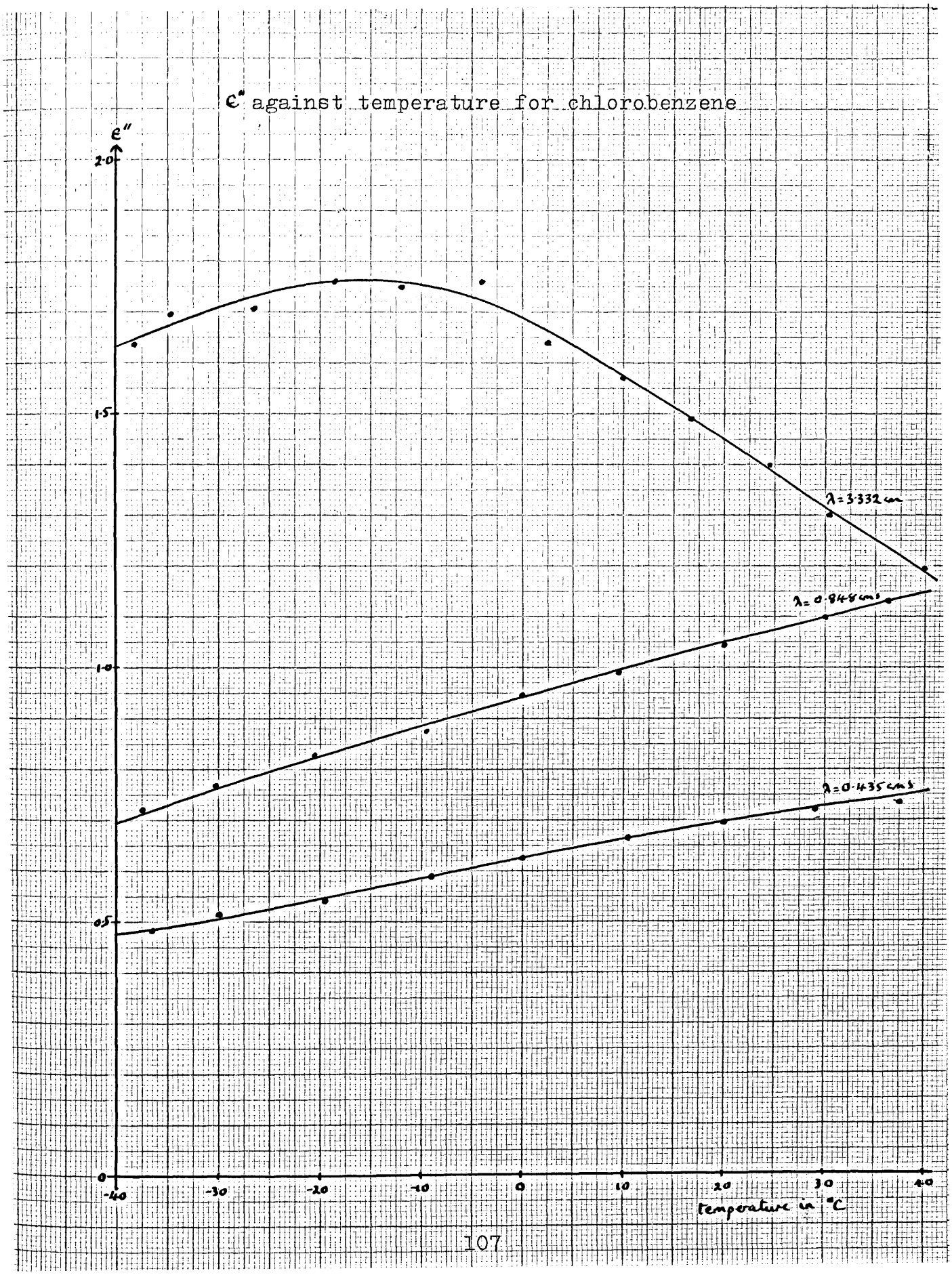

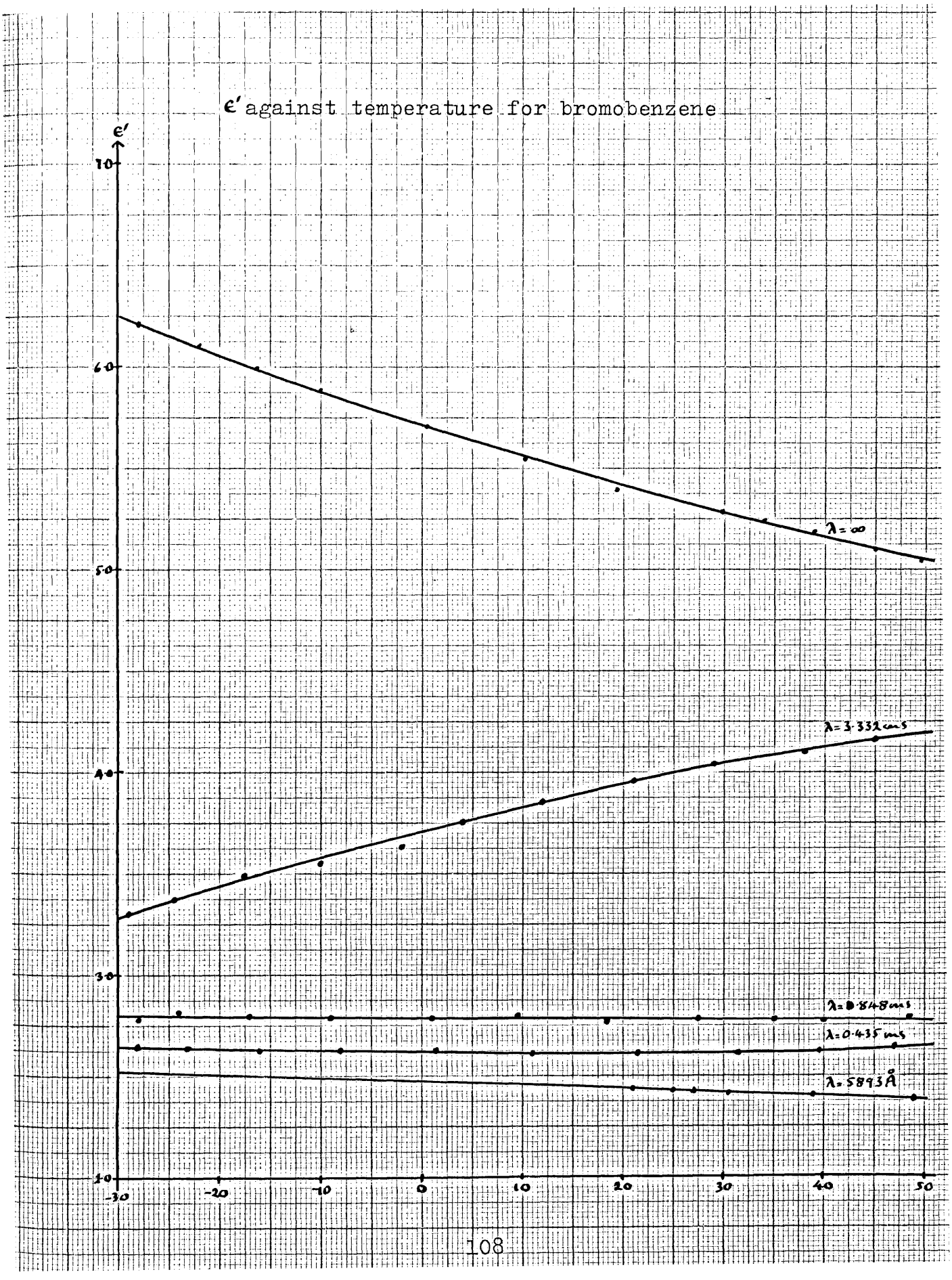
ε'against temperature for bromobenzene
ε'
70
60
50
40
30
20
-30
-20
-10
0
10
20
30
40
50
λ=∞
λ=3·332cms
λ=0·848cms
λ=0·435cms
λ=5893Å

ϵ'' against temperature for bromobenzene

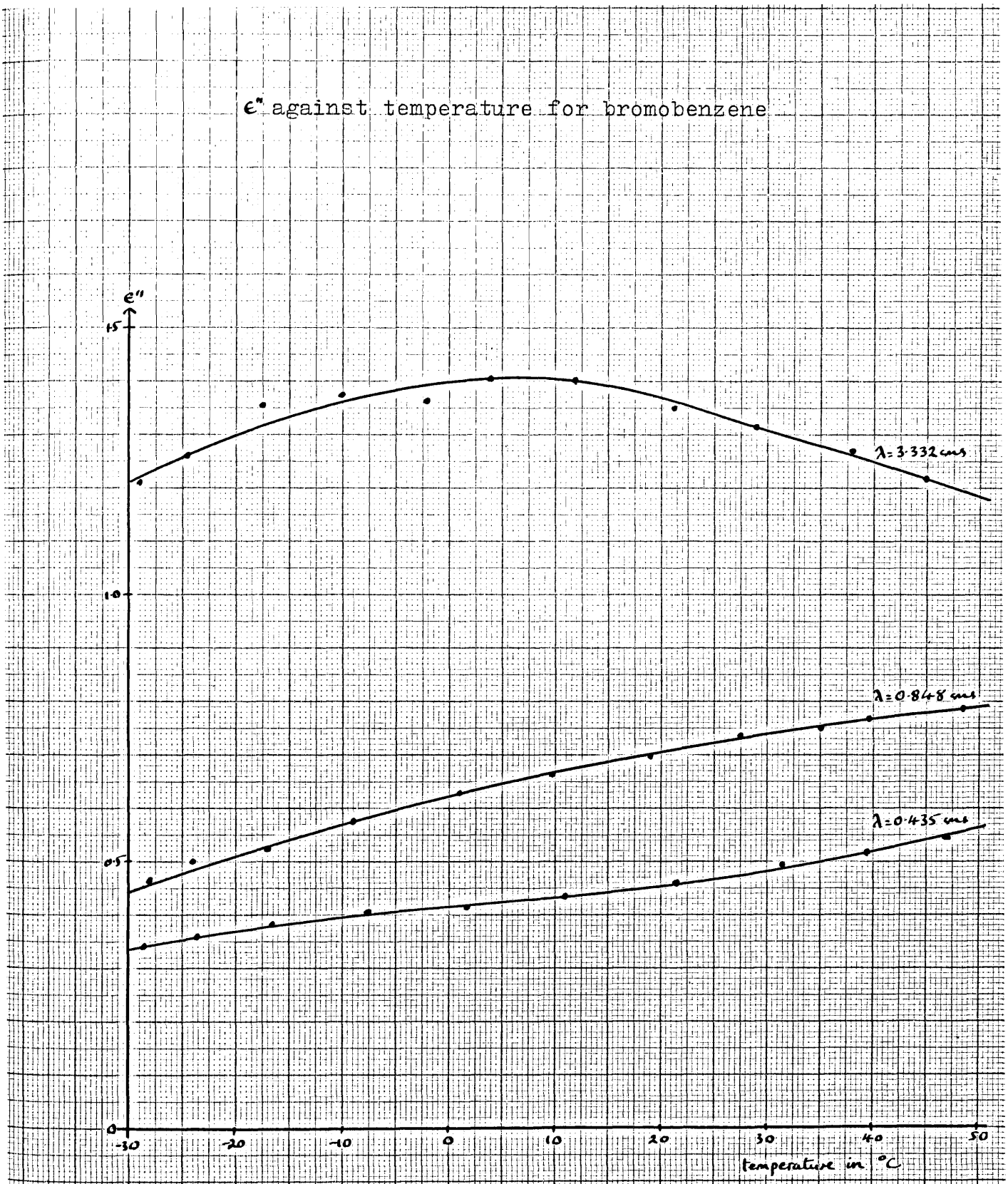

ϵ' against temperature for iodobenzene

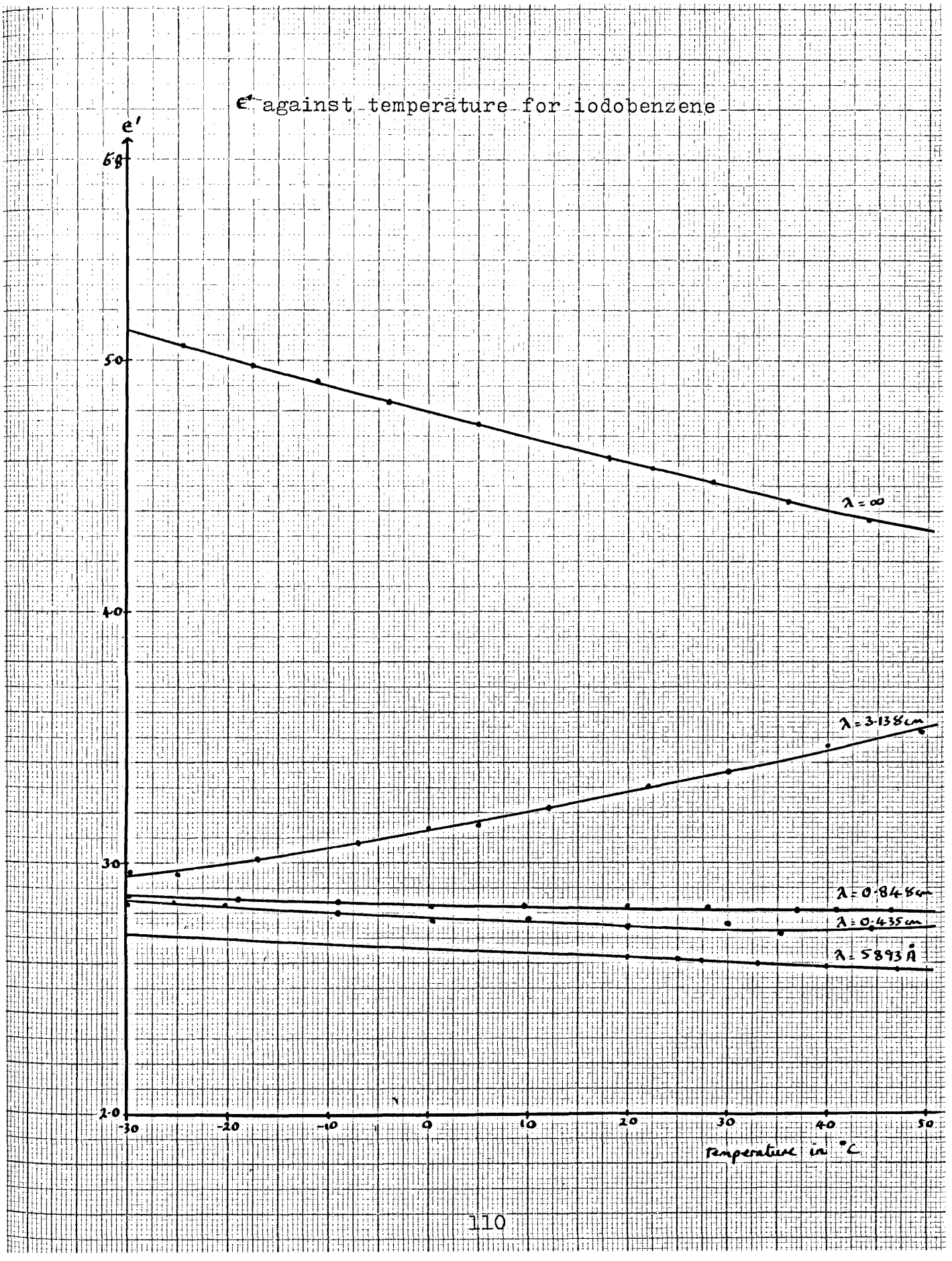

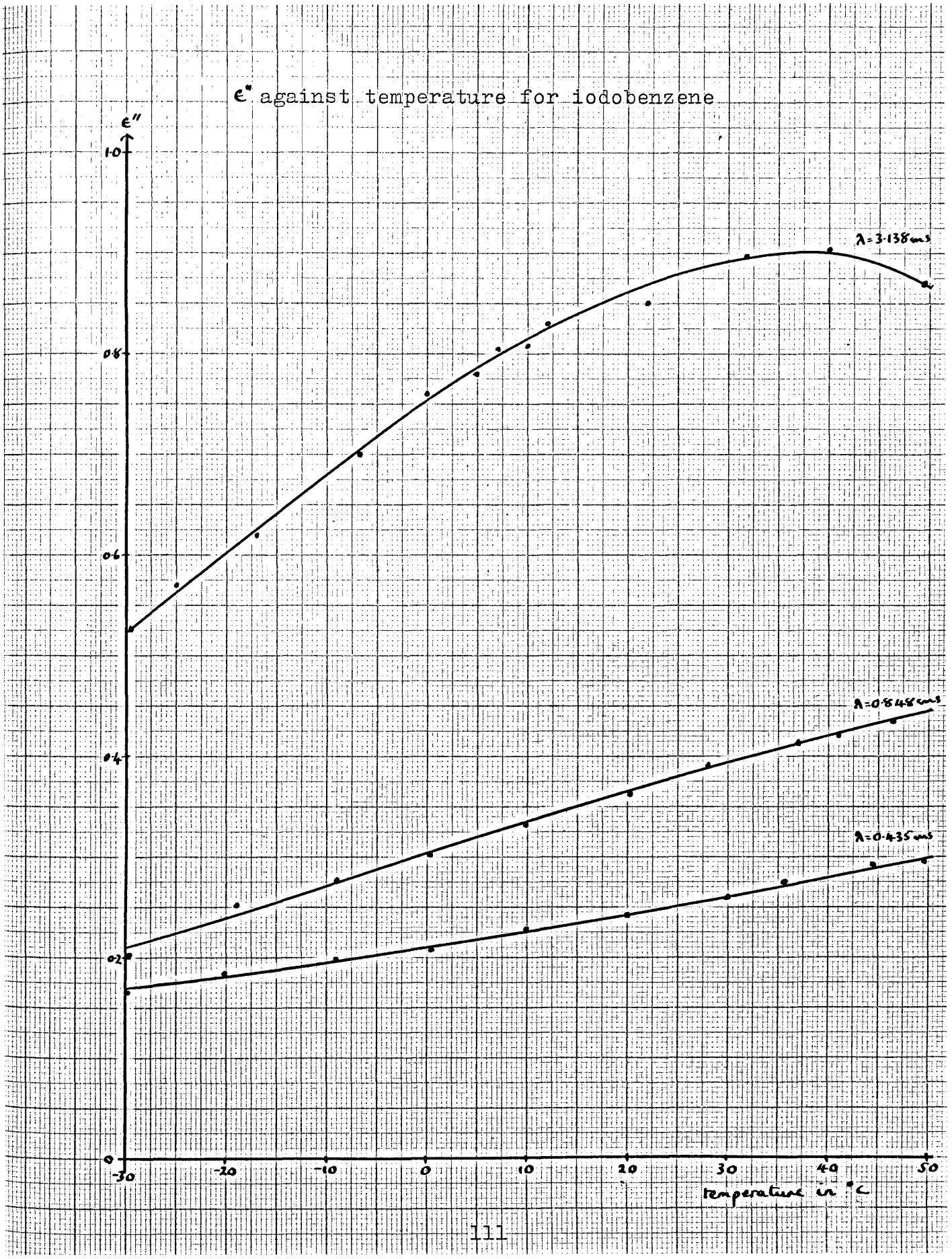
ε" against temperature for iodobenzene
ε"
1·0
0·8
0·6
0·4
0·2
0
λ = 3·138 cms
λ = 0·848 cms
λ = 0·435 cms
-30
-20
-10
0
10
20
30
40
50
Temperature in °C

ϵ' against temperature for nitrobenzene

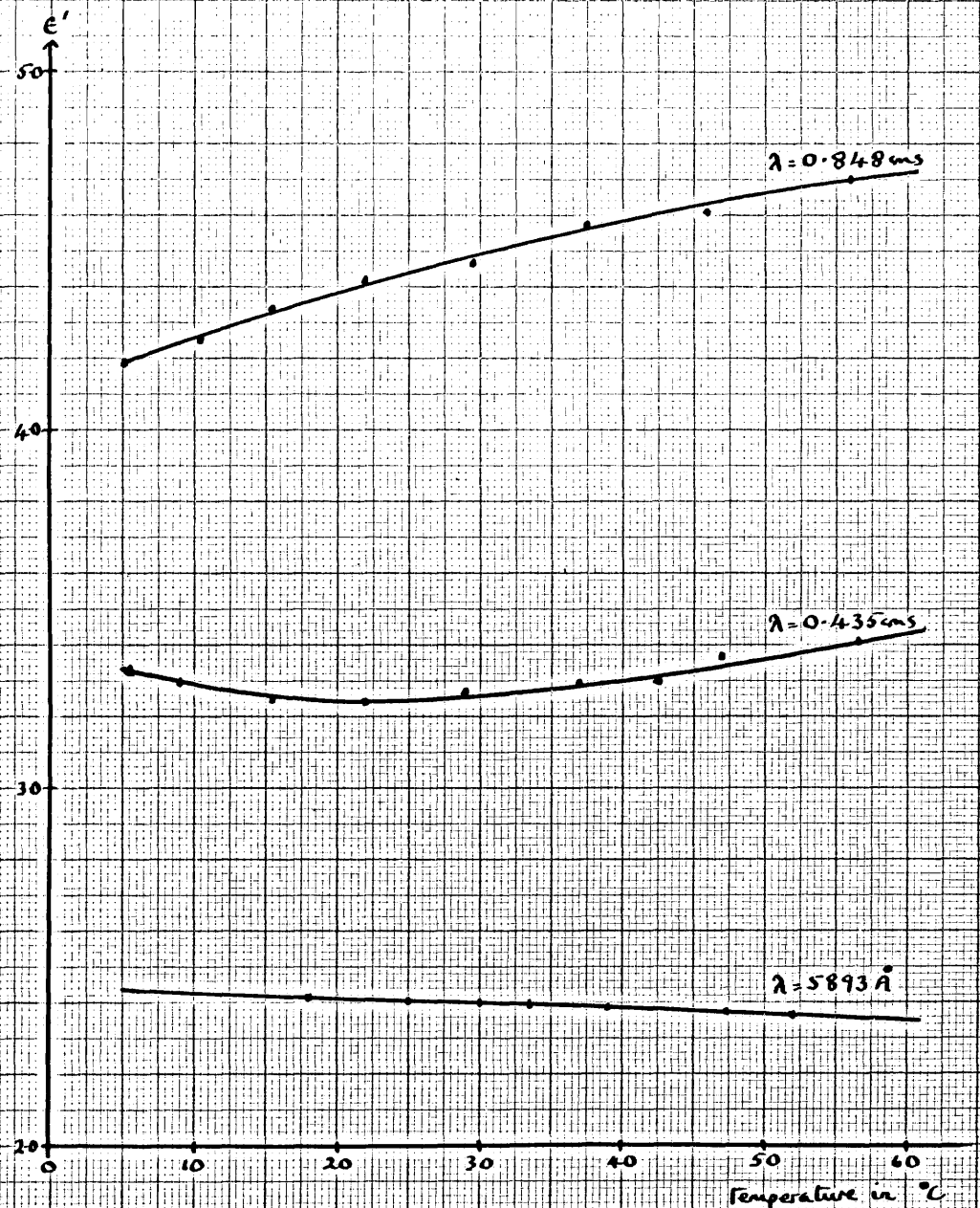

ϵ'' against temperature for nitrobenzene

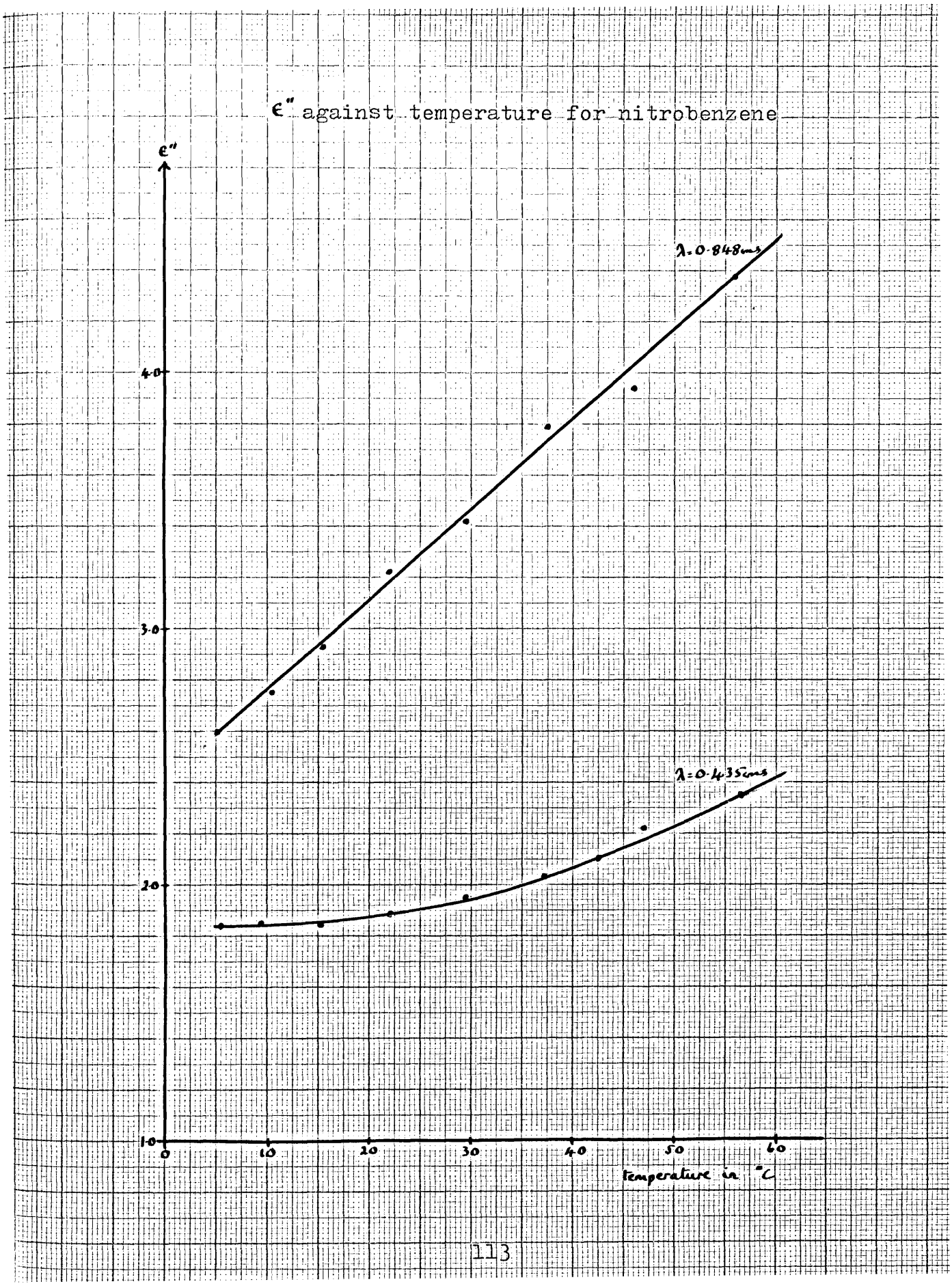

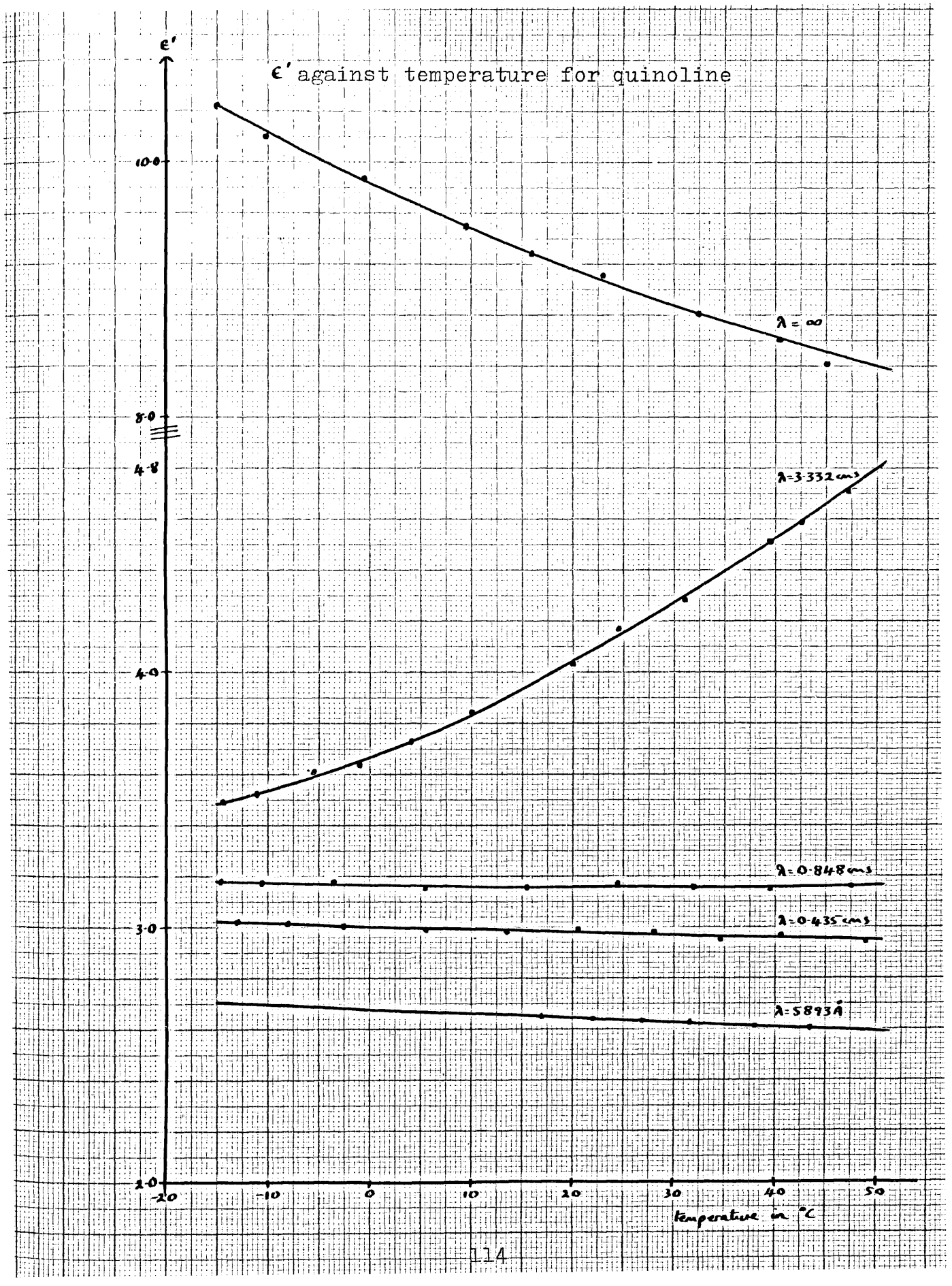
ε'
ε' against temperature for quinoline
10·0
8·0
4·8
4·0
3·0
2·0
λ = ∞
λ=3·332 cms
λ=0·848 cms
λ=0·435 cms
λ=5893 Å
-20
-10
0
10
20
30
40
50
Temperature in °C

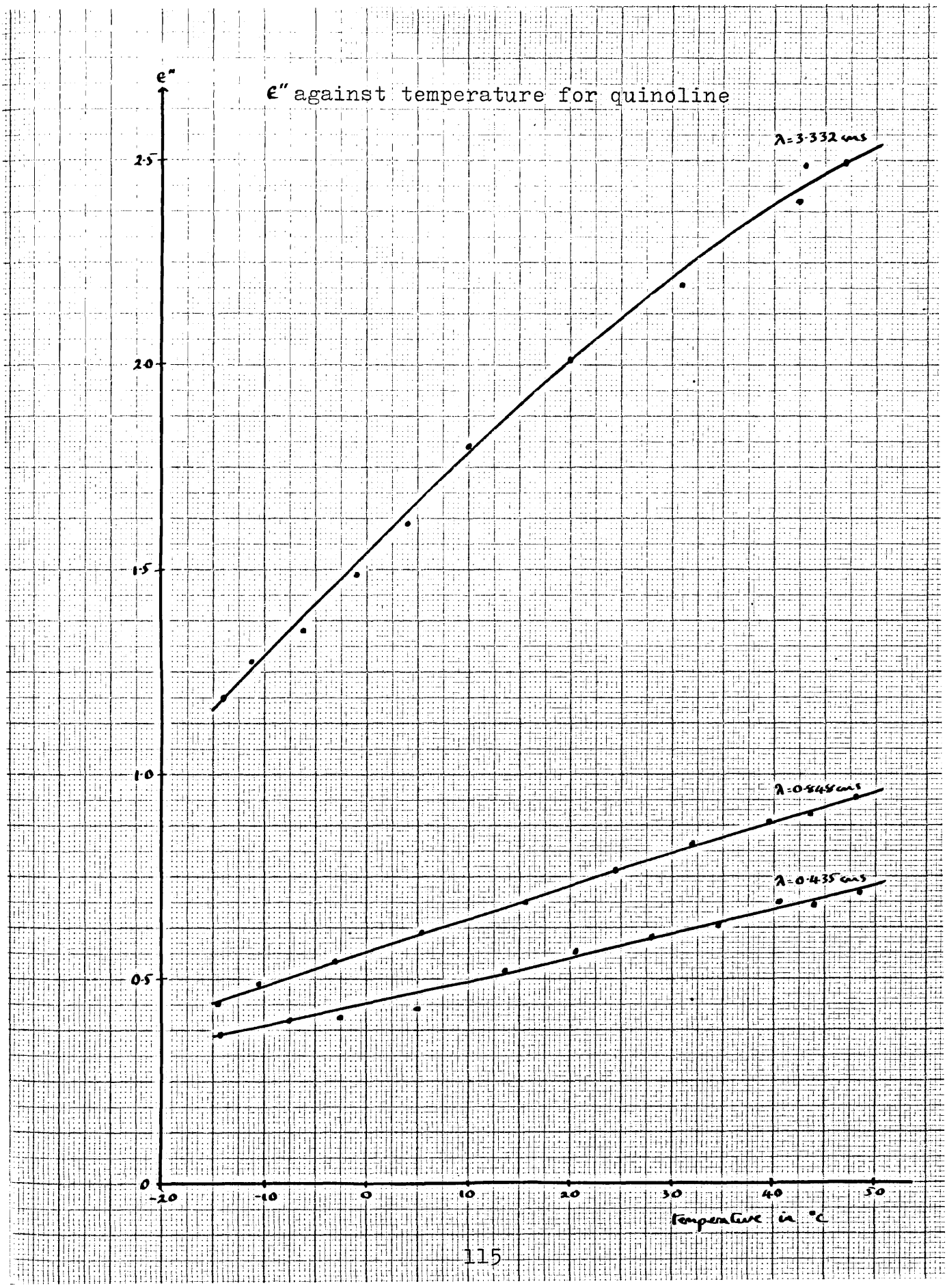
ε″ against temperature for quinoline
ε″
2·5
2·0
1·5
1·0
0·5
0
-20
-10
0
10
20
30
40
50
Temperature in °C
λ = 3·332 cms
λ = 0·848 cms
λ = 0·435 cms

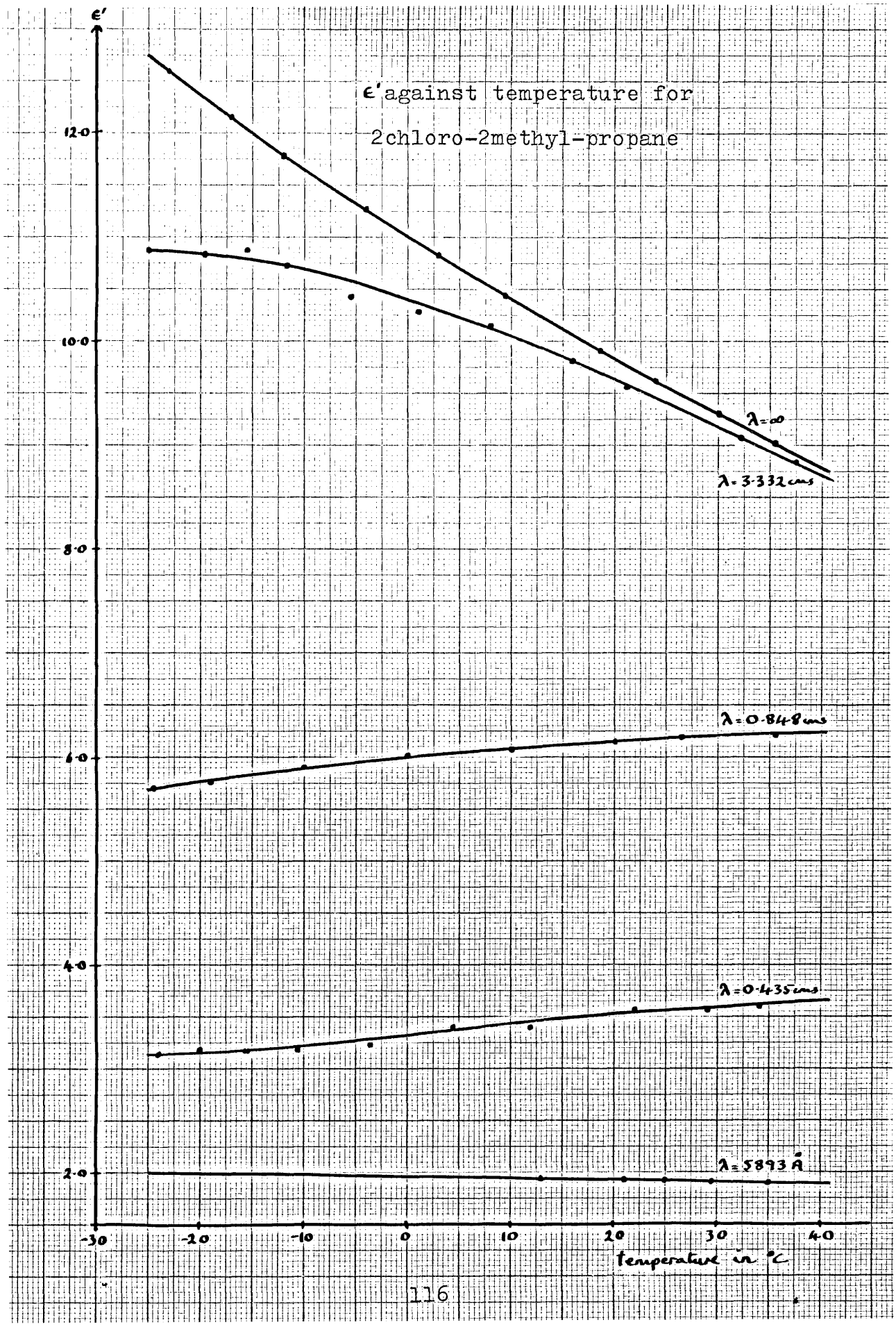
ε'
ε'against temperature for
2chloro-2methyl-propane
12·0
10·0
8·0
6·0
4·0
2·0
λ=∞
λ=3·332cms
λ=0·848cms
λ=0·435cms
λ=5893 Å
-30
-20
-10
0
10
20
30
40
temperature in °C

ϵ'' against temperature for 2chloro-2methyl-propane

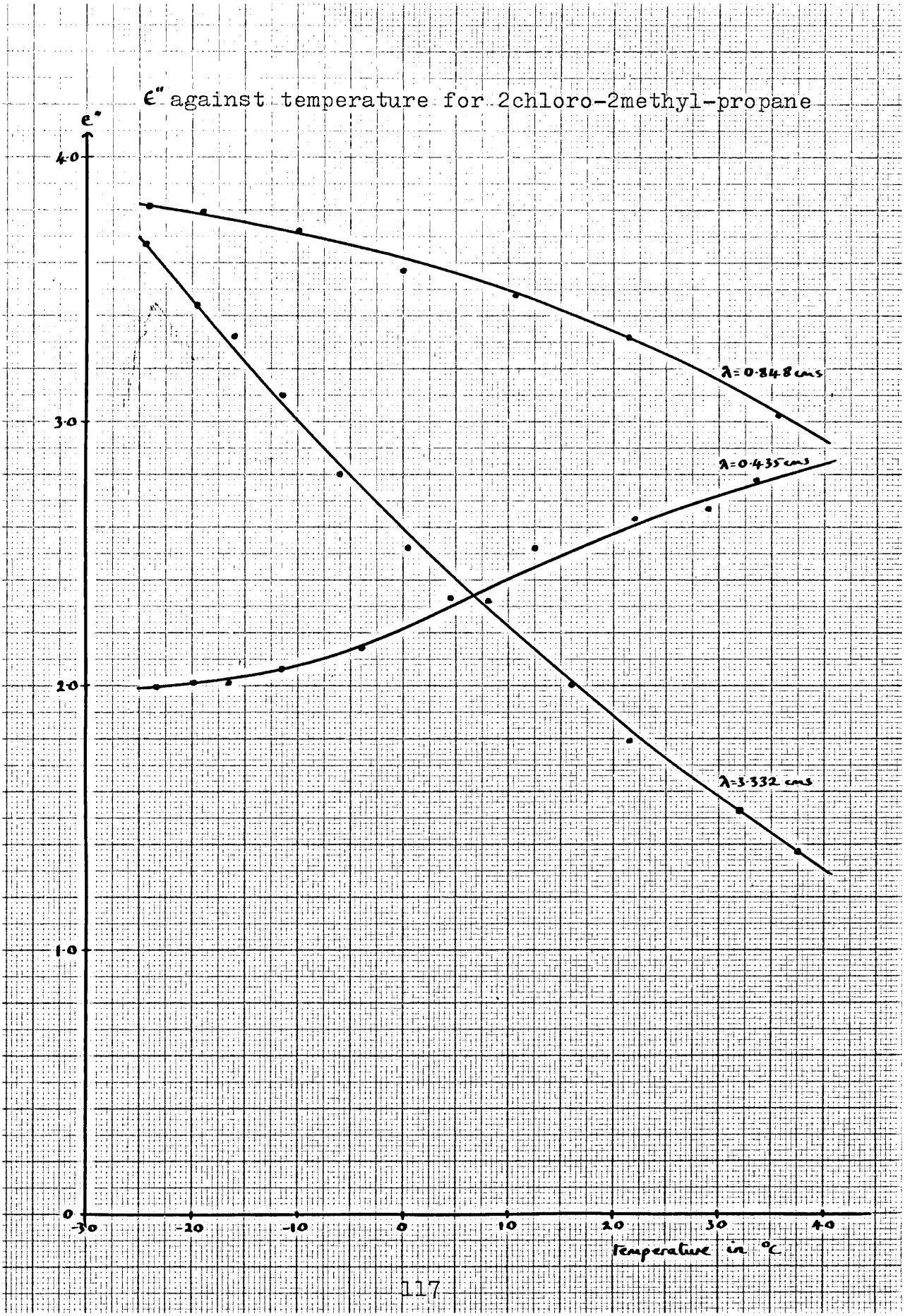

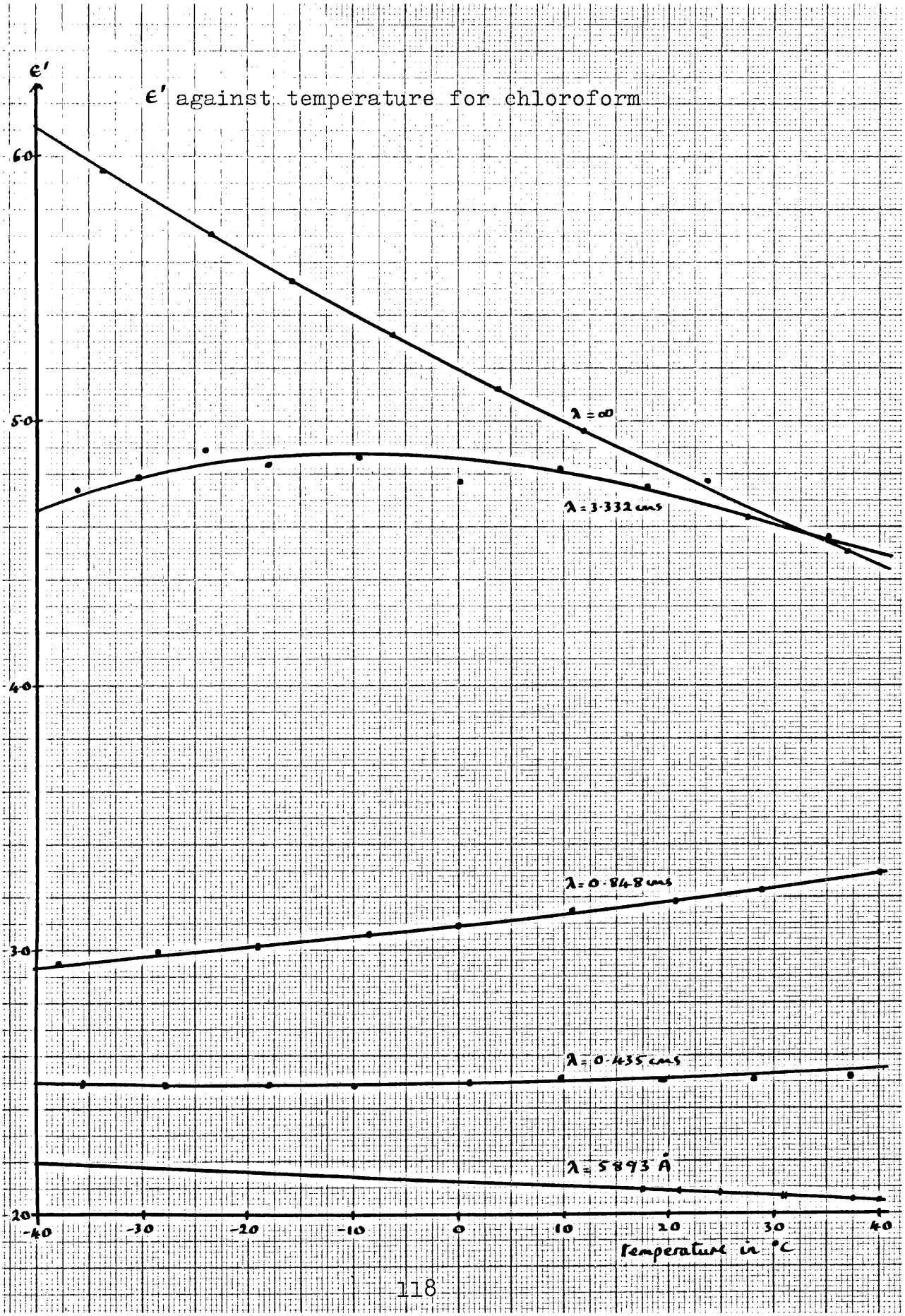
ε'
ε' against temperature for chloroform
6·0
5·0
4·0
3·0
-20
λ = ∞
λ = 3·332 cms
λ = 0·848 cms
λ = 0·435 cms
λ = 5893 Å
-40
-30
-20
-10
0
10
20
30
40
Temperature in °C

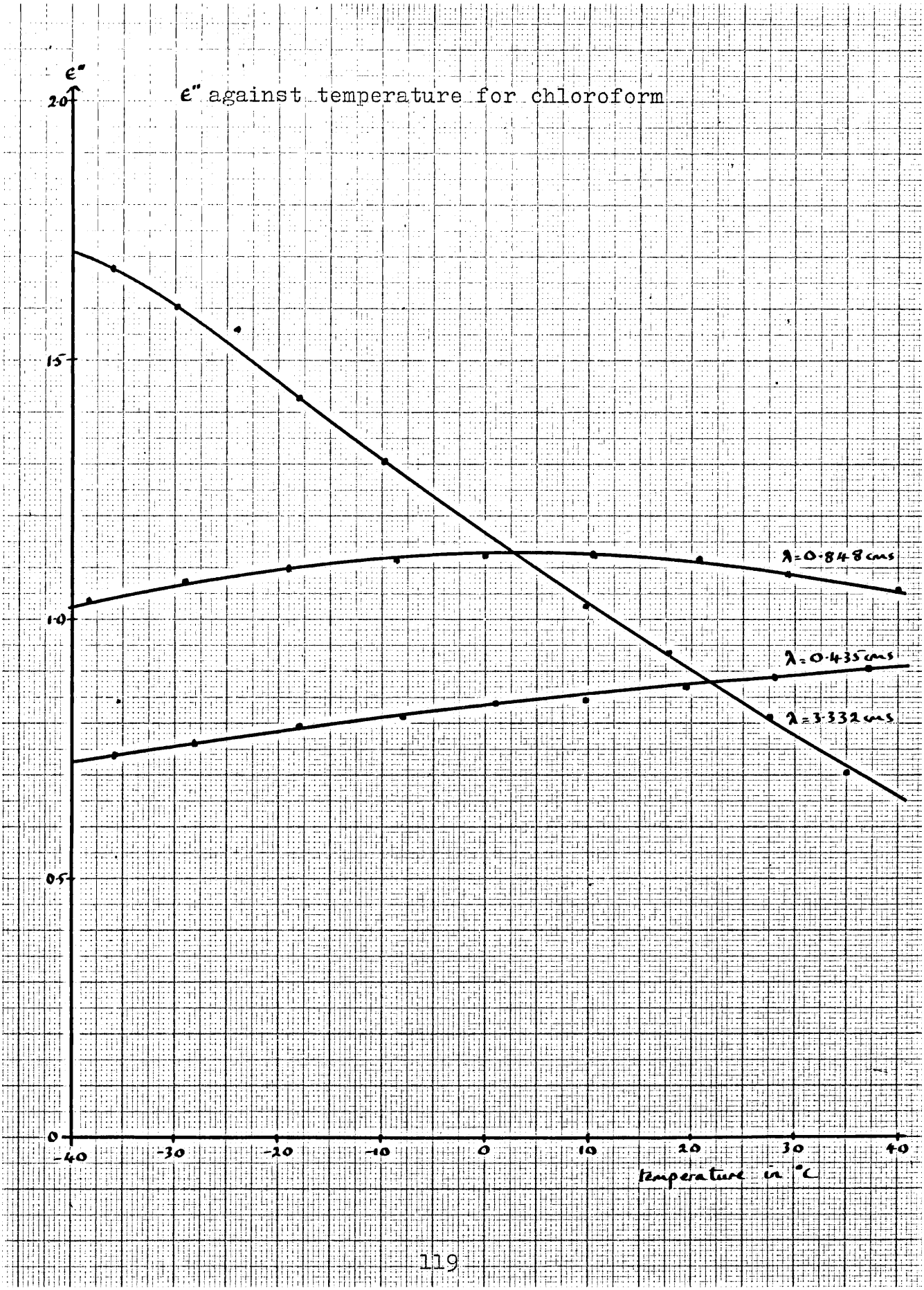
ε"
ε" against temperature for chloroform
2·0
1·5
1·0
0·5
0
λ = 0·848 cms
λ = 0·435 cms
λ = 3·332 cms
-40
-30
-20
-10
0
10
20
30
40
Temperature in °C

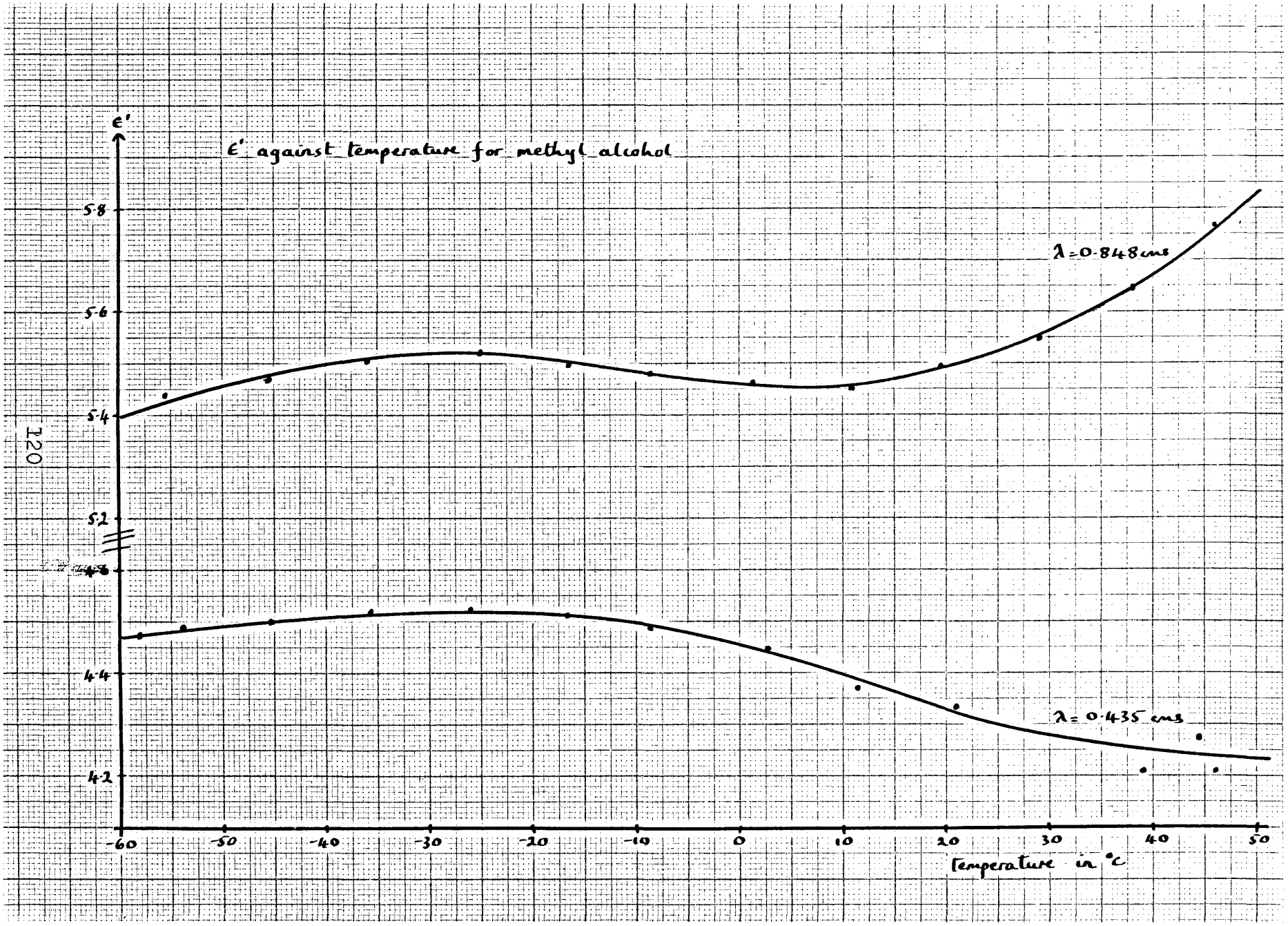
ε'
ε' against temperature for methyl alcohol
5·8
5·6
5·4
5·2
4·4
4·2
λ = 0·848 cms
λ = 0·435 cms
-60
-50
-40
-30
-20
-10
0
10
20
30
40
50
Temperature in °C

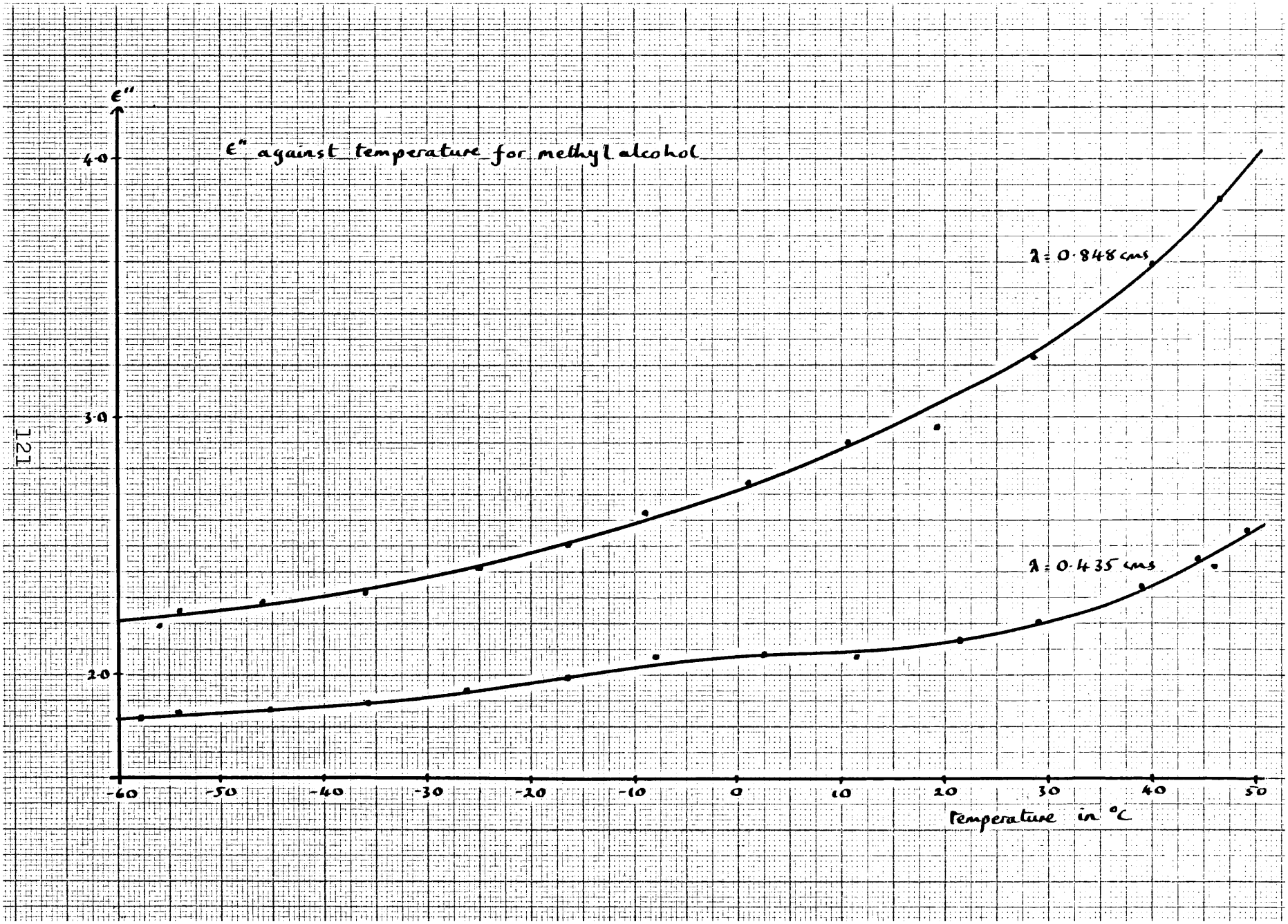
ε"
ε" against temperature for methyl alcohol
4·0
3·0
2·0
λ = 0·848 cms
λ = 0·435 cms
-60
-50
-40
-30
-20
-10
0
10
20
30
40
50
Temperature in °C

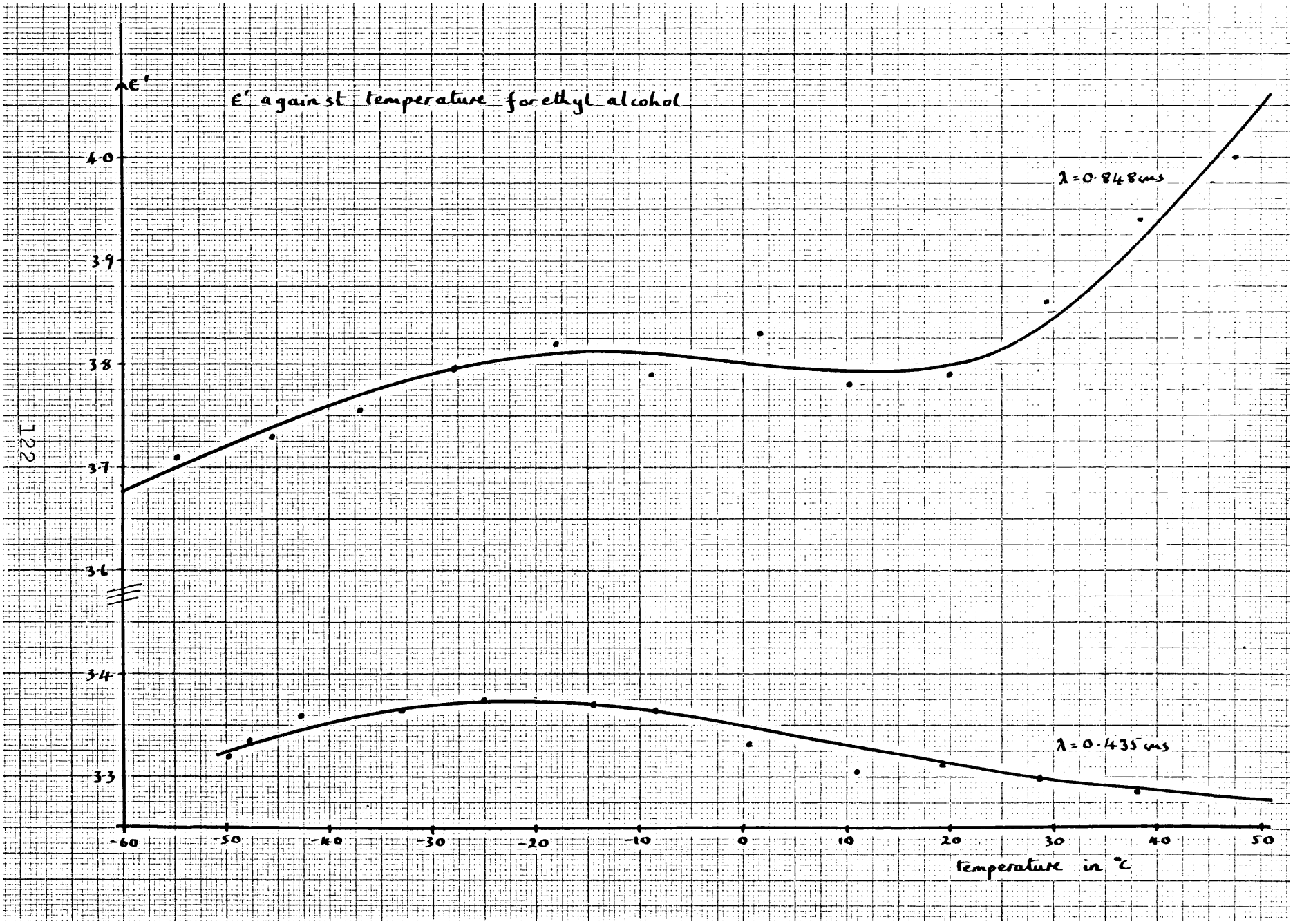
ε'
ε' against temperature for ethyl alcohol
4·0
3·9
3·8
3·7
3·6
3·4
3·3
λ = 0·848 cms
λ = 0·435 cms
-60
-50
-40
-30
-20
-10
0
10
20
30
40
50
Temperature in °C
122

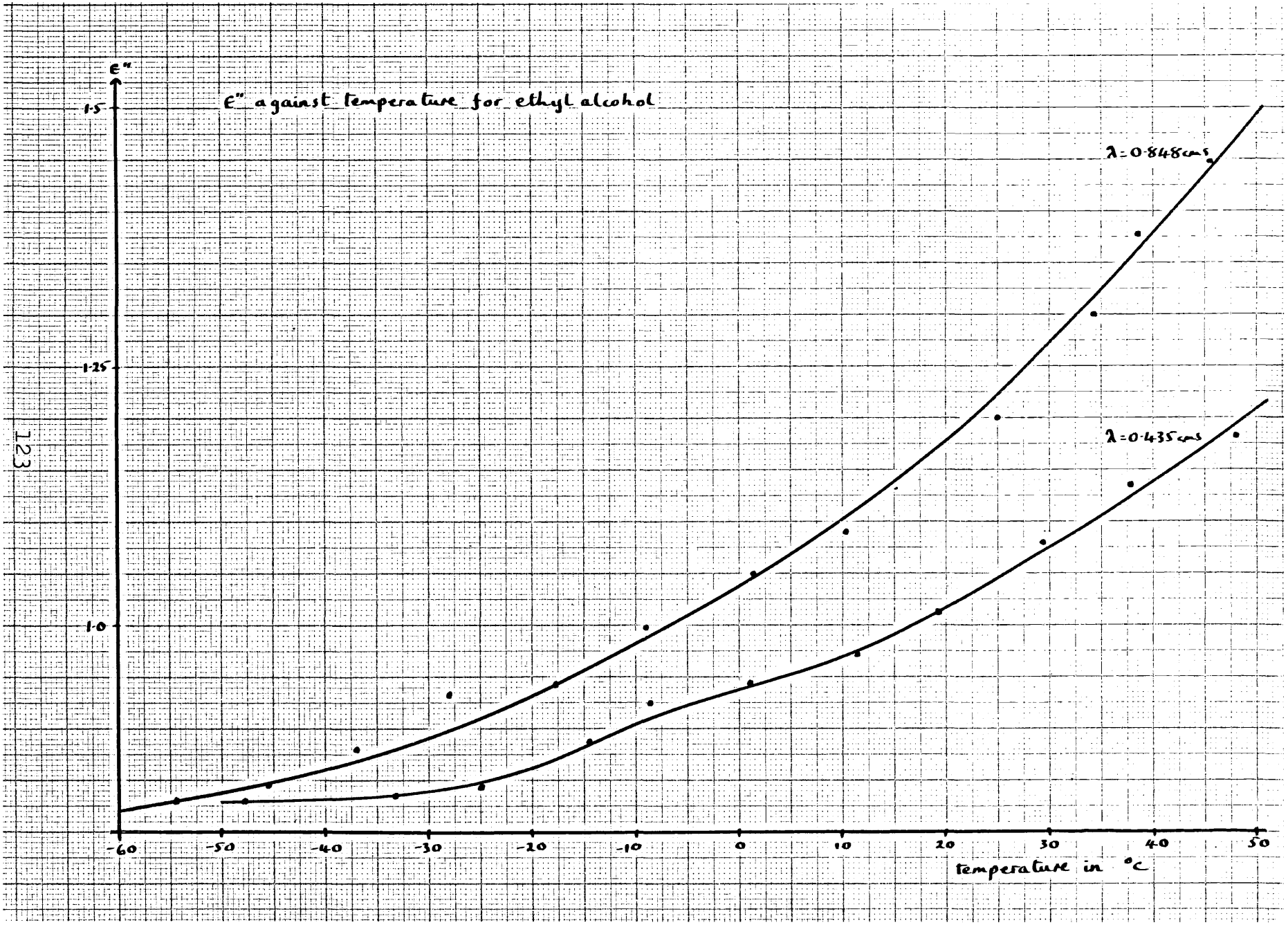
ε″
ε″ against temperature for ethyl alcohol
1·5
1·25
1·0
λ = 0·848 cms
λ = 0·435 cms
-60
-50
-40
-30
-20
-10
0
10
20
30
40
50
temperature in °C

123

Tables of the static permittivity, the complex permittivity at each wavelength, and the refractive index at the sodium-D line, all at various temperatures.

Chlorobenzene

temp °C	ϵ_s	$\lambda = 3.332$cm ϵ'	ϵ''	$\lambda = 0.848$cm ϵ'	ϵ''	$\lambda = 0.435$cm ϵ'	ϵ''	n_D
40	5.33	4.70	1.19	2.97	1.15	2.64	0.757	1.5138
30	5.49	4.70	1.31	2.94	1.10	2.60	0.728	1.5194
20	5.66	4.67	1.45	2.91	1.05	2.58	0.696	1.5250
10	5.84	4.59	1.57	2.87	1.00	2.58	0.663	1.5303
0	6.05	4.46	1.70	2.84	0.940	2.58	0.623	1.5359
-10	6.27	4.29	1.76	2.82	0.882	2.60	0.582	1.5412
-20	6.51	4.09	1.76	2.80	0.824	2.61	0.542	1.5468
-30	6.76	3.87	1.72	2.79	0.762	2.62	0.508	1.5521
-40	7.03	3.63	1.63	2.79	0.694	2.63	0.477	1.5577
-45	7.16	3.51	1.58	2.79	0.660	2.63	0.462	1.5603

Bromobenzene

temp °C	ϵ_s	λ = 3.332cm ϵ'	ϵ''	λ = 0.848cm ϵ'	ϵ''	λ = 0.435cm ϵ'	ϵ''	n_D
50	5.04	4.20	1.18	2.77	0.788	2.67	0.562	1.5435
40	5.15	4.14	1.25	2.78	0.765	2.63	0.517	1.5491
30	5.27	4.04	1.31	2.78	0.734	2.61	0.483	1.5548
20	5.41	3.94	1.37	2.78	0.702	2.61	0.456	1.5604
10	5.56	3.83	1.40	2.78	0.667	2.62	0.431	1.5660
0	5.71	3.70	1.40	2.78	0.621	2.62	0.414	1.5718
-10	5.86	3.58	1.36	2.79	0.570	2.63	0.394	1.5772
-20	6.04	3.43	1.30	2.79	0.509	2.64	0.367	1.5839
-30	6.24	3.28	1.21	2.79	0.443	2.64	0.333	1.5883

Iodobenzene

temp °C	ϵ_s	λ = 3.138cm ϵ'	ϵ''	λ = 0.848cm ϵ'	ϵ''	λ = 0.435cm ϵ'	ϵ''	n_D
50	4.32	3.54	0.870	2.80	0.443	2.74	0.300	1.6021
40	4.41	3.46	0.901	2.81	0.419	2.73	0.279	1.6078
30	4.50	3.37	0.890	2.81	0.391	2.73	0.259	1.6135
20	4.59	3.28	0.861	2.82	0.365	2.74	0.240	1.6192
10	4.69	3.20	0.813	2.82	0.335	2.76	0.224	1.6248
0	4.80	3.13	0.754	2.83	0.305	2.78	0.209	1.6304
-10	4.90	3.06	0.680	2.84	0.274	2.80	0.194	1.6361
-20	5.01	3.00	0.603	2.85	0.241	2.82	0.181	1.6417
-30	5.12	2.95	0.522	2.87	0.211	2.85	0.171	1.6473

Nitrobenzene

temp °C	ϵ_s	$\lambda = 0.848$cm ϵ'	ϵ''	$\lambda = 0.435$cm ϵ'	ϵ''	n_D
60	28.4	4.73	4.51	3.43	2.41	1.5324
50	30.3	4.66	4.15	3.36	2.22	1.5374
40	32.2	4.58	3.82	3.30	2.06	1.5425
30	34.1	4.49	3.47	3.26	1.95	1.5477
20	35.9	4.38	3.12	3.25	1.88	1.5527
10	37.8	4.25	2.77	3.28	1.84	1.5578
6	38.6	4.20	2.62	3.32	1.84	1.5598

Quinoline

temp °C	ϵ_s	$\lambda = 3.332$cm ϵ'	ϵ''	$\lambda = 0.848$cm ϵ'	ϵ''	$\lambda = 0.435$cm ϵ'	ϵ''	n_D
50	8.39	4.80	2.53	3.16	0.952	2.95	0.729	1.6105
40	8.61	4.53	2.39	3.16	0.878	2.96	0.668	1.6158
30	8.87	4.27	2.21	3.16	0.802	2.97	0.611	1.6210
20	9.16	4.04	2.01	3.16	0.724	2.98	0.550	1.6263
10	9.47	3.83	1.78	3.16	0.644	2.99	0.495	1.6316
0	9.83	3.66	1.54	3.17	0.563	3.00	0.437	1.6368
-10	10.23	3.54	1.29	3.17	0.484	3.01	0.383	1.6421
-15	10.45	3.48	1.16	3.18	0.440	3.02	0.358	1.6442

2chloro-2methyl-propane

temp °C	ϵ_s	λ = 3.332cm ϵ'	ϵ''	λ = 0.848cm ϵ'	ϵ''	λ = 0.435cm ϵ'	ϵ''	n_D
40	8.75	8.68	1.30	6.24	2.93	3.66	2.84	1.3731
30	9.27	9.17	1.57	6.21	3.15	3.59	2.72	1.3793
20	9.80	9.63	1.88	6.16	3.34	3.52	2.57	1.3857
10	10.38	10.04	2.22	6.08	3.49	3.44	2.41	1.3920
0	11.00	10.41	2.59	5.99	3.61	3.32	2.22	1.3983
-10	11.67	10.69	3.00	5.88	3.71	3.22	2.07	1.4046
-20	12.37	10.84	3.45	5.75	3.79	3.16	2.01	1.4110
-25	12.74	10.87	3.69	5.68	3.82	3.14	1.99	1.4141

Chloroform

temp °C	ϵ_s	λ = 3.332cm ϵ'	ϵ''	λ = 0.848cm ϵ'	ϵ''	λ = 0.435cm ϵ'	ϵ''	n_D
50	4.29	4.36	0.54	3.34	1.01	2.58	0.93	1.4259
40	4.45	4.50	0.66	3.29	1.05	2.55	0.91	1.4322
30	4.63	4.61	0.78	3.23	1.09	2.53	0.89	1.4384
20	4.81	4.71	0.90	3.18	1.11	2.52	0.88	1.4447
10	5.00	4.80	1.03	3.13	1.13	2.51	0.86	1.4518
0	5.20	4.85	1.16	3.09	1.13	2.50	0.83	1.4572
-10	5.40	4.87	1.31	3.05	1.12	2.49	0.81	1.4634
-20	5.63	4.86	1.46	3.01	1.09	2.49	0.78	1.4696
-30	5.86	4.79	1.61	2.97	1.07	2.49	0.75	1.4758
-40	6.11	4.66	1.71	2.94	1.03	2.50	0.73	1.4821
-50	6.38	4.42	1.73	2.90	0.98	2.51	0.69	1.4883
-55	6.52	4.26	1.71	2.88	0.95	2.52	0.67	1.4915

Methyl Alcohol

temp °C	λ = 0.848cm ϵ'	ϵ''	λ = 0.435cm ϵ'	ϵ''
50	5.82	4.02	4.23	2.55
40	5.67	3.59	4.25	2.33
30	5.55	3.28	4.28	2.20
20	5.48	3.06	4.33	2.13
10	5.45	2.88	4.40	2.09
0	5.45	2.72	4.46	2.08
-10	5.48	2.60	4.50	2.03
-20	5.51	2.49	4.52	1.97
-30	5.52	2.39	4.52	1.92
-40	5.49	2.32	4.51	1.89
-50	5.45	2.26	4.50	1.86
-60	5.40	2.21	4.47	1.83

Ethyl Alcohol

temp	$\lambda = 0.848$cm		$\lambda = 0.435$cm	
^{o}C	ϵ'	ϵ''	ϵ'	ϵ''
50	4.05	1.49	3.28	1.21
40	3.94	1.38	3.29	1.14
30	3.85	1.27	3.30	1.08
20	3.80	1.18	3.31	1.02
10	3.79	1.10	3.33	0.97
0	3.80	1.04	3.35	0.94
-10	3.81	0.98	3.36	0.91
-20	3.81	0.93	3.37	0.86
-30	3.79	0.89	3.37	0.84
-40	3.76	0.86	3.35	0.83
-50	3.72	0.84	3.33	0.83
-60	3.68	0.82		

Tables of ϵ_∞ and λ_c calculated from ϵ' and ϵ'' at each wavelength and temperature. ϵ_∞ has an error of $\pm$ 2%, and λ_c of $\pm$ 3%-4%, though for $\epsilon_\infty(3)$ and $\lambda_c(3)$ at the higher temperatures where $\epsilon_s - \epsilon'$ is small, this error is much larger.

Chlorobenzene

temp	$\epsilon_\infty(3)$	$\epsilon_\infty(8)$	$\epsilon_\infty(4)$	ϵ_∞	$\lambda_c(3)$	$\lambda_c(8)$	$\lambda_c(4)$
40	2.42	2.43	2.42	2.42	1.74	1.74	1.61
30	2.49	2.47	2.41	2.48	1.99	1.96	1.73
20	2.55	2.51	2.42	2.53	2.28	2.22	1.92
10	2.61	2.54	2.44	2.58	2.65	2.52	2.14
0	2.65	2.57	2.47	2.62	3.13	2.89	2.42
-10	2.74	2.60	2.51	2.66	3.78	3.32	2.74
-20	2.81	2.62	2.54	2.70	4.58	3.82	3.14
-30	2.84	2.65	2.56	2.74	5.60	4.42	3.54
-40	2.84	2.68	2.58	2.78	6.93	5.18	4.01
-45	2.82	2.69	2.59	2.80	7.70	5.59	4.26

Bromobenzene

temp	$\epsilon_\infty(3)$	$\epsilon_\infty(.8)$	$\epsilon_\infty(.4)$	ϵ_∞	$\lambda_c(3)$	$\lambda_c(.8)$	$\lambda_c(.4)$
50	2.53	2.50	2.53	2.52	2.36	2.44	1.84
40	2.59	2.53	2.52	2.55	2.72	2.64	2.13
30	2.63	2.56	2.53	2.59	3.12	2.89	2.44
20	2.66	2.59	2.54	2.62	3.57	3.17	2.66
10	2.69	2.62	2.55	2.66	4.10	3.51	2.97
0	2.72	2.65	2.57	2.69	4.79	4.00	3.23
-10	2.75	2.68	2.58	2.72	5.58	4.58	3.56
-20	2.78	2.71	2.60	2.75	6.68	5.41	4.04
-30	2.79	2.73	2.61	2.77	8.17	6.61	4.70

Iodobenzene

temp	$\epsilon_\infty(3)$	$\epsilon_\infty(.8)$	$\epsilon_\infty(.4)$	ϵ_∞	$\lambda_c(3)$	$\lambda_c(.8)$	$\lambda_c(.4)$
50	2.56	2.68	2.68	2.68	2.78	2.91	2.30
40	2.61	2.70	2.67	2.69	3.31	3.24	2.62
30	2.67	2.72	2.69	2.71	3.99	3.65	2.97
20	2.71	2.74	2.71	2.73	4.78	4.12	3.36
10	2.76	2.76	2.73	2.76	5.76	4.74	3.75
0	2.79	2.78	2.76	2.78	6.93	5.46	4.19
-10	2.81	2.80	2.78	2.80	8.50	6.37	4.71
-20	2.82	2.83	2.81	2.82	10.62	7.59	5.26
-30	2.83	2.85	2.83	2.84	13.02	9.06	5.79

Nitrobenzene

temp	$\epsilon_\infty(.8)$	$\epsilon_\infty(.4)$	$\lambda_c(.8)$	$\lambda_c(.4)$
60	3.87	3.20	4.46	4.51
50	3.99	3.17	5.24	5.27
40	4.06	3.15	6.13	6.09
30	4.08	3.14	7.23	6.88
20	4.07	3.14	8.56	7.56
10	4.02	3.18	10.38	8.15
6	4.00	3.23	11.12	8.57

Quinoline

temp	$\epsilon_\infty(3)$	$\epsilon_\infty(.8)$	$\epsilon_\infty(.4)$	ϵ_∞	$\lambda_c(3)$	$\lambda_c(.8)$	$\lambda_c(.4)$
50	3.02	2.99	2.85	3.01	4.59	4.48	3.18
40	3.13	3.01	2.88	3.07	5.69	5.26	3.68
30	3.21	3.04	2.91	3.13	6.94	6.04	4.20
20	3.25	3.07	2.93	3.16	8.49	7.03	4.89
10	3.27	3.10	2.95	3.18	10.53	8.31	5.69
0	3.28	3.12	2.97	3.20	13.37	10.02	6.76
-10	3.29	3.14	2.99	3.22	17.28	12.44	8.20
-15	3.29	3.15	3.00	3.23	20.00	14.01	9.03

2chloro-2methyl-propane

temp	$\epsilon_\infty(3)$	$\epsilon_\infty(8)$	$\epsilon_\infty(4)$	ϵ_∞	$\lambda_c(3)$	$\lambda_c(8)$	$\lambda_c(4)$
40		2.82	2.08	2.82		0.73	0.78
30		2.97	2.29	2.97		0.82	0.91
20		3.09	2.47	3.09		0.92	1.06
10		3.25	2.60	3.25		1.04	1.25
0		3.38	2.68	3.38	0.76	1.18	1.50
-10	1.51	3.50	2.71	3.50	1.09	1.32	1.77
-20	3.06	3.58	2.72	3.58	1.48	1.48	1.99
-25	3.59	3.62	2.73	3.62	1.69	1.57	2.10

Chloroform

temp	$\epsilon_\infty(3)$	$\epsilon_\infty(.8)$	$\epsilon_\infty(.4)$	ϵ_∞	$\lambda_c(3)$	$\epsilon_\infty(.8)$	$\epsilon_\infty(.4)$
50		2.27	2.08	2.18		0.80	0.80
40		2.33	2.12	2.23		0.94	0.90
30		2.39	2.15	2.27		1.09	1.02
20		2.42	2.19	2.30		1.24	1.15
10		2.45	2.21	2.33		1.40	1.27
0	1.01	2.49	2.24	2.36	1.01	1.58	1.41
-10	1.66	2.51	2.27	2.39	1.36	1.78	1.56
-20	2.08	2.55	2.29	2.42	1.76	2.03	1.76
-30	2.39	2.59	2.32	2.45	2.23	2.30	2.02
-40	2.64	2.61	2.35	2.48	2.83	2.62	2.17
-50	2.89	2.63	2.38	2.51	3.74	3.02	2.43
-55	2.96	2.64	2.40	2.52	4.41	3.24	2.58

References

1) P.Debye; 'Polar Molecules' New York, 1929

2) J.Wyman; J. Amer. Chem. Soc. 58, 1482, 1936

3) L.Onsager; J. Amer. Chem. Soc. 58, 1486, 1936

4) J.G.Kirkwood; Jour. Chem. Phys. 7, 911, 1939

5) H.Fröhlich; Trans. Farad. Soc. 44, 238, 1948

6) W.M.Heston, E.J.Hennelly, C.P.Smyth;
J. Amer. Chem. Soc. 72, 2071, 1950

7) K.S.Cole, R.H.Cole; Jour, Chem. Phys. 9, 341, 1941

8) W.F.Brown; 'Handbuck der Physick', vol XVII, Berlin 1956.

9) .R.H.Cole; Jour. Chem. Phys. 6, 385, 1938

10) J.G.Powles; Jour. Chem. Phys. 21, 633, 1953

11) C.H.Collie, J.B.Hasted, D.M.Ritson;
Proc. Phys. Soc. 60, 145, 1948

12) J.Ph.Poley; App. Sci. Res. 4B, 337, 1955

13) F.W.Heinenken, F.Bruin; Physica 23, 57, 1957

14) R.W.Rampolla, R.C.Miller, C.P.Smyth,
Jour. Chem. Phys. 30, 566, 1959

15) W.E.Vaughan, C.P.Smyth; Jour. Phys. Chem. 65, 94, 98,1961.

16) W.E.Vaughan, W.S.Lovell, C.P.Smyth;
Jour. Chem. Phys. 36, 535, 1962

17) S.K.Garg, C.P.Smyth; Jour. Chem. Phys. 42, 1397, 1965

18) G.W.Chantry, H.A.Gebbie; Nature, 208, 378, 1965

19) H.A.Gebbie, N.W.B.Stone, F.D.Findlay, E.C.Pyatt;
Nature 205, 378, 1965

20) Y.Leroy, E.Constant; C.R.Acad. Sci. 262B, 1391, 1966

21) D.Chanal, E.Décamps, A.Hadni, H.Wendling;
J. de Physique 28, 165, 1967

22) T.Powles; Trans. Farad. Soc. 44, 802, 1948

23) E.Constant, Y.Leroy, L.Raczy;
C.R.Acad. Sci. 261, 4687, 1965

24) D.H.Whiffen; Trans. Farad, Soc. 46, 124, 1950

25) W.M.Heston, C.P.Smyth; J. Amer. Chem. Soc. 72, 99, 1950

26) S.K.Garg, H.Kilp, C.P.Smyth;
Jour. Chem. Phys. 43, 2341, 1965

27) G.W.Chantry, H.A.Gebbie, B.Lassier, G.Wyllie;
Nature 214B, 163, 1967

28) N.E.Hill; Proc. Phys. Soc. 82, 723, 1963

29) B.Lassier, C.Brot; Chem. Phys. letters 1, 581, 1968

30) A.E.Stanevich, N.G.Yaroslavskii;
Optics and Spectroscopy 10, 278, 1961

31) S.Roberts, A.von Hippel; 'Dielectrics and Waves'

32) A.G.Mungall, J.Hart; Canadian J. Phys. 35, 995, 1957

33) J.A.Saxton, R.A.Bond, G.T.Coats, R.M.Dikinson;
Jour. Chem. Phys. 37, 2132, 1962

34) C.Pine, W.G.Zoellner, J.H.Rohrbaugh;
Jour. Opt. Soc. Amer. 49, 1202, 1959

35) A.Gerschel, C.Brot; Rev. Phys. Appl. 1, 113, 1966

36) S.Roberts, A.von Hippel; J. App. Phys. 17, 610, 1946

37) R.Papoular; C.R.Acad. Sci. 254, 1763, 1962

38) J.A.Lane, J.A.Saxton; Proc. Royal Soc. London
213A, 400, 1952

39) E.H.Grant; Brit. J. App. Phys. 10, 87, 1959

40) S.Mallikarjun, N.E.Hill; Trans. Farad. Soc. 61, 1389,1965

41) E.Fatuzzo, P.R.Mason; J. App. Phys. 36, 427, 1965

42) L.A.Sayce, H.V.A.Briscoe; Jour. Chem. Soc. 127, 315, 1925

43) S.Mallikarjun; thesis offered for a Ph.D. degree,
London University, 1964

44) S.Sugden; Jour. Chem. Soc. 770, 1933

45) J.E.Chamberlain; Private communication.

46) N.E.Hill; Trans. Farad. Soc. 55, 2000, 1959

Acknowledgements

The author wishes to thank Dr.N.E.Hill of Bedford College, London, for all her help. Also the workshop of Bedford College for help in making apparatus, and to Dr.J.E.Chamberlain of the National Physical Laboratory, Teddington, for providing some of his experimental data on chlorobenzene.